universität wien

MASTERARBEIT

Titel der Masterarbeit

„Iron oxide solubility in artificial sea water in the presence of siderophores and humic substances“

Verfasserin

Monika Laux, BSc.

Angestrebter akademischer Grad

Master of Science (MSc)

Wien, 2014

Studienkennzahl lt. Studienblatt:	A 066 862
Studienrichtung lt. Studienblatt:	Masterstudium Chemie
Betreuerin / Betreuer:	ao. Univ.-Prof. Mag. Dr. Regina Krachler

TABLE OF CONTENTS

ZUSAMMENFASSUNG

Huminstoffe werden seit vielen Jahren wissenschaftlich untersucht. Dennoch bleiben die Charakterisierungen schwierig, da nach wie vor keine Strukturformeln bekannt sind. Auch hinsichtlich ihrer Funktion in biologischen Systemen gibt es nach wie vor Unklarheiten. Besonders die Bedeutung für den biogeochemischen Eisenkreislauf ist umstritten. Eisen spielt in den oberflächlichen Schichten der Ozeane eine wichtige Rolle, da es in weiten Teilen den limitierenden Faktor für die Primärproduktion des Phytoplanktons darstellt. Diese Stellung als limitierender Faktor rührt daher, dass Eisen(III) im Meerwasser nur eine geringe Löslichkeit aufweist. Organische Verbindungen terrestrischen und ozeanischen Ursprunges können diese Löslichkeit erhöhen.

In dieser Arbeit wurden die Versuche zur Charakterisierung von Huminstoffen aus Feuchtgebieten und deren Eisentragfähigkeit von Krachler et al., Kittinger und Plessl fortgeführt. Dazu wurden zwei natürliche Wasserproben aus Hochlandmooren in Nordschottland beziehungsweise Oberösterreich untersucht. Des Weiteren wurden zwei kommerziell erhältliche Referenzsubstanzen aus einem Sumpfgebiet in Georgia und einem Trinkwasserreservoir in Norwegen analysiert.

Dabei kam ein mehrstufiges Experiment zum Einsatz: Nach dem Ausfällen von in Meerwasser nicht löslichen Anteilen erfolgte eine Trennung mittels einer Größenausschlusschromatographie in mehrere Fraktionen, die anschließend getrocknet und erneut in künstlichem Meerwasser gelöst wurden. Ein marines Siderophor wurde ebenfalls in künstlichem Meerwasser gelöst und mit allen Proben wurden Löslichkeitsversuche durchgeführt, die die Bedingungen im offenen Ozean simulieren sollten. Die Bestimmung der Eisenlöslichkeit erfolgte mit Gammaspektroskopie nach Zusatz eines ^{59}Fe Tracers.

Die Ergebnisse zeigen, dass die Werte für die Komplexbildungskonstanten der Eisen-Huminstoffkomplexe gerade so weit unter jenem des Siderophors liegen, dass ein entscheidender Beitrag der terrestrischen Huminstoffe zum

bioverfügbaren Eisenreservoir im Ozean wahrscheinlich ist, aber trotzdem ein Ligandenaustausch mit Siderophoren als Aufnahmemechanismus nahe liegt.

Abstract

Humic substances have been subject of scientific investigation for many years. Nevertheless characterizations stay difficult, because there are no structural formulas known yet. Also in respect of their biological function there are still ambiguities. Especially the significance for the global biogeochemical iron cycle is under controversial discussion. Iron plays a vital role in the euphotic zone of the ocean, since it represents the limiting factor for primary production of phytoplankton in wide regions. This is due to the limited solubility of iron(III) in seawater. Terrestrial-derived and marine organic compounds are capable of enhancing this solubility.

With this thesis I continued the experiments made by Krachler et al., Kittinger and Plessl, who tried to characterize humic substances from wetlands and their capacity to act as an iron carrier. For this purpose two natural water samples from peat land run offs from northern Scotland and Upper Austria were investigated. Moreover two commercially available reference substances from a swamp in South Georgia and a drinking water reservoir in Norway were analyzed. In this case a multistage experiment was deployed. After precipitation of the fraction not soluble in seawater, further separation was conducted by size exclusion chromatography. The resulting fractions were dried and re-dissolved in artificial seawater. A marine siderophore was dissolved in artificial seawater as well. With all samples experiments were performed, which intended to simulate the conditions of the open ocean. The iron solubility was determined using gamma spectroscopy after addition of a ^{59}Fe tracer.

The results show that the values for the complex formation constants of the humic substances are just below the value of the siderophore. This suggests a significant contribution of the terrestrial humic substances to the bioavailable iron reservoir. But still a ligand exchange with siderophores is a possible uptake mechanism.

LIST OF ABBREVIATIONS

AAS	Atomic absorption spectrometry
CLE-CSV	competitiv ligand exchange cathodic stripping voltammetry
DOC	dissolved organic carbon
DOM	dissolved organic matter
EIFEX	European Iron Fertilization Experiment
EN ISO	European Norm International Organization for Standardization
FA	fulvic acids
FFF	filed flow fractionation
GHP	gamma ray sterilized hydrophilic polypropylene
Ga	billion years
HA	humic acids
HPG	high purity germanium
HS	humic substances
HNLC	high nutrient low chlorophyll
IHSS	International Humic Substance Society
LNLC	low nutrient low chlorophyll
MS	mass spectrometry
NOM	natural organic matter
NPDOC	non purge able dissolved organic carbon
PET	Polyethylene terephthalate
PTFE	Polytetrafluoroethylene
PE	polyethylene
SEC	size exclusion chromatography
SPE	solid phase extraction
TOC	total organic carbon
s	standard deviation
CI	Confidence interval

INTRODUCTION

Iron

Iron is the fourth most abundant element on the earth's crust (4.7wt%) and is even more prevalent in its core (90wt%) (Hollemann, Wiberg, 1985). Consistently it is essential for all life processes. Nevertheless it is vanishingly rare in the today's oceans and limits primary production across large areas. The reason for this paradox lies in the chemistry of iron and in the Earth's history.

Because of its high binding energy per nucleon Fe is the heaviest element which can be formed by exothermic nuclear fusion. It is therefore the final product of this process in stars and a relatively abundant element in rocky planets. Oxygen, silicon, carbon, magnesium and sulfur are very prevalent also but have a lower density than iron and formed the earth's crust and atmosphere mainly as silicates and CO_2 (Turner and Hunter, 2001).

Under the reductive conditions of the primordial atmosphere iron appeared mainly as Fe II in FeS_2, $FeSiO_3$, FeO, $FeCO_3$. (Kendall et al., 2012)

At the time when life developed (~3.8 Ga before present) Fe was readily soluble in the mildly reducing Archean ocean, as there was no free O_2. The availability in high concentrations and the two oxidation states (Fe(II), Fe(III)) differing by only one electron and relatively close in terms of free energy, made it particularly well suited for the function of transfer, transport and storage of energy (Turner and Hunter, 2001). The parallel high availability of sulfide in ancient oceans lead to the formation Fe-S clusters and redox systems as cofactors in many enzymes of essential biological functions.

After the evolution of oxygenic photosynthesis O_2 was generated and CO_2 was consumed. For about 1 Ga the O_2 in the ocean was reduced by organic compounds, SH_2 and in particular the available Fe(II) which lead to the deposit of the banded iron formations. About 2 Ga ago most of the oxygen sinks were saturated and could not capture the oxygen produced by

cyanobacteria anymore. O_2 levels in the oceans and in the atmosphere rose and stabilized at the current level of about 21%. The ubiquitous O_2 leads to oxidative weathering of iron containing rocks and surface waters transferring the readily soluble Fe(II) into sparingly soluble Fe(III). Only at anoxic conditions in ground waters and marine sediments Fe(II) can exist in higher concentrations (Turner and Hunter, 2001).

Speciation of iron

Redox reactions, inorganic and organic complexation, adsorption and precipitation control the concentration of iron in natural waters. Oxidative weathering of silicate rocks leads to river input of Fe(III) from the weathering products although most of it is immediately immobilized as iron oxides. A fraction of the iron load in rivers is colloidal or suspended. During estuarine mixing the particulate and dissolved inorganic and organic colloids flocculate due to the major change of pH and ionic strength (Krachler et al., 2005, Kendall et al., 2012)

Dissolved iron can exist in seawater in two oxidation states, Fe(II) and Fe(III), free or complexed with inorganic and organic ligands. The formation of organic complexes is important at a pH near 8. Liu and Millero, have determined the solubility of Fe(III) in NaCl solutions as a function of pH, temperature and ionic strength. These results clearly show that the solubility in seawater (0.2 to 0.3 nM) is much higher than in NaCl solutions (0.010 nM) at the same pH, temperature and ionic strength (Liu and Millero, 1999).

$[Fe(III)\ (H2O)_6]^{3+}$ is hydrolysed by OH^- to $Fe(OH)_3$ which is subsequently aged by dehydration and crystallization to FeOOH, $5Fe_2O_3.9H_2O$ and finally Fe_2O_3 with decreasing solubility (Kendall et al., 2012), (Turner and Hunter, 2001). The dissolved inorganic species of Fe(III) in seawater are predominantly the hydrolysis products $Fe(OH)_2^+$, $Fe(OH)_3^0$ and $Fe(OH)_4^-$ (Kuma 1996).

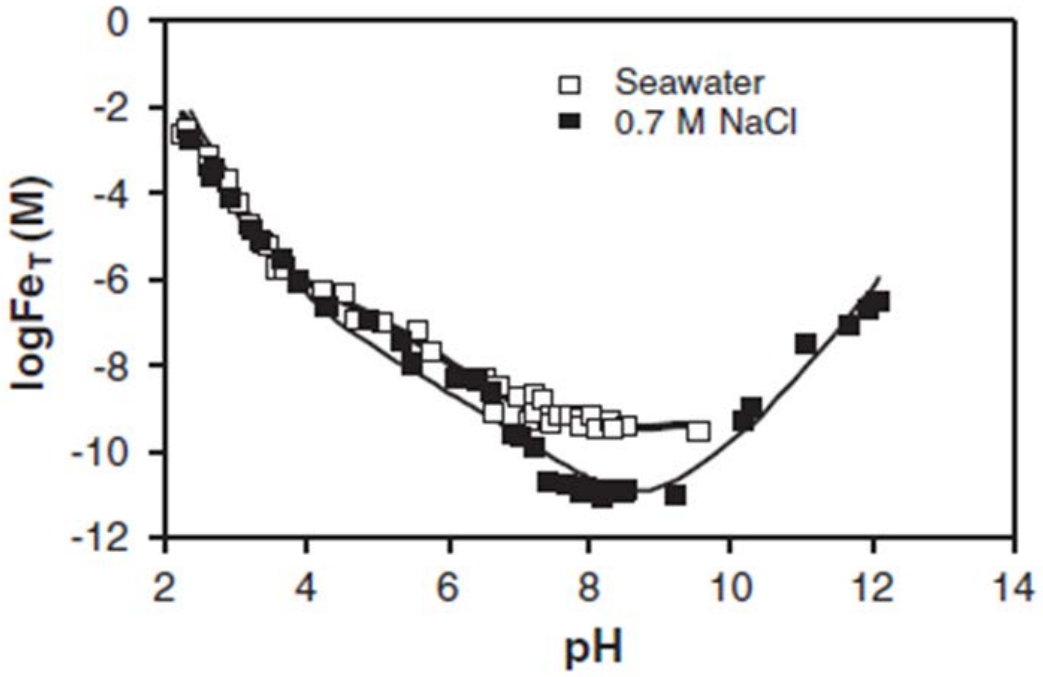

Figure 1: A comparison of the solubility of Fe(III) (M) as a function of pH in seawater and 0.7 m NaCl (Liu and Millero, 1999) at 25 °C

The higher solubility of Fe(III) in seawater compared to NaCl at the same ionic strength is due to the formation of complexes of Fe^{3+} with organic ligands (Liu and Millero, 1999).

The biogeochemical significance of iron

Iron is essential to most organisms. It is generally found in the center of metalloproteins that mediate redox reactions. Some of these proteins serve as enzymes that facilitate the transfer of electrons used to generate chemical energy for the cell. Some major Fe containing enzymes include hydrogenases, iron-sulfur proteins and cytochromes. Ferredoxin is one of the most common ones and contains Fe_2S_2. Ferredoxins catalyze electron transfer reactions of photosynthesis and phosphorylation and therefore are necessary for most primary production. Nitrogenase catalyzes the breaking of the triple bonds between each nitrogen atom in nitrogen fixing organisms (Kendall et al., 2012).

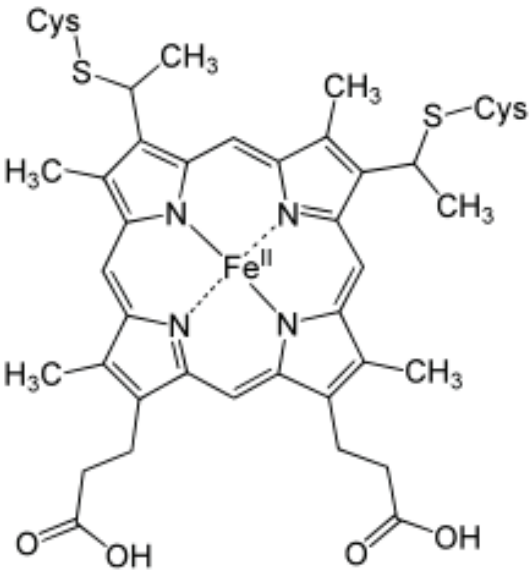

Figure 2: Hem c, drawing by Yikrazool

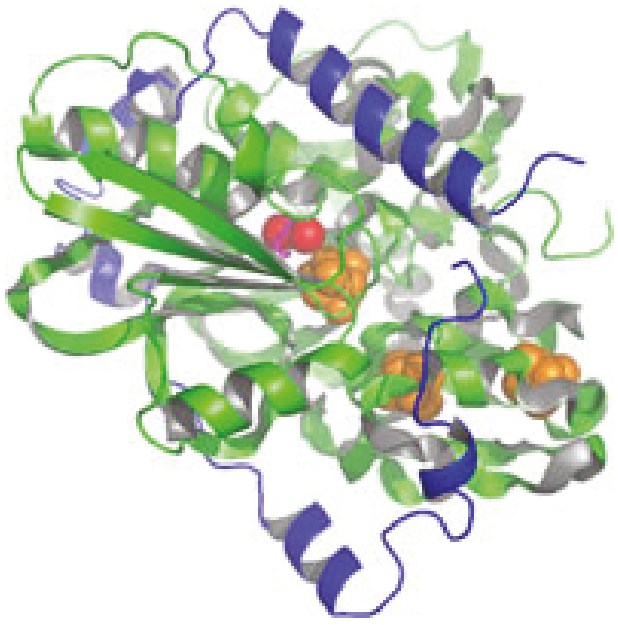

Figure 3: 3D structure of Hydrogenase (http://www.bbsrc.ac.uk)

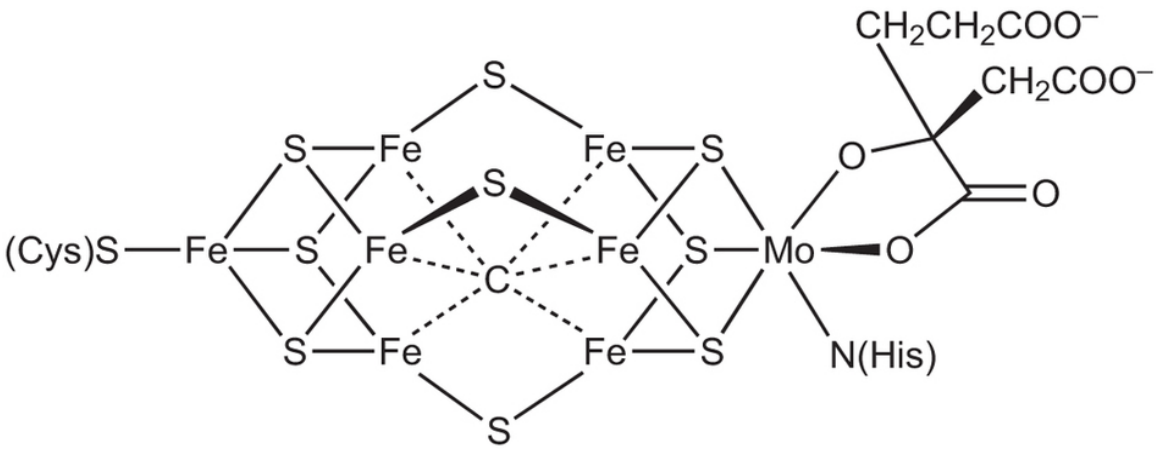

Figure 4: Nitrogenase, FeMo Co factor (Nature Chemistry 5, 559–565 (2013)

HNLC regions, High nutrient low chlorophyll regions of the oceans have high average concentration of the macro nutrients nitrate and phosphate and silicate (figures 5 to 7). In spite of this the chlorophyll annual average is only modest (under 0.5 mg/m^3). These regions are the subarctic Pacific, the equatorial Pacific and the Southern Ocean.

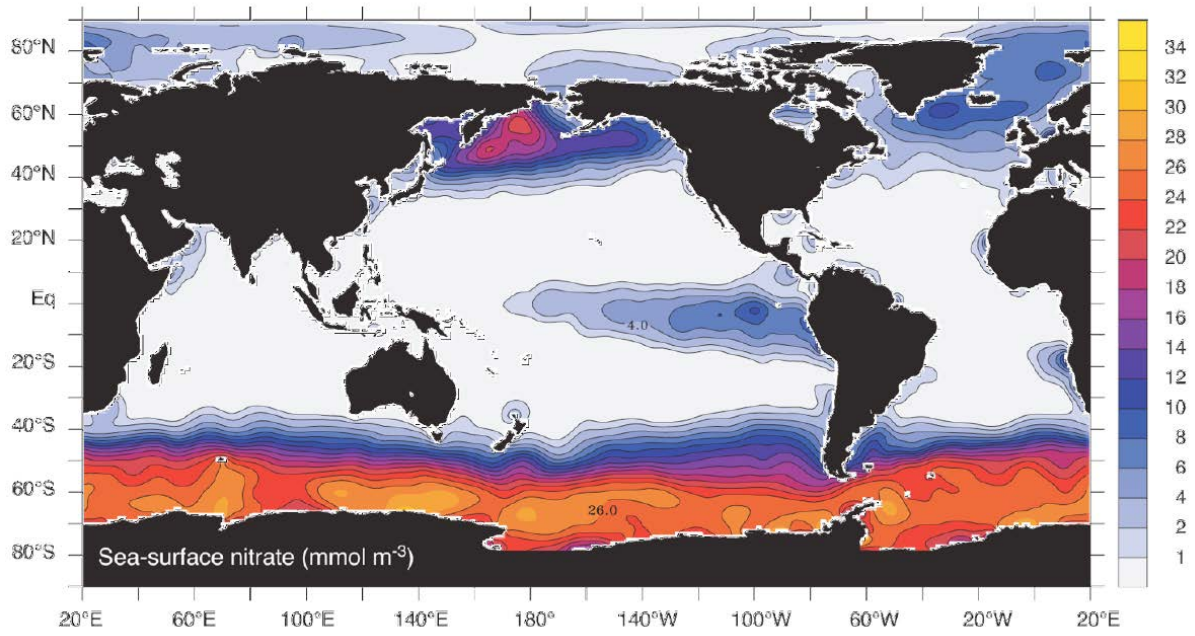

Figure 5: Sea-surface nitrate [mmol/m^3],
from Ocean Biogeochemical Dynamics, Ed: Jorge L. Sarmiento & Nicolas Gruber, Princeton University Press 2006, edited by Thomas Reinthaler

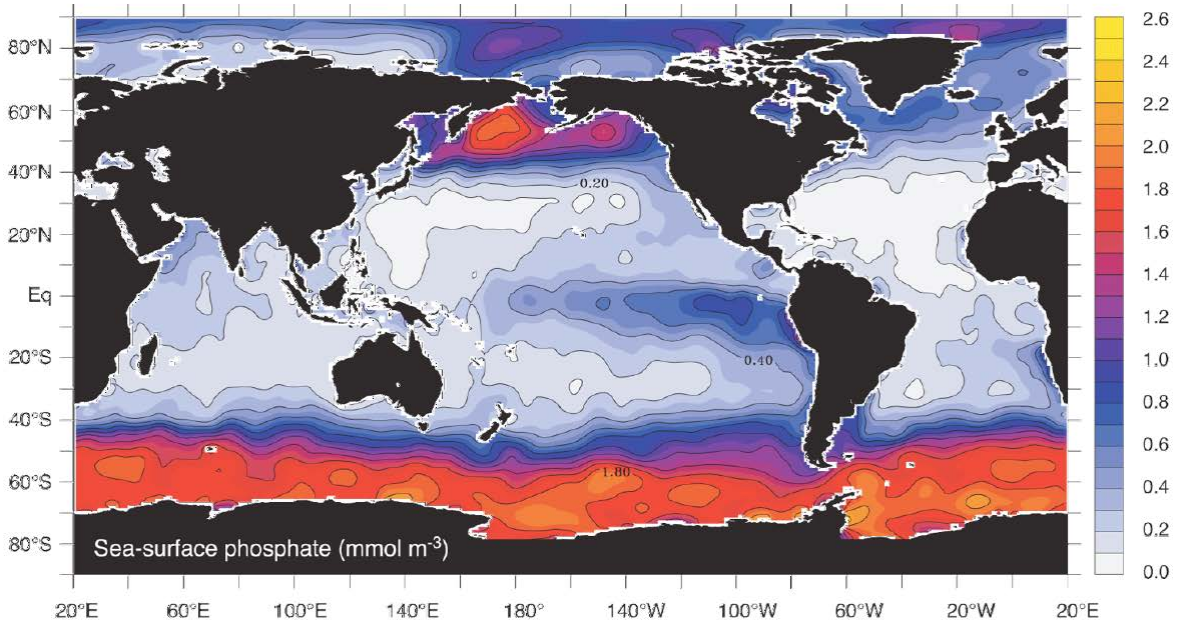

Figure 6: Sea-surface phosphate [mmol/m^3]
from Ocean Biogeochemical Dynamics, Ed: Jorge L. Sarmiento & Nicolas Gruber, Princeton University Press 2006, edited by Thomas Reinthaler

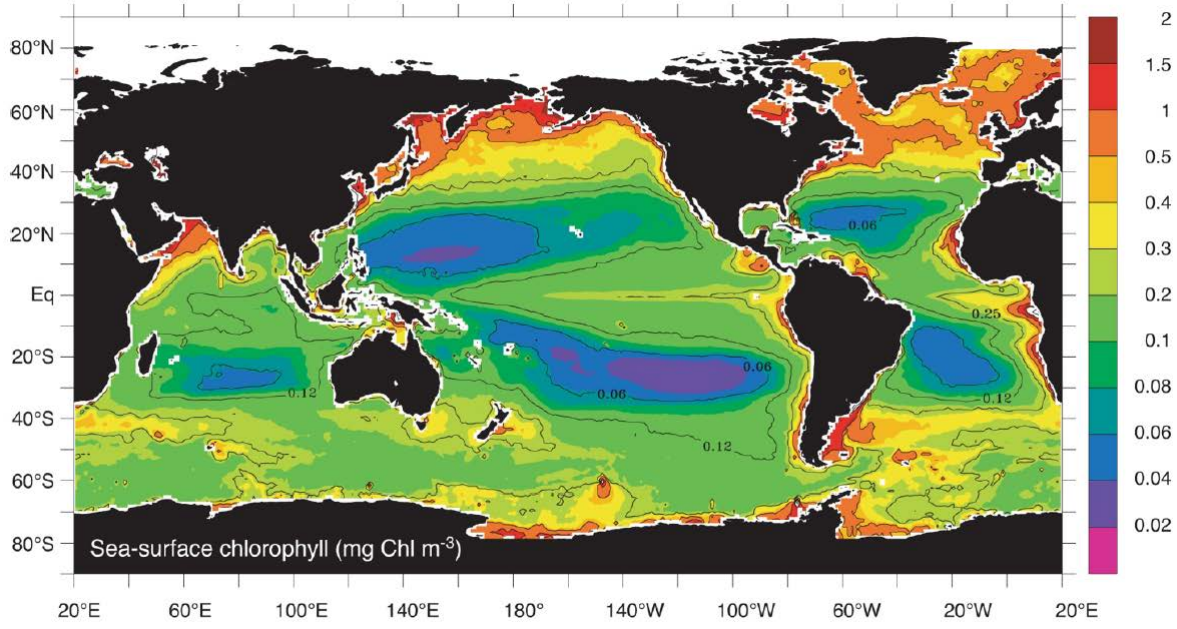

Figure 7: Sea-surface phosphate [mmol/m^3],
from Ocean Biogeochemical Dynamics, Ed: Jorge L. Sarmiento & Nicolas Gruber, Princeton University Press 2006, edited by Thomas Reinthaler

There are some regions with high productivity in the Antarctic, but they are all on the eastside and close to land. The circumpolar current flows to the east and provides these areas with dust, river discharge and ice melt. As the Redfield ratios C:N:P = 106:16:1 are reasonably constant, the rate of primary production depends on the amount of nitrate and phosphate provided by upwelling water in most regions of the ocean especially the subtropical gyres. In contrast to that in the HNLC regions nitrate and phosphate are not limiting new production. They are all sites where the general circulation of the ocean induces large scale upwelling of deep waters to the surface (Turner and Hunter, 2001). Martin and Fitzwater first demonstrated that iron is the limiting factor in these ecosystems (Martin and Fitzwater, 1988). Their results were proved by several iron fertilization experiments (Figure 8).

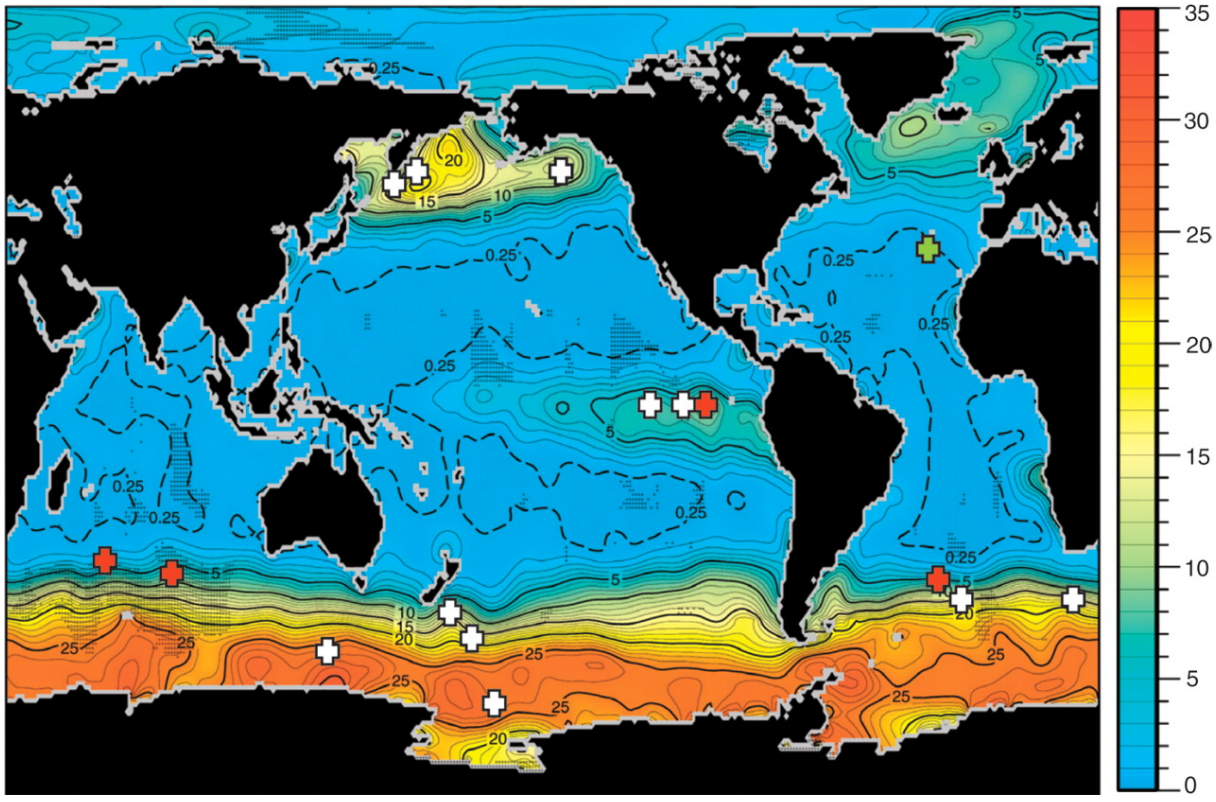

Figure 8: Annual surface mixed-layer nitrate concentrations in units of μmol liter−1 , with approximate site locations of FeAXs (white crosses), FeNXs (red crosses), and a joint Fe and P enrichment study of the subtropical LNLC Atlantic Ocean (FeeP; green cross).

FeAXs shown are SEEDS I and II (northwest Pacific; same site but symbols are offset), SERIES (northeast Pacific), IronEX I and II (equatorial Pacific; IronEX II is to the left), EisenEx and EIFEX (Atlantic polar waters; EIFEX is directly south of Africa), SOIREE (polar waters south of Australia), SOFEX-S (polar waters south of New Zealand), SOFEX-N (subpolar waters south of New Zealand), and SAGE (subpolar waters nearest to New Zealand). FeNX sites shown are the Galapagos Plume (equatorial Pacific), Antarctic Polar Front (polar Atlantic waters), and the Crozet and Kerguelen plateaus (Indian sector of Southern Ocean; Crozet is to the left of Kerguelen) (Boyd, Philip W., et al., 2007).

Of particular interest are the results of the European Iron Fertilization Experiment (EIFEX) which was carried out in 2004 in an eddy of the circumpolar current at the Antarctic polar front. A large diatom bloom peaked in the fourth week after fertilization and was followed by a mass mortality. This caused a drawdown of carbon of approximately 50% of the biomass produced in the bloom (Smetacek, 2012).

Usualy the drawdown of particulate carbon from the euphotic zone to the mesopelagic zone is just 20%. In depths between 100 and 1000 m most of the carbon gets remineralized and stays dissolved as CO_2 (Krachler et al., 2010). Together with the solubility pump, this biological carbon pump removes a huge amount of CO_2 from the atmosphere for decades to centuries (Falkowski, Barber et al. 1998). The efficiency of the biological pump is highly dependent on the bioavailability of nutrients in the surface waters, especially iron in the HNLC regions (Martin and Fitzwater, 1988).

Eolian dust deposition after erosion from arid regions is suggested to be the main source of iron in the open ocean (Raven et Falkowski, 1999). Other sources are coastal sediments, aerosols, upwelling and ice melt (Cassar 2007). River discharge and ground water are considered to bet important sources for iron in coastal regions, but the importance for the open ocean is still under investigation. As mentioned before most of the iron is removed in mixing zones as solubility decreases with increasing salinity and pH. Therefore it was considered for a long time, that this largely colloidal iron is

effectively removed in estuaries by flocculation or precipitation as Hydroxide (Krachler et al., 2010). As the pH rises above 8 in the open ocean, the solubility further decreases (Byrne und Kester 1976). Only underneath the photic zone the pH decreases to 7.7 and iron concentrations slightly rise again (Kuma et al, 1996).

But meanwhile it was shown that iron in seawater can be complexed by organic ligands and these complexes are stable and able to escape the mixing zone and make a contribution to the bioavailable iron in open ocean water (Gledhill and van den Berg, 1994; Kuma et al., 1996; Rose et al. 2003, Krachler et al., 2010). UV irradiation experiments of coastal and open ocean water showed that the ligands of the complexes were decomposed and iron solubility decreased especially in coastal waters. This indicates the importance of ligands of riverine origin (Kuma et al., 1996).

But the stability and solubility of these complexes strongly depend on the nature of the ligands (Riedl, 1994). The iron transport capacities of river waters differ greatly. A mountainous river in the Austrian Alps would add only about 5% of its dissolved Fe load to coastal waters. A small tributary draining a sphagnum peat-bog, which acts as a source of humic substances to the river water, would add approximately 20% of its original Fe load to the ocean's bio-available iron pool (Krachleret al., 2005).

Examination of the kinetics of complexation of iron by terrigenous NOM show, that the complex formation constants are comparable to those of strong iron binding ligands like siderophores. Therefore these complexes will have a strong effect on the iron solubility in coastal waters (Rose et. al., 2003). Measurements with cathodic stripping voltammetry proved the existence of humic substance iron complexes in the open ocean (Laglera and van den Berg, 2009). Thus humic substances may contribute to the iron fertilization of the ocean and furthermore through the biological carbon pump make a contribution to the removal of Carbon from the atmosphere (Plessl 2012).

Humic Substances

Humic substances (HS) are ubiquitous components of the natural organic matter derived from plant decomposition. They are present in soil and aquatic environments and consist predominantly of polyphenols and benzoic/carboxylic acids. HS are operationally divided into humic acids (HA) and fulvic acids (FA) on the basis of their solubility, as HA precipitate at pH 1, while FA are soluble. (Laglera, van den Berg 2009). Humins are not soluble in aquatic solutions of any pH (IHSS 2007). HA have a molecular weight between 2000 and 5000 Da, whereas FAs have a molecular weight between 500 and 2000 Da. Aquatic fulvic acids are a major fraction of DOM in natural waters and account for 50–80% of the total amount of dissolved organic carbon (Krachler et al., 2005).

Humic substances consist of chemically variable and functionally heterogeneous polymers. The most important functional groups are Carboxyl, Carbonyl, Amino, Imino, Hydroxy- und Sulfhydryl groups (Bliefert 2002). There are different pathways suggested for the origin of HS. One of the versions considers the HS as modified lignins. In this case the degradation of the cormophytal material by microorganisms is carried out only incompletely and results in the formation of o-Hydroxyphenols and the oxidation of aliphatic side chains to carboxylic acids (Stevenson 1994). A second pathway suggested by Stevenson describes the complete decomposition of lignin or other carbon sources like celluloses and subsequently polymerization to polyphenols by random reactions. Another pathway is a kind of Maillard reaction, a condensation of amino acids or peptides with reducing sugars, both species released by biota in the course of degradation processes (Stevenson 1994, Ziechmann 1996). In addition different environmental conditions seem to favor different pathways. In peat bogs the pathway deriving from lignin seems to be of greater significance, whereas in deciduous forests the poly phenols from the degradation of leaves have a key role, and in areas with highly continental climate the sugar-amino acid condensation prevails. The content of humic substances in the soil strongly depends on its nature. Arable soils contain

about 1-2%, black soils 2-8% and pastures 10%, while the portion in boggy soils can be up to 20% (Bliefert 2002).

As a consequence of all this no uniform structural formulas for HS are known. Even if one distinct formula was known, the next molecule might look completely different (Ziechmann 1996). But to investigate HS with the same properties and origin and to characterize them is of scientific value.

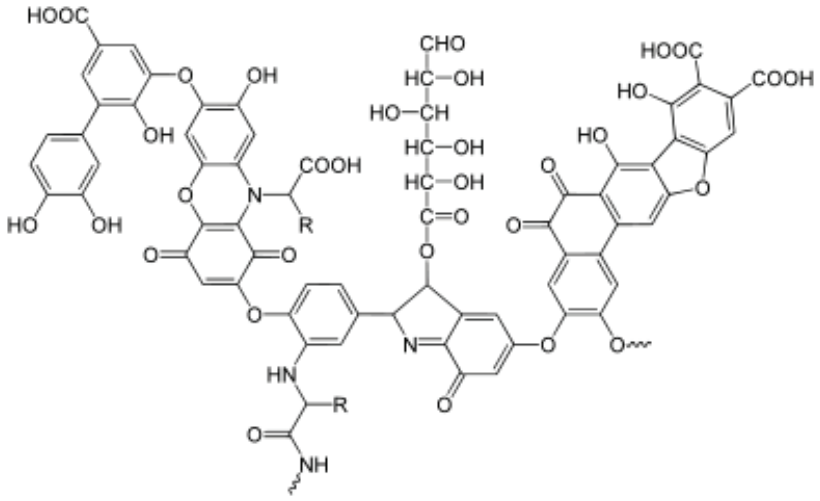

Figure 9: structure proposed for humic substance, drawing by Yikrazuul

Of particular interest are HS from peat bogs. They content a lot of iron. Peat bogs are ecosystems with a peat forming flora and a peat layer of at least 30 cm height (Colditz 1994). Bogs are wet habitats that occur mainly on an impermeable pad in valleys or on slopes. Accordingly, the soils are low in air and oxygen. Sphagnum mosses emit hydrogen ions into the environment when they take up nutrients. In this way they create an acidic environment that impedes the growth of competitors. Even their own lower parts die and create the peat. Peat mosses grow very slowly. The annual growth in Central Europe is 0.5 to 1.5 mm.

Once the contact with the groundwater is lost, the only source of water is the rain. But sphagnum mosses have the ability to store water up to 25 times of their own weight. In addition to the mosses, there are a number of other plants, specialized on survival in the bog like the downy birch (*betula*

pubescens), the mountain pine (*pinus mugo*), sundew (*drosera rotundifolia*) and some representatives of the family of heather plants (*ericaceae*). In peat lands dead plant material is not completely degraded but is subject to incomplete humification. This partly degraded organic material builds up the peat together with the sphagnum mosses (Colditz 1994). Moreover it leads to the high content of HS and DOM in the run off streams (black water). In addition the HS are strong chelate ligands which enhance the weathering rates of iron-silicate minerals and greatly increase the solubility of the essential trace metal iron in river water. (Krachler et al., 2010)

River catchments with high proportions of peat land have been found to be linked to enhanced peat-derived DOM concentrations. (Aitkenhead et al., 1999, Elder et al., 2000). This suggests that the iron transport capacity of a river is closely related to the vegetation types in its watershed, as soils are the source of both, dissolved iron as well as dissolved organic matter to the river water (Krachler et. al. 2005).

Figure 10 : Spagnum mosses at Tannermoor, Austria

Siderophores

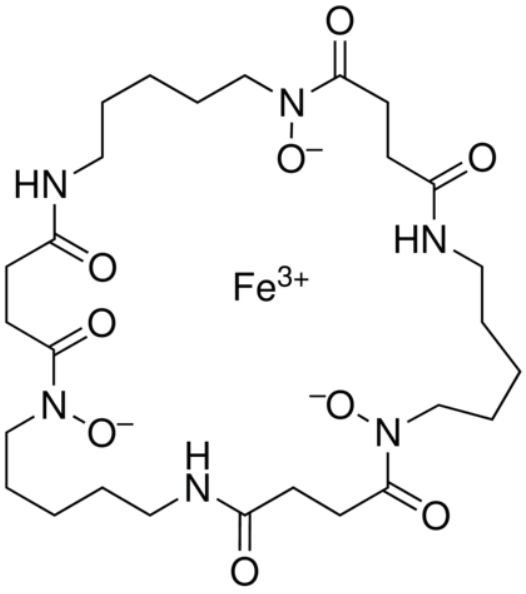

Figure 11: Ferrioxamine E,
picture by Sigma Aldrich

Other types of natural organic ligands that are capable of forming strong iron chelate complexes are siderophores. They are important in iron acquisition for diverse organisms even in the dilute nature of the pelagic marine environment. But only a small number of marine photosynthetic organisms produce their own siderophores. Most chelators structurally characterized carry hydroxamate and/or catecholate functional groups (Hopkins and Morel, 2009).

Heterotrophic marine bacteria often produce siderophores when attached to particles such as marine snow, phytoplankton, or zooplankton. Under these conditions loss to diffusion is reduced in part due to the amphiphilic character of most marine siderophores. This distinctive characteristic of marine siderophores is the frequent presence of a hydrophobic fatty acid tail imparting the amphiphilic character to the compound (Martinez et al. 2003). These siderophores seem to be produced as a response to iron addition in contrast to those of coastal microorganisms or graminaceous plants, which produce siderophores only in iron deficiency. This response may be an adaption to the surface ocean where newly available iron is rapidly lost by

precipitation and settling to deep seawaters if not complexed by dissolved chelators.

However marine cyanobacteria and eukaryotic marine phytoplankton seem not to be able to produce siderophores themselves. But they seem to be capable of accessing siderophore bound iron (Hopkins and Morel, 2009). Mawji et alt. detected specific siderophores in the open ocean of the Atlantic. The trihydroxamate siderophores ferrioxamine E and G, both produced by heterotrophic bacteria, were found at concentrations up to 10 pM each binding as much as 5% of the total dissolved iron in surface waters. (Mawji et al. 2008, Hopkins and Morel, 2009).

Objective

The objective of this master thesis was to get some insight into the role of humic substances obtained from wetlands in the iron-binding under the dilute conditions of the open ocean. Although structure and chemical properties of fulvic acids have been studied extensively, little is known about their functioning as transport vehicles for essential trace metals in the continental runoff (Krachler 2005). As Seawater contains a complex mix of siderophores, organic exudates and autochthonous humic materials which combine to stabilize dissolved iron (Hopkins and Morel, 2009), I used artificial seawater made of ultrapure chemicals to see the influence of land-derived humic substances alone.

In order to be able to assess the results we also studied the behavior of Ferrioxamine E as a standard siderophore produced by marine bacteria. Siderophores act as specific ligands for Fe(III) with extremely high iron-binding ability. Therefore I tried to get information about the conditional complex stability constants of both species. This can lead to conclusions about the proportion of dissolved iron associated to HS of terrestrial origin.

Starting from the radiotracer experiments of Krachler et al. (Krachler et al., 2005, Krachler et al., 2010), it was my task to develop a highly accurate method for the determination of conditional complex forming constants of iron chelate complexes with organic ligands in seawater. This method reflects the natural conditions closer than the method employed by Kuma et al. (Kuma et al. 1996) and by Liu and Millero (Liu, X. & Millero 1999, 2002).

MATERIALS AND METHODS

Sampling

Two freshwater samples from the north of Scotland and Upper Austria, two reference materials and a commercially available siderophore were studied The two freshwater samples were derived from surface waters which drain peat bogs and therefore are tea colored and contain a lot of humic substances. The sample from Scotland was taken from the "Craggie Burn" at N 58° 25.817 E 003° 54.317 at 88 m altitude on August 18th, 2011. The sample from Upper Austria was taken from the "Tannermoor" at N 48° 30.340' E 014° 51.731' at 921 m altitude on April 13th, 2013. Tannermoor, situated in the north eastern part of Upper Austria, Muehlviertel, is one of Austria's largest remnant peat-bogs covering an area of approximately 1 km^2. Tannermoor brook is draining the peat-bog and absolutely unpolluted (Krachler et al., 2005).

Water samples were collected from the surface using a HNO_3 cleaned polyethylene bottle that had been rinsed with Milli-Q water. The samples were immediately passed through a Sarbotan 300 Capsules (0,45 µm+0,2 µm PTFE membrane, Sartorius stedim) to remove particulate material, eukaryotes and bacteria. The samples were stored in 10L PP bottles, which had been cleaned with HNO3 and rinsed with Milli-Q water, at 4°C until further treatment.

The Reference Substances Suwannee River NOM (1R101N) and Nordic Reservoir NOM (1R108N) were purchased from the International Humic Substances Society (IHSS). The Suwannee River rises in the Okefenokee Swamp in South Georgia and flows southwest to the Gulf of Mexico. The Okefenokee Swamp contains extensive peat deposits. At the time of collection of the IHSS standard aquatic samples, the water level in the Okefenokee Swamp was regulated by a series of dams in a sill along the western edge of the swamp. The IHSS samples were collected at the southernmost dam on this sill. (N 30°48' W 082°25', 35 m sea level) (IHSS). The Nordic Reservoir NOM

sample was obtained from a drinking water reservoir at Vallsjøen, Skarnes, Norway from October 29th to November 3rd, 1997. The reservoir islocated at 225 m above sea level and has a maximum depth of about 14 m. The sample was obtained from the Sør-Odal County Waterworks intake pipe (N60° 15', E 011° 52') that draws water from at depth of 10m (pH = 5.6, EC = 2.1 mS/m and DOC = 10.7 mg/L). The water temperature was 4°C. The HS were isolated by reversed osmosis and are stored as desalted (H^+-saturated), freeze-dried solid powders (IHSS).

Chemicals

Ultrapure mineral acids were prepared in house (Muthgasse) by double sub boiling distillation of 65% nitric acid and sub boiling distillation of 37% hydrochloric acid of p.a. grade (Merck KGaA, Darmstadt) respectively, using a duo PUR quartz sub boiling unit (MLS Lab Systems GmbH, Leutkirch). Ultrapure Water was obtained sub boiling distillation of purified water (18.2 MΩcm) using an ultra-clear system (Sg water GmbH, Barsbüttel). Sodium hydroxide monohydrate (Suprapure, Merck) and purified water where used to prepare the 0.5 M NaOH solution. For preparation of the artificial seawater the following salts were used: NaCl: (Sigma Aldrich 38979, Trace select), Na_2SO_4:(Sigma Aldrich 204447, ≥ 99.99%), KCl: (Sigma Aldrich 05257, Trace select), $NaHCO_3$: (Sigma Aldrich 31437, p.a. >99.7%), KBr: (Sigma Aldrich 90737, Trace select), H_3BO_3 (Fluka 15660 p.a.; Sigma Aldrich 202878, 99.999%), NaF (Sigma Aldrich 450022, 99.99%), $MgCl_2.6H_2O$ (Alfa Aesar 10797, 99.999%; Sigma Aldrich 255777, 99.995%), $SrCl_2.6H_2O$ (Sigma Aldrich 204463, 99.995%), Na_2CO_3 (Fluka 71347, Trace select).

$CaCl_2.2H_2O$ was not available in the desired purity, therefore other hydrates were used: $CaCl_2.xH_2O$ (Alfa Aesar 10680, 99.9965%; $CaCl_2$ anhydrous: Sigma Aldrich 499609, 99.99%). When none of the pure chemicals was available $CaCl_2.2H_2O$ (Sigma Aldrich 21100, p.a.) was used to prepare the artificial seawater. Ferrioxamine E (from *Streptomyces antibioticus,* Fluka 38266, ≥95%) was used to prepare the siderophore solutions.

50 ml PE tubes (VWR), 15 ml PE tubes, setra cups, 2l PE Bottles and pipette tips were cleaned in the ISO 6 (EN ISO 14644) cleanroom in a nitric acid bath (10% W/W nitric acid p.a. in deionized water) for 24 hours and in a 1% nitric acid bath (1% w/w nitric acid, sub boiled in purified water) for another 24 hours. Afterwards there where rinsed with purified water, dried under laminar flow and stored in PE bags until further use.

Artificial seawater and salting out

For the salting out of the samples and for the solubility experiments artificial seawater was used, which contained the major components of sea salt as proposed by Kester et al. (Kester et al. 1967).

The seawater was prepared in a cleanroom (EN ISO 14644: ISO 8, Laminar flow) by weighing the NaCl, Na_2SO4, KCl, KBr, H_3BO_3, $SrCl_2{\cdot}6H_2O$, NaF in acid rinsed setra cups and rinsing them into an acid rinsed 2 L PE bottle with HQ water. $MgCl_2{\cdot}6H2O$ in the required purity is extremely hygroscopic and has to be weight very fast.

Table 1: Salts composition as proposed by Kester et al. (1967)

Salt	Mass (g/L)
NaCl	23.926
$MgCl_2{\cdot}6H_2O$	10.831
$CaCl_2{\cdot}2H_2O$	1.518
Na_2SO_4	4.008
KCl	0.667
$NaHCO_3$	0.196
KBr	0.098
H_3BO_3	0.026
$SrCl_2{\cdot}6H_2O$	0.024
NaF	0.003

$CaCl_2 \cdot 2H_2O$ was not available in the required purity and was replaced by other chemicals like $CaCl_2.xH_2$ O and anhydrous $CaCl_2$ and finally by $CaCl_2 \cdot 2H_2O$ of p.a. grade. Then the bottle was filled with purified water to obtain approximately 1900 g seawater and stirred until all the salts were completely dissolved. Then the $NaHCO_3$ was weighed and rinsed into the seawater to prevent the precipitation of carbonate. Subsequently the pH was measured using a PHM92 pH-Meter Radiometer Copenhagen) with a mikro electrode (inLab Micro, Mettler Toledo). A Na_2CO_3 (0.2g in 80ml H_2O) solution in purified water was added dropwise (again to prevent the precipitation of carbonate) until the pH was 8.20. Afterwards purified water was added until the weight of 2046.6 g, according to the average density of seawater.

To obtain more sample material of the humic substances each one liter of the water sample was concentrated in a rotary evaporator (Rotavapor R-210, Büchi) to approximately 100ml. To simulate the conditions of the estuarine mixing zone 100ml of the artificial seawater was added. The mixture was shaken well and stored at 8° C for 72 hours to obtain a constant DOC and iron concentration (Plessl 2012).

Approximately 20 mg of the reference substances were dissolved in 5ml seawater and shaken until no further humic substances was dissolved. To separate the soluble humic substances from the insoluble ones the mixtures were filtered with syringe filters (Acrodisc 25 mm, 0.2 µm GHP membrane, PALL).

SEC Chromatography

The concentrated and filtered mixtures of humic substances were separated according to their size via size exclusion chromatography (SEC) as described by C. Plessl (Plessl 2012) and Kittinger (Kittinger 2010). Two SR 25/100 chromatography columns (GE Healthcare) where filled with Sephadex LH 20 purchased from GE healthcare as stationary phase. Sephadex LH-20 is made from hydroxypropylated dextran beads that have been cross linked to yield a polysaccharide network, with an exclusion size of 4000 to 5000 Dalton. The

particle size of the dry beads is 18-111 µm. (GE Healthcare 2006). Both columns combined added up to a 158 cm bed with a diameter of 2.5 cm. The columns were connected with a liquid chromatography device (ÄKTApurifier 10, GE Healthcare). The mobile phase was H_2O (A) with 4.5 % Methanol (B). Flow rate was 0.1 ml/min. The samples were injected by filling a 2ml sample loop manually with a syringe and switching the injection valve automatically. Detection was carried out at 254 nm by the UV detector UV 900 (GE Healthcare). Fractions were collected with the automatic fraction collector FRAC900. By this means it is possible to collect the fractions over the time of one week, which is the total runtime of the SEC chromatography under the described conditions. The fractions containing humic substances (Peak 0, Peak 1 and Peak 2) were dried in a concentrator (Savant ISS 110 SpeedVac Concentrator, Thermo Scientific) at low concentration speed and stored at 4 - 8°C until further use.

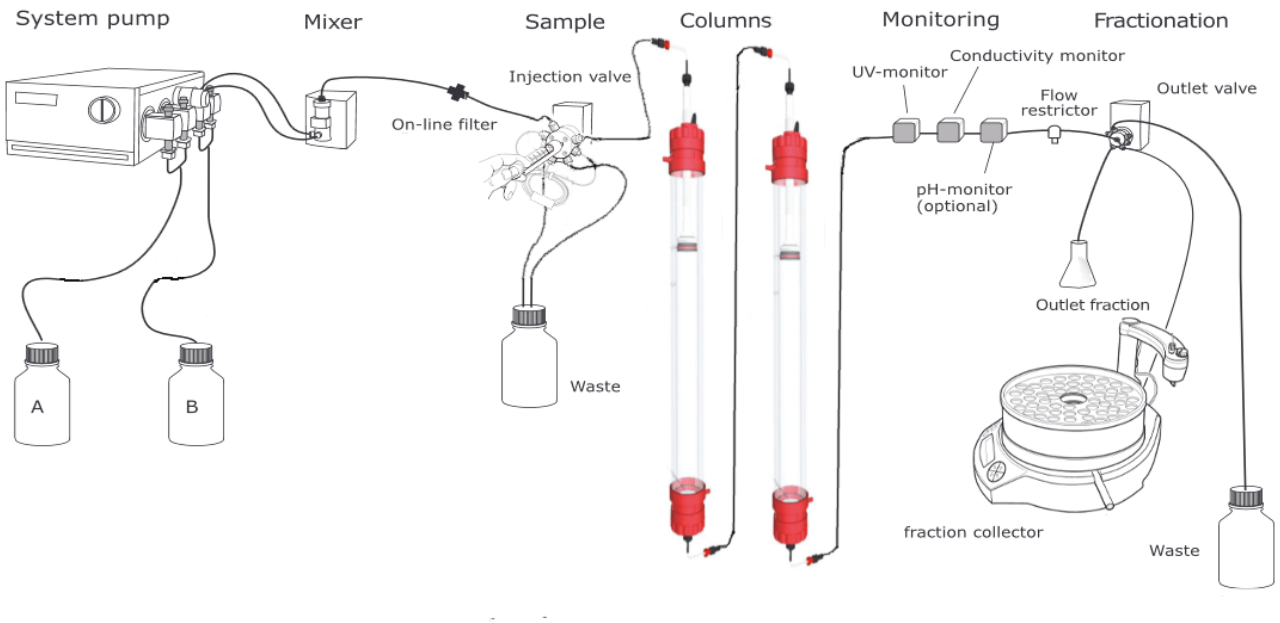

Figure 12: ÄKTApurifier 10, modified from Äktapurifier user guide, GE Healthcare

Sample preparation

The dried humic substance fractions were dissolved in 5 ml artificial seawater. DOC concentrations were measured with a TOC-VCPH total organic carbon analyzer by Shimadzu. DOC was measured as NPDOC—non purge able dissolved organic carbon, bringing the samples to pH≈2 with HCl (p.a. by Fluka) and sparging them with carrier gas for 5 min. prior to combustion.

Initial iron concentrations in the concentrated sample solutions were determined by flame atomic absorption spectrometry (flame AAS). Because of the inevitable matrix effect of seawater the method of standard addition was applied.

The device used was the AAnalyst 200 from Perkin Elmer. In flame AAS, the sample is aspirated and transformed into an aerosol by means of a concentric nebulizer. In the spray chamber it is mixed with fuel gas (acetylene) and oxidant (compressed air) and passes collision surfaces thus only the finest drops can reach the flame. In the slot burner with a lateral length of 10 cm the mixture produces a flame with a maximum temperature of 2400°C. In the flame the desolvation, volatilization and dissociation produce atoms and ions (Skoog, Holler, Crouch, 2013).

The light sources of choice are element-specific hollow cathode lamps. The cathode of this lamp consists of the element to be analyzed and the anode consists of tungsten. The lamp is filled with neon or argon at a pressure of 130 to 650 Pa. When high voltage is applied the atoms of the cathode are sputtered and will glow discharge and emit the desired wavelength. On the basis of low pressure and low temperature in the lamp the bandwidth of the emitted radiation is about two orders of magnitude smaller than the bandwidth of absorption in the flame (Skoog, Holler, Crouch, 2013).

Based on the DOC values the dilution and amount of sample solution were calculated to produce the desired concentrations between 0,5 and 50 nM DOC according to the concentration ranges of terrigenous organic matter in the ocean by Hernes and Benner (Hernes and Benner 2006). The Iron

concentrations were chosen to provide a low excess of Iron, just enough to form a sediment, but no particles, that would sweep away the samples.

Each 50 ml PE tube was filled with the amount of artificial seawater needed to add up to 40 ml altogether with the other solutions. Then the required amount of HS solution in artificial seawater, the corresponding amount of $FeCl_3$ in 0.5 M HCl and the corresponding amount of 0.5 M NaOH to neutralize the HCl were added. Finally 10µl of ^{59}Fe radiotracer ($^{59}FeCl_3$ in 0.5 M HCl NEZ037 from Perkin-Elmer) with a half-life of 44.6 days was added in the radiochemistry laboratory. Additional Fe concentrations in all treatments due to the addition of the ^{59}Fe tracer were estimated to be less than 0.1% of the initial Fe concentration. Then the tubes were closed and sealed with parafilm and shaken (Vibramax 100, Heidolph) with 300rpm at room temperature or at 20 °C in the incubator for 7 days to allow precipitation and the radioactive equilibrium to establish. Subsequently, the tubes were centrifuged for 4 h at 4000 rpm in order to separate the "water column" from the solid phase. Immediately after the soft stop of the centrifuge a 5 mL "water column" sample from each tube was pipetted into a clean 20 ml PET vial of identical geometry for the gamma spectroscopy. The pH values in the tubes were measured afterwards with the pH meters Pro Lab 2000 and Pro Lab 860 using the same type of electrode: IL Micro pHT-A (all from SCHOTT Instruments).

Gamma spectroscopy

Carrier free radioactive ^{59}Fe was purchased from Perkin Elmer as $^{59}FeCl_3$ in 0.5 M HCl. The ß$^-$ decay of ^{59}Fe (half-life 44.5 d) is followed by emission of gamma rays (1099 keV: 56.59%, 1292 keV: 43.2%) as shown in the decay scheme (figure 13).

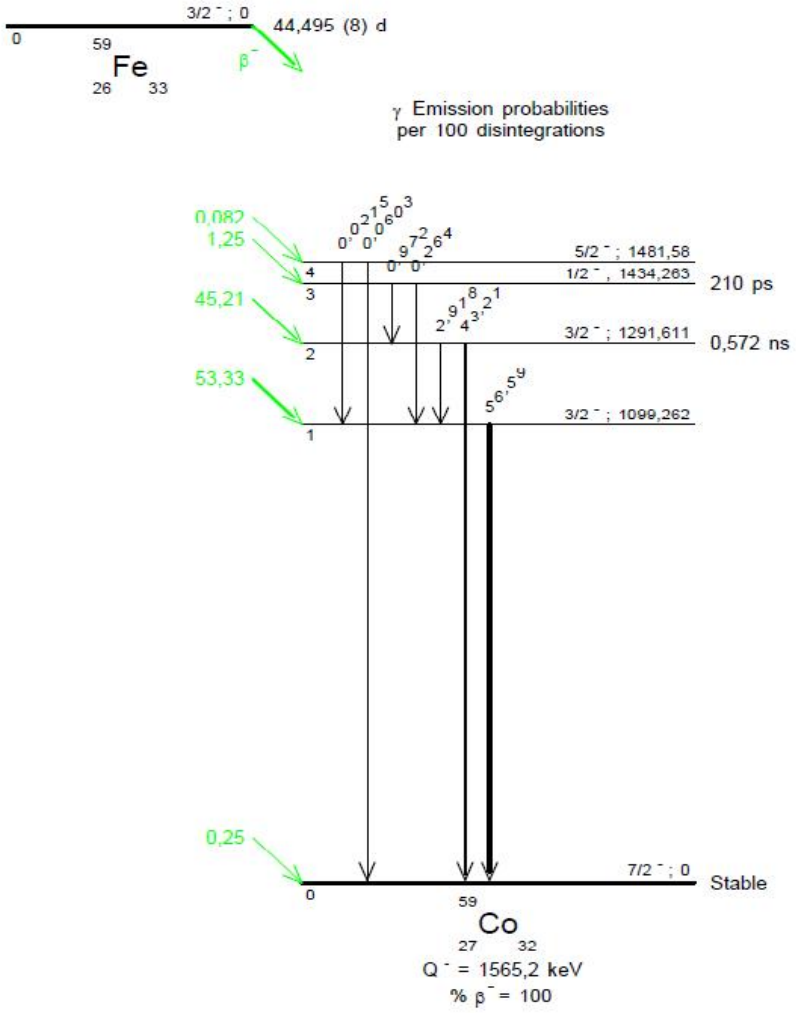

Figure 13: decay scheme of ^{59}Fe,
BIPM, Table de Radionucléides, 2004

The gamma rays of ^{59}Fe in the aliquot were counted using the Germanium high purity reversed electrode semiconductor detector Canberra GR2020. The

gamma rays interact with the Germanium by producing free electrons and holes that travel to the electrodes due to the applied voltage. The resulting current is proportional to the energy of the gamma quant and can be amplified and then analyzed by a multichannel analyzer. In the obtained spectrum of counts versus energy of the gamma quanta, the area under the peak is proportional to the activity of the sample. The volume of the germanium crystal is big enough to suppress the Compton scattering. Cooling of the crystal with liquid nitrogen to 77 K avoids thermal noise (Figure 14) (Hamidatou et al 2013).

For my experiments only the 1292 keV peak was evaluated. The efficiency of the detector was not determined, because only a relative count rate was needed to determine the iron concentrations in the vials. The reference solution was 10 µl tracer in 39.99 ml 0.5 M HCl. An aliquot of 5 ml in the 20 ml vial with the same geometry as the sample vials was measured to represent completely dissolved iron. The activity added to each sample and the reference solution was about 80000Bq until about 1000Bq. Each vial with aliquot was measured until 1000 counts were obtained. This results in an uncertainty of ±3%

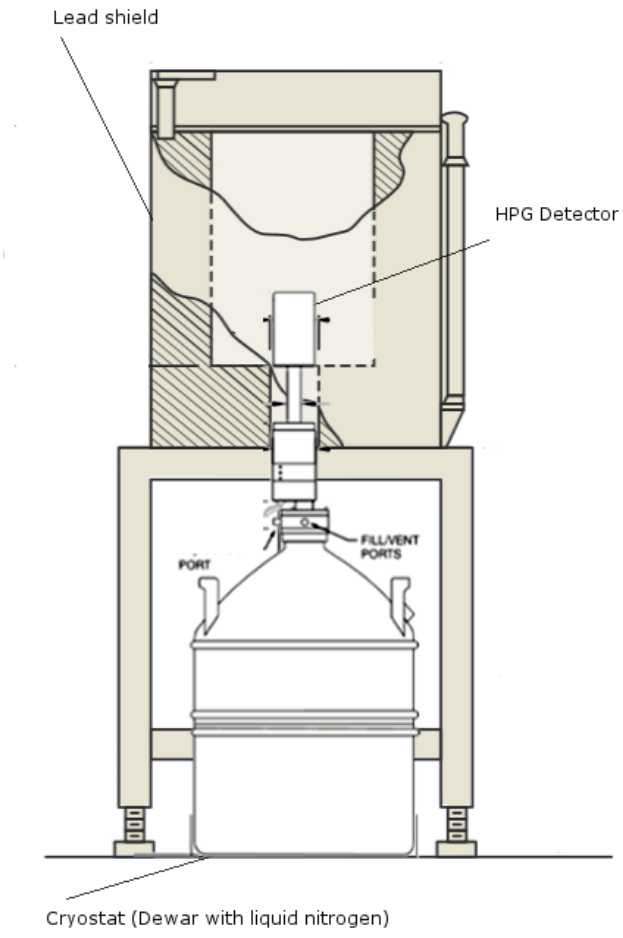

Figure 14: schematic diagram of the HP germanium detector, modified from www.canberra.com

Data Evaluation

The molecular weights of the peaks of the samples from Scotland and Georgia where determined by E. Neubauer with FlowFFF UV-Vis (E. Neubauer, Department of Environmental Geosciences, University of Vienna, 2013, personal communication)

With these values of the molecular weights (table 2) the molar concentrations of the HS could be calculated from the DOC values assuming that carbon is one half of the molecular weight. For the samples from Upper Austria and Sweden the molecular weights of the Scottish sample were used for the calculations.

The tables in the appendix show the results of the Gamma spectroscopy measurements, pH values and the iron concentrations of HS samples and the amount of iron added as $FeCl_3$. From table 14 the values for the iron concentrations of the HS solutions were calculated assuming saturation with iron and one humic substance molecule complexing one iron atom. The concentration of total dissolved iron $[Fe_T]$ in in the sample can be calculated based on the equation:

$$[Fe_T] = 25 \frac{cpm_{sample}}{cpm_{HCl}} Fe_S \qquad \text{Eq. (1)}$$

Where cpm are the counts per minute of the 5ml aliquots of the sample solution and the tracer in 0.5 M HCl respectively and Fe_S is the sum of iron from the HS and the iron added. With a linear relationship between the dissolved iron and the ligand concentration $[L_T]$ the following applies:

$$[Fe_T] = [Fe'] + A\,[L_T] \qquad \text{Eq. (2)}$$

Where $[Fe´]$ is the solubility of iron in pure seawater which is the sum of the concentration of all dissolved inorganic iron(III) species. A is the slope of the straight line and $[L_T]$ is the total ligand concentration as derived from the mass of HS added to 40 mL inorganic seawater and the molar mass of this HS fractions determined experimentally by FlowFFF.

According to Rue and Bruland (Rue and Bruland, 1995) the equation for the conditional complex formation constant can be derived from the following equations and assumptions:

For the Fe(III)-L complex, 1:1 stoichiometry is assumed and no correction for ionic strength have to be applied. This results in the following mass balance equations:

$$[Fe_T] = [Fe'] + [FeL] \qquad \text{Eq. (3)}$$

$$[L_T] = [L] + [FeL] \qquad \text{Eq. (4)}$$

[FeL] is the concentration of the undissociated Fe(III)-L complex. [L] denotes the free ligand concentration.

Furthermore it is assumed that the thermodynamic equilibrium of the dissolved inorganic iron (III) species with the solid iron oxid phases present in the sample has been established. The corresponding solubility product expression for Fe(OH)3) is:

$$K_{sp} = [Fe^{3+}]\,[OH^-]^3 \qquad \text{Eq. (5)}$$

According to equation (5), $[Fe^{3+}]$ is constant for given values of K_{sp} and $[OH^-]$, which implicates that [Fe'] is constant too.
The mass action law representing the equilibrium between [Fe'], [L] and [FeL] is:

$$K_{cond.} = \frac{[FeL]}{[Fe'][L]} \qquad \text{Eq. (6)}$$

Equation (6) defines the conditional stability constant $K_{cond.}$ as formulated by Rue and Bruland (Rue and Bruland, 1995).

[Fe'] can, in a first approximation be assumed to have the same value in all samples of a particular series of experiments.

$$[Fe'] = [Fe_T]_0 \qquad \text{Eq. (7)}$$

Where $[Fe_T]_0$ represents the total dissolved iron concentration in equilibrium with the solid iron oxide phase in inorganic seawater (HS concentration $[LT]_0$=0 mol/L).

Replacing [FeL] in equation (3) by an expression containing $[L_T]$ and K_{cond}. leads to the following equation:

$$[Fe_T] = [Fe'] + [L_T]\frac{[Fe'].K_{cond.}}{1+[Fe'].K_{cond.}} \qquad \text{Eq. (8)}$$

If the plot of measurable $[Fe_T]$ against given $[L_T]$ yields a straight line according to equation (8), the data can be interpreted as 1:1 complex between Fe(III) and ligands with closely similar $K_{cond.}$.

$K_{cond.}$ can be calculated from the slope A of the straight line by linear regression and [Fe´] corresponds to the axis intercept. If the axis intercept is negative or more than one order of magnitude smaller than [Fe´], than [Fe´] measured for the particular set of measurements yields the more accurate result.

$$K_{cond.} = \frac{A}{[Fe'](1-A)} \qquad \text{Eq. (9)}$$

Error calculation and error estimation

According to Skoog, Holler and Crouch (Skoog, Holler, Crouch, 2013).the variance of the calculated value $K_{cond.}$ can be expressed by the partial derivations of the equation (9) and the variances of [Fe´].

$$s^2_{\mathrm{K_{cond.}}} = \left(\frac{\partial K_{cond.}}{\partial A}\right)^2 s_A^2 + \left(\frac{\partial K_{cond.}}{\partial [Fe']}\right)^2 s^2_{[Fe']} \qquad \text{Eq. (10)}$$

This results in the following equation for the standard deviation:

$$s_{\mathrm{K_{cond.}}} = \sqrt{\left(\frac{1}{[Fe'](1-A)^2}\right)^2 s_A^2 + \left(\frac{A}{(1-A)[Fe']^2}\right)^2 s^2_{[Fe']}} \qquad \text{Eq. (11)}$$

A, $s_{A,}$ [Fe´] and $s_{[Fe´]}$ can be derived from the linear regression. If [Fe´] is the measured value for a particular set of measurements, then $s_{[Fe´]}$ is the standard deviation for these measurements, or has to be estimated, g.e. from the linear regression. The standard deviation of the gamma measurements has to be considered also. For the coefficient of variation equation (1) has to be derived by $cpm_{sample,}$ cpm_{HCL} and $Fe_{S.}$

$$\frac{s_{[Fe_T]}}{[Fe_T]} = \sqrt{\left(\frac{s_{cpm_{sample}}}{cpm_{sample}}\right)^2 + \left(\frac{s_{cpm_{HCl}}}{cpm_{HCl}}\right)^2 + \left(\frac{s_{Fe_S}}{Fe_S}\right)^2} \qquad \text{Eq. (12)}$$

The coefficients of variation for the gamma measurements are 3% and for the iron measurements by flame AAS is estimated to be 5%. The resulting coefficients of variation for [Fe'] would be at least 6,6%.

For the decadic logarithm of $K_{cond.}$ applies:

$$s = 0{,}434\ \frac{s_{K_{cond.}}}{K_{cond.}} \qquad \text{Eq. (13)}$$

Finally, the following applies for the confidence interval (CI) at a confidence level of 95%:

$$CI = \pm 1{,}96\ s \qquad \text{Eq. (14)}$$

RESULTS

Separation by SEC showed similar results for all samples. The chromatograms showed three peaks that were baseline separated. The following chromatograms (Fig. 15 to Fig 18) show typical separations of the different analytes. The other chromatograms, the fractions of which were used for further analysis are found in the appendix.

The three peaks were denoted Peak 0, Peak 1 and Peak 2. Peak 2 was not found or analyzed in previous studies (Plessl 2012). Plessl conducted SPE (solid phase extraction) prior to SEC. When he conducted SEC without SPE he found three peaks, from this fact he concluded, that the third peak was a fraction that could not be eluted from the SPE column.

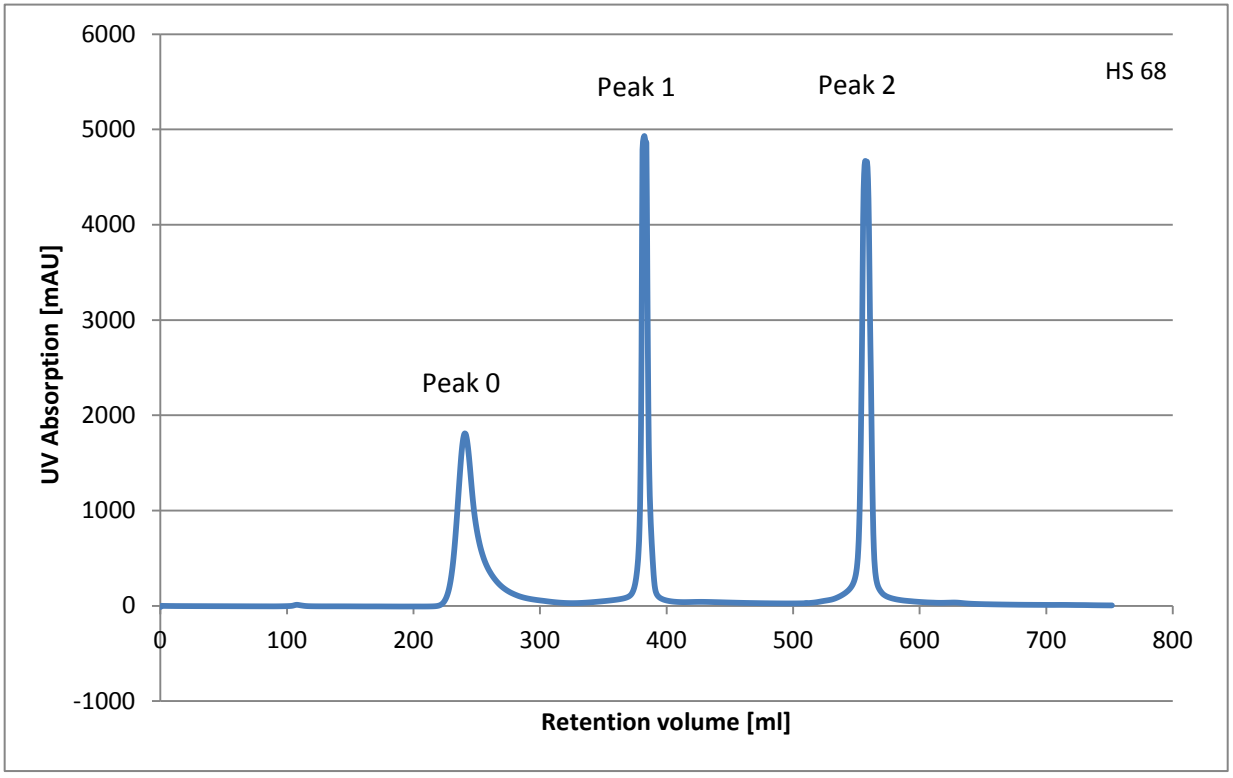

Figure 15: HS 68 Craggie burn, UV Absortion

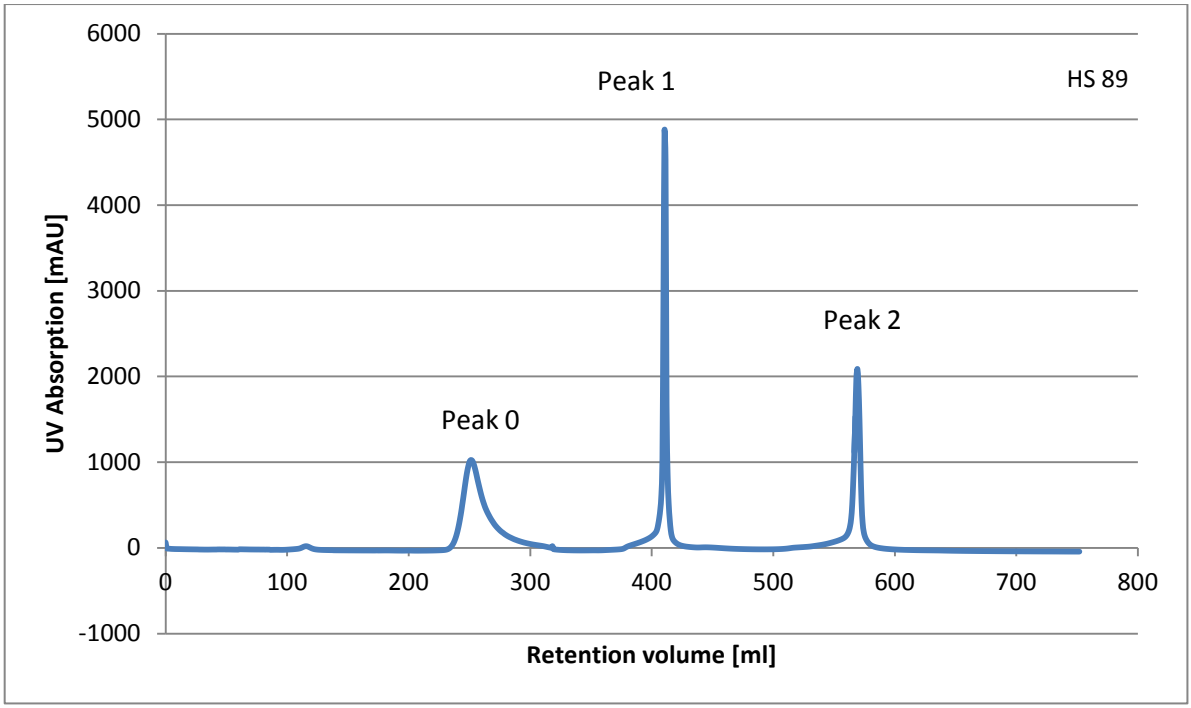

Figure 16 HS 89 Tannermoor

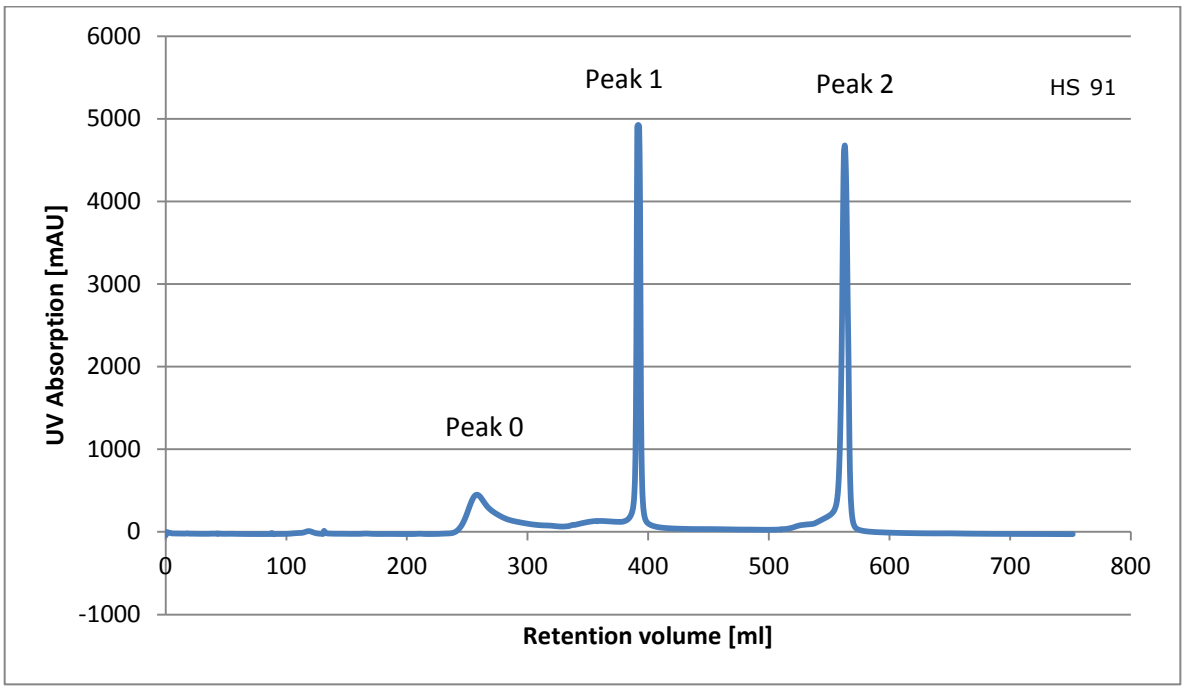

Figure 17 HS 91 Suwannee River

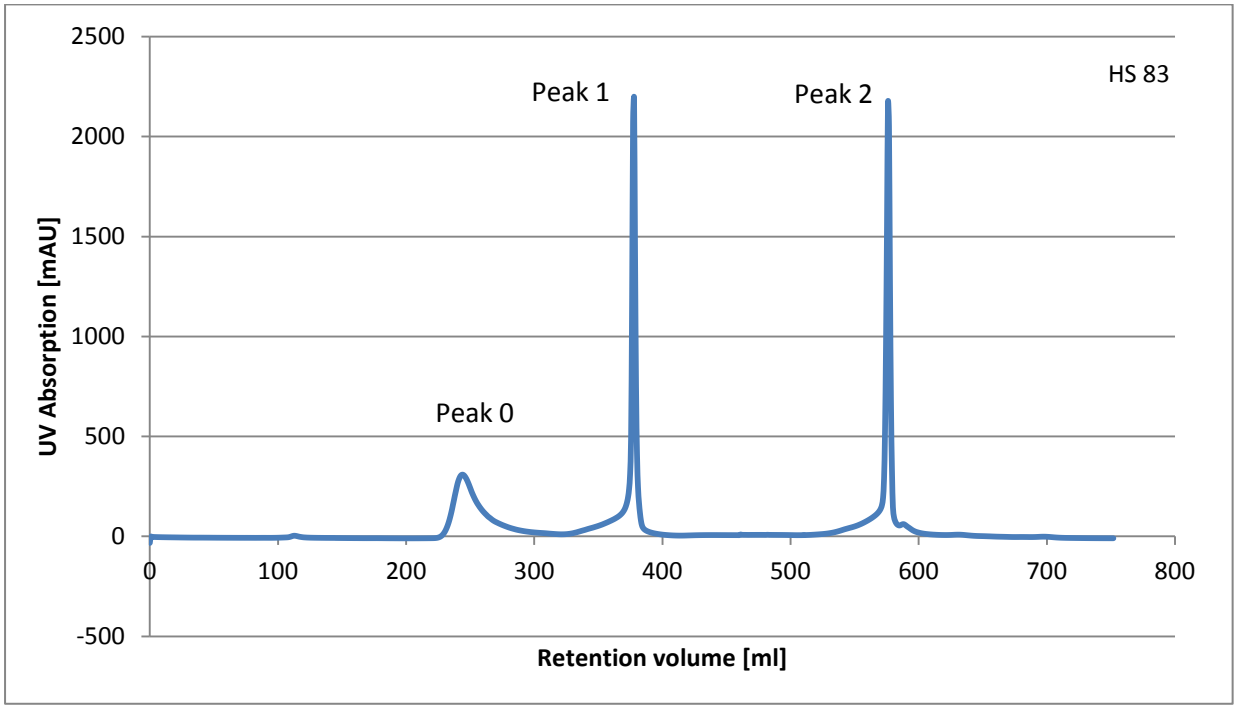

Figure 18 HS 83 Nordic Reservoir

Table 2: Molecular weights of HS

	Molecular weight [g/mol]		
Sample	Peak 0	Peak 1	Peak 2
Craggie Burn	3317	2420	2814
Suwannee River	3348	2117	2575

Table 2 shows the molecular weights of the peaks determined by E. Neubauer with FlowFFF UV-Vis (E. Neubauer, Department of Environmental Geosciences, University of Vienna, 2013, personal communication).

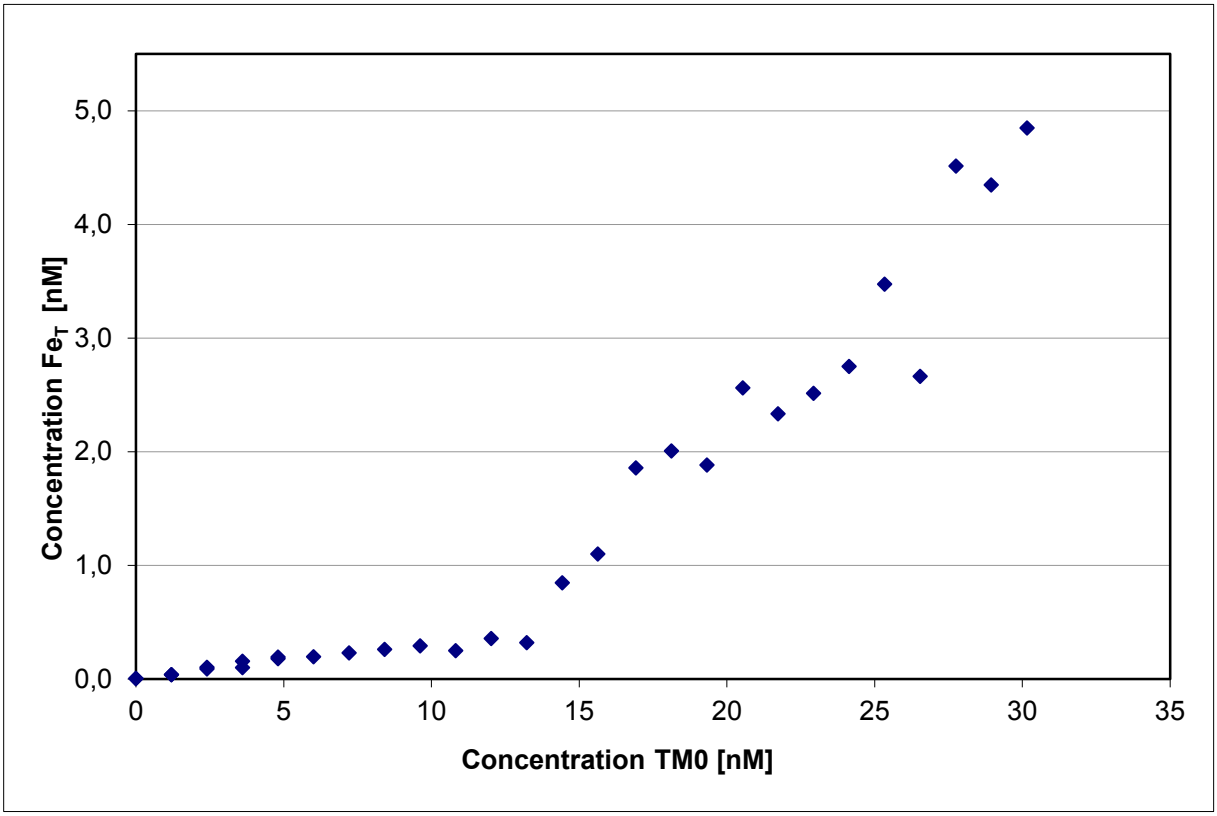

Figure 19: Iron solubility in artificial seawater in dependence of different Tannermoor Peak 0 concentrations

Figure 19 shows the plot of the first experiments with samples from the Tannermoor. When the concentration of HS increases 15nM, the characteristic of the curve is changing. This leads to the hypotheses that there is only a certain linear range, in which the assumption of a 1:1 complex is valid.

Table 3 shows the abbreviations for the several peaks of the HS.

Table 3: Abbreviations of HS fractions

Sample name	Peak 0	Peak 1	Peak 2
Tannermoor	TM0	TM1	TM2
Suwannie River	SR0	SR1	SR2
Craggie Burn	CB0	CB1	CB2
Nordic Reservoir	NR0	NR1	NR2

The plots of [Fe_T] against [L_T] for all three peaks of the 4 different water samples and Ferrioxamine are shown in figure 20 to 24. Only the points that were used for the linear regression are shown. The calculated equations are shown next to the lines.

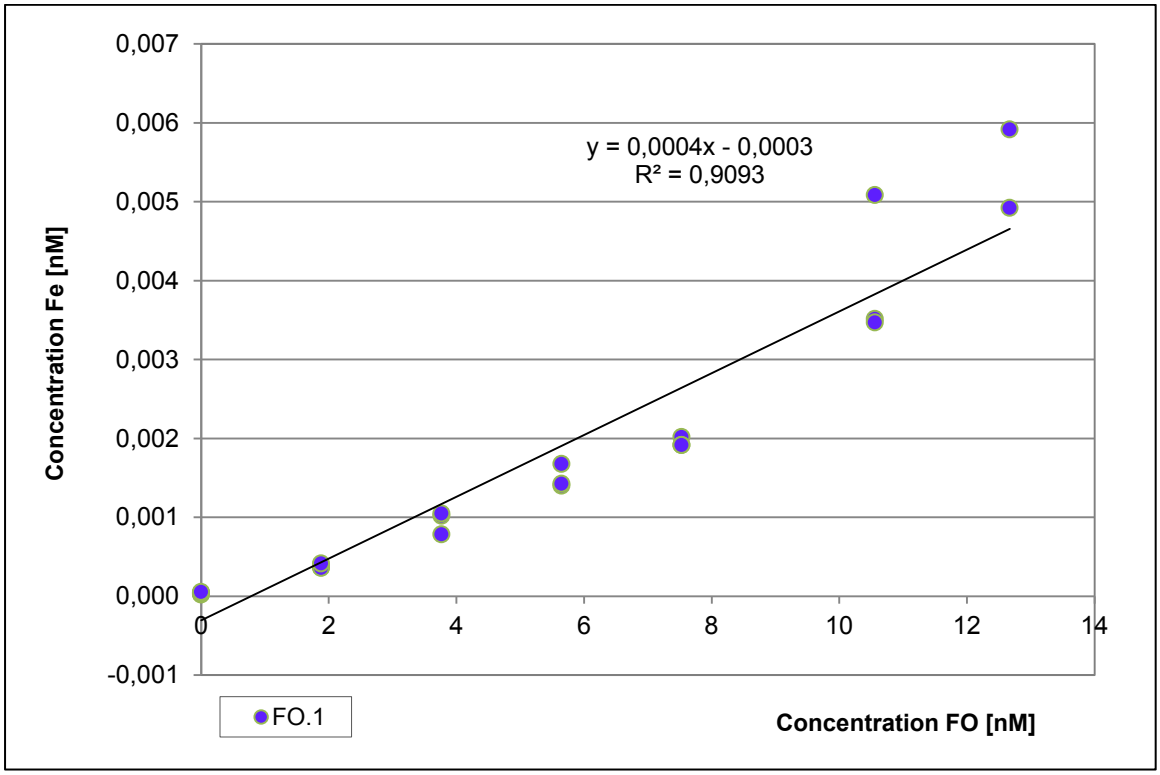

Figure 20: Iron solubility in artificial seawater in dependence of Ferrioxamine E concentration

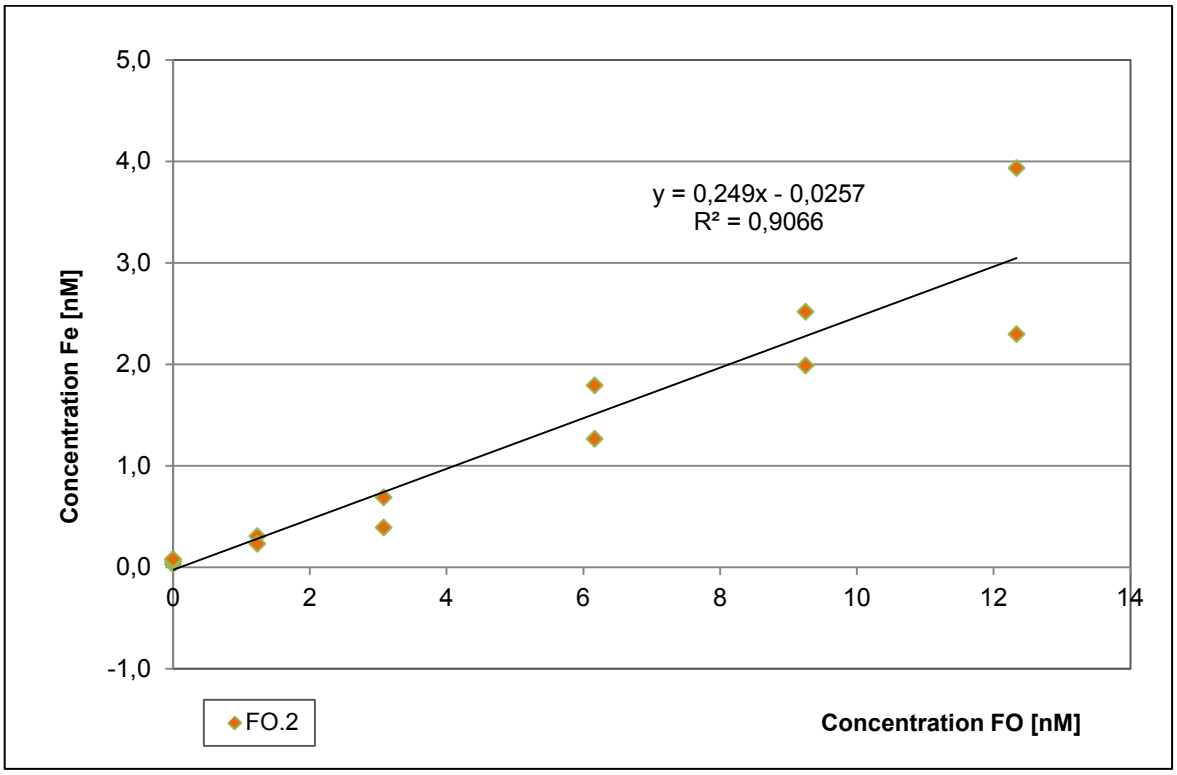

Figure 21: Iron solubility in artificial seawater in dependence of Ferrioxamine E concentration

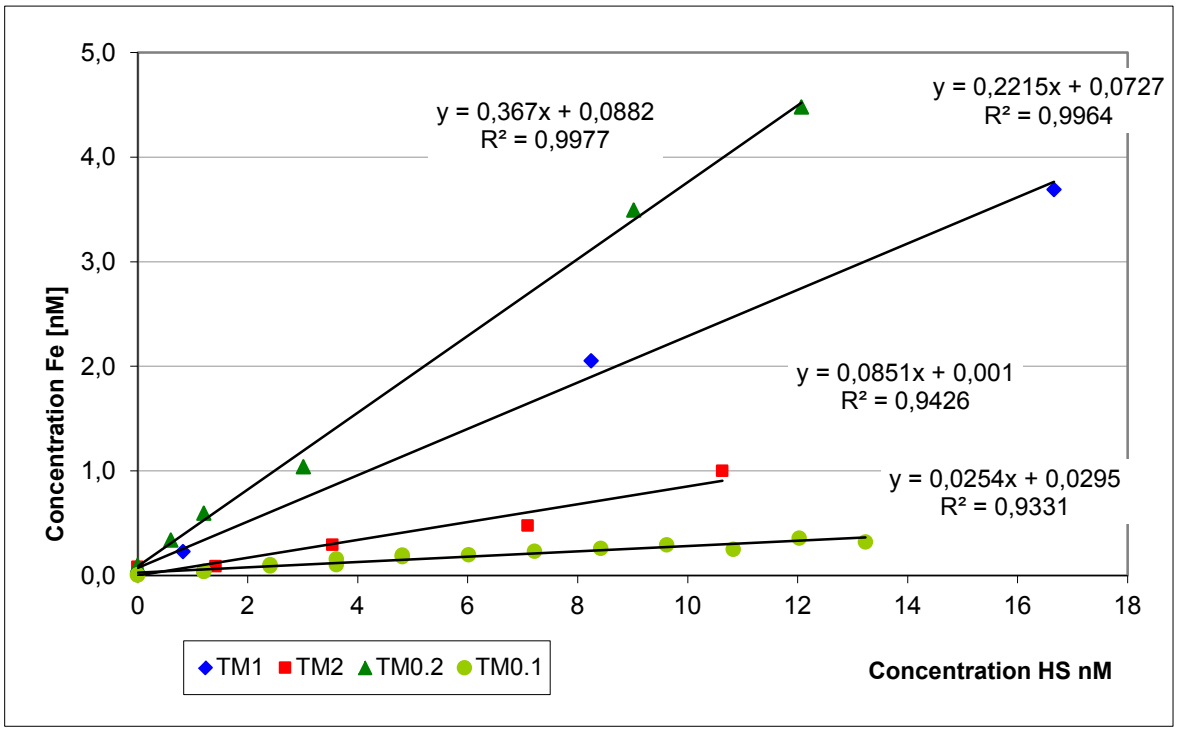

Figure 22: Iron solubility in artificial seawater in dependence of different Tannermoor fraction concentrations

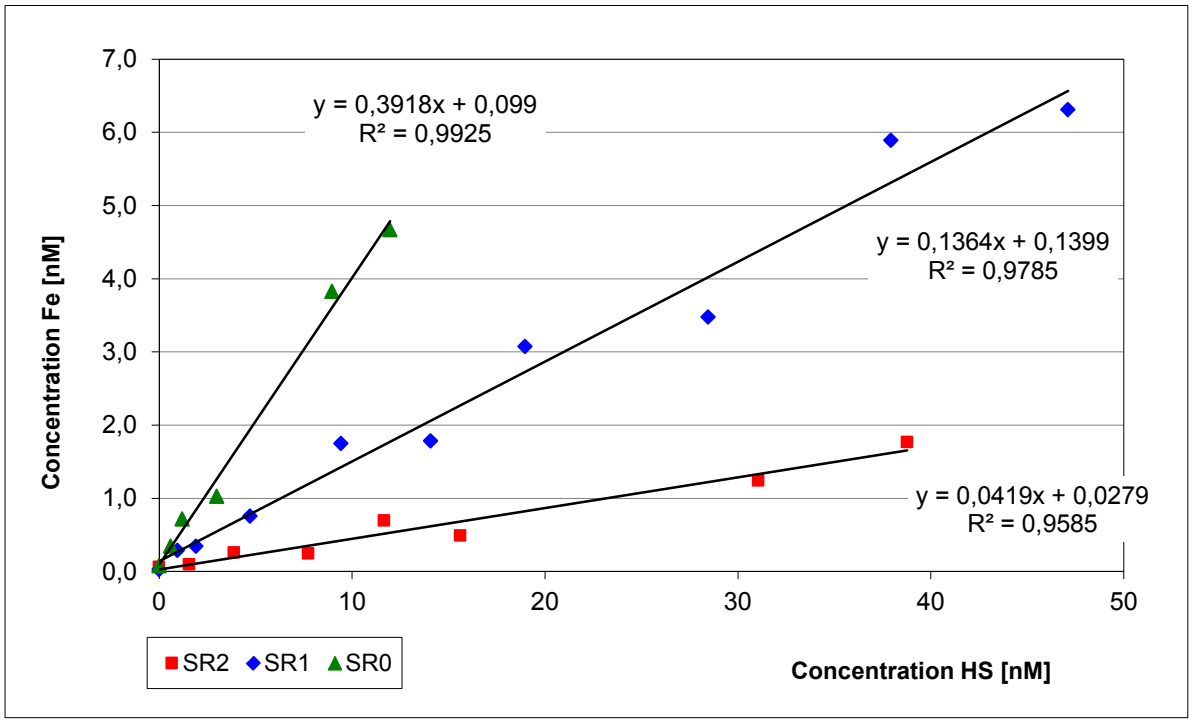

Figure 23: Iron solubility in artificial seawater in dependence of different Suwannee river fraction concentrations

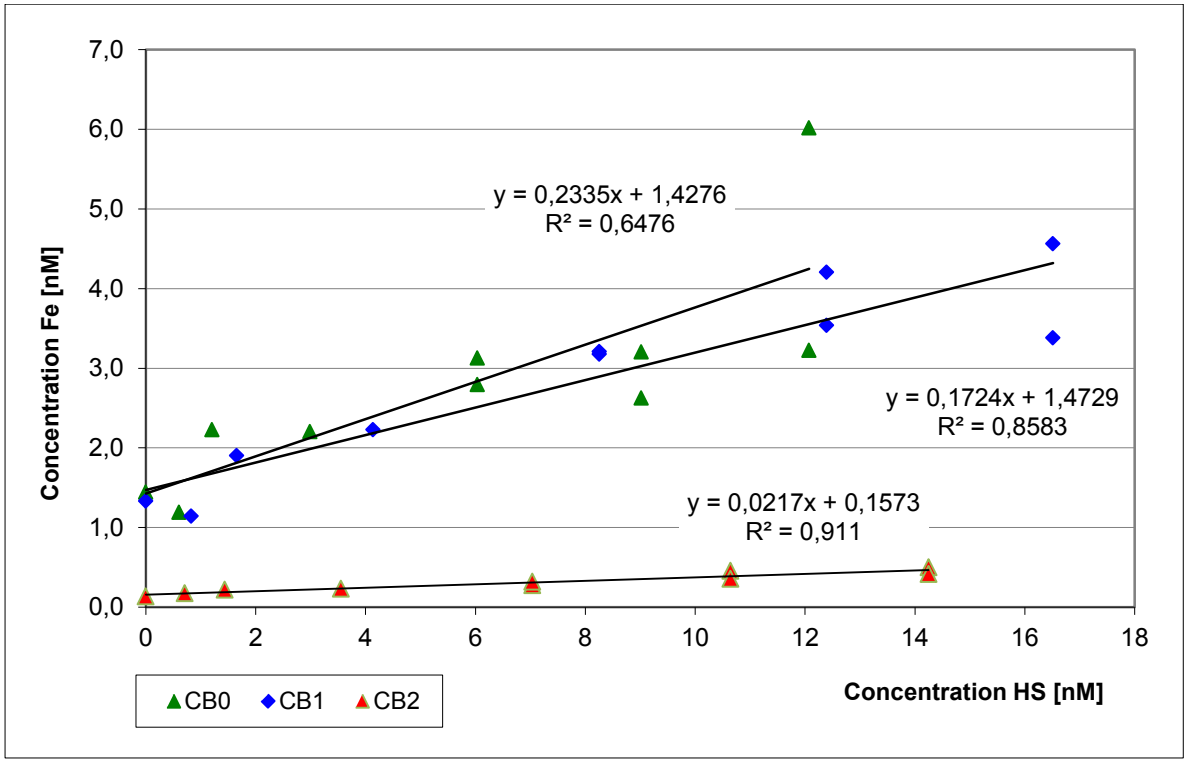

Figure 24: Iron solubility in artificial seawater in dependence of different Craggie burn fraction concentrations

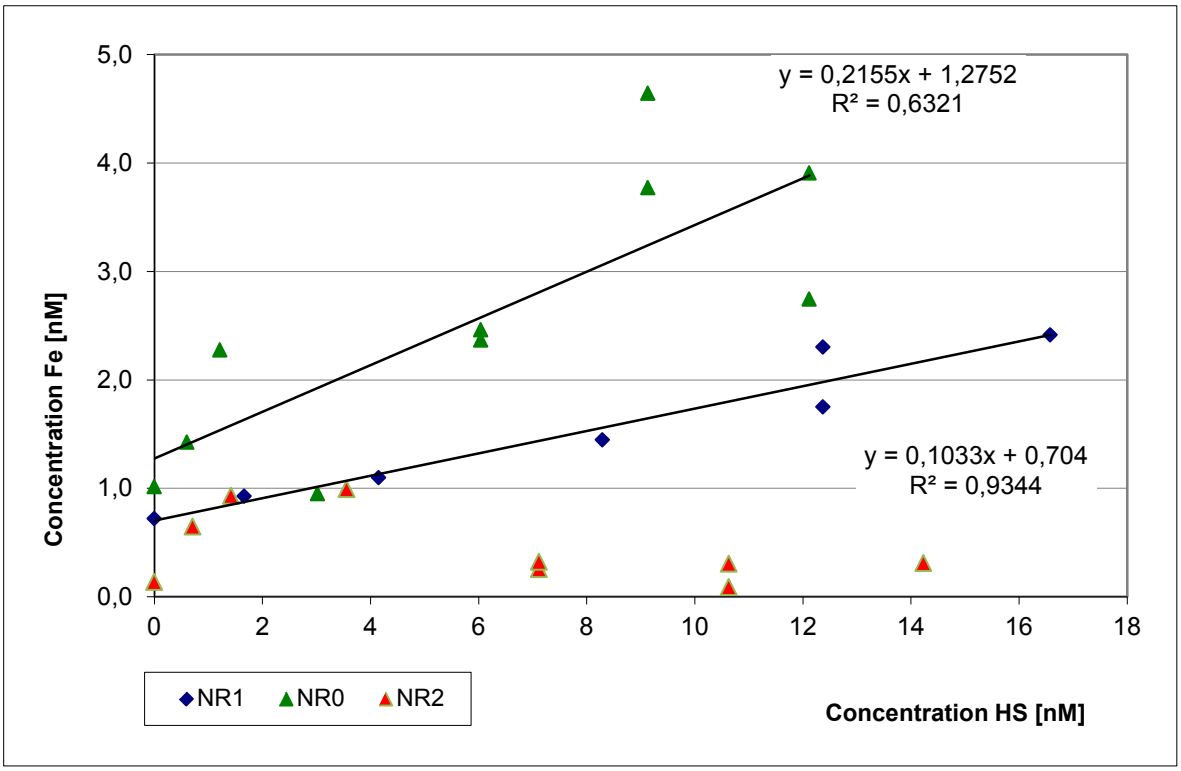

Figure 25: Iron solubility in artificial seawater in dependence of different Nordic reservoir fraction concentrations

For NR2 no linear range could be found for concentrations up to 15 nM. Therefore, $K_{cond.}$ could not be calculated. For TM2 The difference between [Fe'] and the axis intercept was too big, therefore [Fe'] was used to calculate $K_{cond.}$. For Ferrioxamine in both plots the Axis intercept was negative, therefore the average of seral measurements of [Fe'] of the same set of experiments were used to calculate $K_{cond.}$ and $s_{[Fe']}$.

The results for $K_{cond.}$ are shown in Table 4

Table 4: Results for Slopes, [Fe'] and $K_{cond.}$

Sample	Slope A	[Fe'] [nM]	log $K_{cond.}$ [L/mol)
TM0 1	0.0254	0.029	8.9 ± 0.1
TM0 2	0.367	0.088	9.8 ± 0.5
TM1	0.221	0.073	9.6 ± 1.0
TM2	0.0851	0.081	9.1 ± 0.8
CB0	0.234	1.43	8.3 ± 0.2
CB1	0.172	1.47	8.2 ± 0.2
CB2	0.0217	0.16	8.1 ± 0.2
SR0	0.392	0.099	9.8 ± 0.9
SR1	0.136	0.14	9.1 ± 1.0
SR2	0.0419	0.028	9.2 ± 0.1
NR0	0.215	1.28	8.3 ± 0.4
NR1	0.103	0.70	8.2 ± 0.2
FO.1	0.0004	0.000034	10.1 ± 0.3
FO.2	0.249	0.057	9.8 ± 2.2

DISCUSSION

Size Exclusion Chromatography:

The SEC was improved to a degree that tempts to assert that the last two fractions might actually be pure substances. The first fractions (CB0, TM0, SR0 and NR0) have a wider range of molecular weight distribution, which is also supported by the results of the flow FFF. But the first fractions do not elute at the size exclusion limit as proposed by Plessl (Plessl 2012). The second and third fractions are associated with peak concentrations of sulphate and chloride respectively, whereas the first fraction seems to contain no salt anions (Krachler personal communication). The first fractions always contain more iron compared to the other ones which is in good accordance with previous studies (see tables in the appendix, Plessl 2012, Kittinger 2010).

MS methods might bring further insight in the structures of the fractions and the associations with anions. But the inorganic salt ions make many ionization methods (e.g. electrospray) impossible.

Method development:

In course of the present work I have successfully developed a method to determine the conditional complex formation constants of iron chelate complexes with organic ligands in seawater. Based on the radio tracer experiments of Krachler et al. (Krachler et al., 2005, 2010) I was searching for a method that combines the easy application and low detection limit of gamma spectroscopy with conditions as close to the natural conditions as possible. The method presented here has certain advantages over the previously exclusively applied electrochemical methods:

1. Very long equilibration times allow to establish equilibration also with components, that react very slow.

2. The possibility to work with extreme dilutions like fM for iron and pM for organic ligands.

3. No need to add competing ligands, buffer solutions or any other chemicals, which do not naturally occur and could distort the results.

However the method still has some imperfections and needs further improvement. The influence of some parameters needs to be examined more closely.

The stability of the HS solutions in seawater varies. In some samples a precipitate formed and these had to be discarded. There seems to be an influence of the way and temperature of drying the HS after SEC.

Long distances between labs expose the samples to uncontrollable conditions and extra shaking. The salts used for preparation of the synthetic seawater were available only in different quality and grade of purity. This fact and temperature changes while transportation led to varying amounts and nature of precipitations. As discussed below the result was that the values for [Fe´] vary in each set of experiments.

It is essential to know the exact iron concentration of the HS solution in artificial seawater. More work has to be done to find a more accurate method of measurement that can deal with the matrix effects.

Iron solubility experiments:
Different conditions for precipitation of the solid phases caused very different values for the solubility of iron in pure synthetic seawater [Fe'], although the values calculated for $K_{cond.}$ showed similar results. This indicates that [Fe'] is highly dependent on the properties of the solid iron oxide phase. The solubility of iron oxides in aqueous systems depends on particle size and nature of the oxide, which affects the lattice energy. Both particle size and lattice energy are heavily influenced by the non-equilibrium supersaturated conditions during precipitation, temperature, shaking intensity and by aging of the precipitate. Calcite precipitation and crystallization of the iron oxide on the calcite surface may also influence the solubility of the iron oxide phase (Clarke, Loeppert, Ehrman, 1985). As the salts used for preparation of the synthetic seawater were available only in different quality and grade of purity, it seems likely, that these impurities exerted additional effects. In

order to achieve a well-defined solid iron oxide phase and comparable results it was necessary to conduct a series of experiments with different HS concentrations in parallel under strictly identical conditions. [Fe'] can then be assumed to have the same value in all samples of a particular series of experiments. The linear shape characteristics of the iron solubility plots confirmed the assumption of a single class of iron binding ligands. Still the results for $K_{cond.}$ in different sets of experiments vary, which might be due to different experimental conditions, which were under constant development. The long storage time of Ferrioxamine might have caused the lesser value for $K_{cond.}$ at FO.1, although no precipitate or cloudiness was noticed. Besides the CI the accordance of the axis intercept and the measured [Fe'] is a degree for the accuracy of the results. This implies that the results of TM0.2 and FO.2 are more trustworthy. This encourages the later conclusions.

Conclusions:

The values found for $K_{cond.}$ are in good agreement with data published by Laglera and van den Berg (Laglera and van den Berg, 2009). The values for log $K_{cond.}$ of the HS in my experiments vary from 8.1 to 9.8. The values found by Laglera and van den Berg by cathodic stripping voltammetry in the presence of a synthetic competing ligand (CLE-CSV) tend to be higher. E.g. log K_{cond} for NOM from the Irish Sea (NOM, Irish Sea) = 10.9±0.2. The different methods can cause different results, as there is no phase separation or precipitation involved at the CLE-CSV method and CSV methods possibly overestimate values for $K_{cond.}$ (Gledhill and Buck, 2012).

If the values of $K_{cond.}$ for the HS are compared to the value of $K_{cond.}$ for Ferrioxamine E, it is remarkable that the siderophore builds slightly more stable complexes than the HS do. This points to another pathway of iron uptake mechanism of iron for phytoplankton. Laglera and van den Berg discussed the importance of HS iron complexes for the dissolved iron pool and for the bioavailable fraction that can increase phytoplankton activity. Photochemical reduction of iron(III) to iron(II), which weakens the metal binding, is one possible way to make iron bioavailable (Laglera and van den Berg, 2009). Ligand exchange of HS and siderophores, especially

hydroxamate species like Ferrioxamine E, seems to be another way to enable the uptake of iron by microorganisms.

ACKNOWLEDGEMENTS

In the first place, I would like to address special thanks to ao. Univ.-Prof. Dr. Regina Krachler, who had the idea for this work and supervised the thesis. She also supported me whenever problems occurred and put a lot of effort into the project.

I also want to thank assoc. Prof. Dr. Stephan Hann for the opportunity to conduct my master thesis' research in the Division for Analytical Chemistry at the University of Natural Resources and Life Sciences.

Special thanks go to ao. Univ. Prof. Dr. Gabriele Wallner, who conducted all the gamma spectroscopy measurement and supported my work in the radiochemistry laboratory.

Furthermore special thanks go to Dr. Franz Jirsa, who has guided me with advice, and performed all the DOC measurements.

Many thanks go to the members of the working group of the division of analytical chemistry at the University of Natural Resources and Life Science, in particular Mario Oberwalder, who made my time enjoyable and helped out with any problems.

Last but not least I want to very especially thank my dear Philipp and my beloved children Florian and Maria for their patience and warmth support.

I want to thank the Wiener ArbeitnehmerInnen Förderungsfond for the financial support during the time of my thesis.

CV

Monika Laux
Pharmareferentin, Chemikerin
Rotenmühlgasse 43/6
1120 Wien
Mobil: 0676/ 4104112
Mail: monika.laux@gmx.at

Persönliches

Geboren am 20. Dezember 1969
in Wien
Lebensgemeinschaft, 2 Kinder

Berufliche Erfahrung

04/2002 – 12/2012	**Pharmareferentin** Pfizer Corporation Austria GmbH selbständige von 4/2002 -10/2003 Indikationsbereiche: Urologie, Pulmologie, Neurologie, Gerinnung, Herz/Kreislauf, Schmerz Betreute Gebiete: Wien, Niederösterreich, Burgenland Niedergelasse Ärzte und Krankenhaus
07/2001 – 12/2001	**PR Assistentin** Info-Service Mag. Kurt Vymazal GmbH Gesundheitskommunikation, Pressearbeit
10/1999 – 06/2001	**Kulturreferentin, Kulturredakteurin** ÖH Uni Wien Organisation von Kulturveranstaltungen Uniaktuell, Leitung der Resorts Kultur und Wissenschaft Verantwortlich für 10 freie Mitarbeiter
09/1998 – 07/2003	**Billeteurin im Etablissement Ronacher** geringfügig beschäftigt bei: Höller & Neischl OEG, Promotersgroup Service Gmbh, VSG-Egger & Klinger GmbH
01/1997 – 12/2002	**Wissenschaftliche Mitarbeiterin, Drogenanalytik** Check It, Drogenpräventionsprojekt des Fonds Soziales Wien
01/2002 – 04/2002 07/1996 – 10/1999	**Wissenschaftliche Mitarbeiterin** Klinisches Institut für Chemische Labordiagnostik, AKH Methodenentwicklung Spiegelbestimmungen und Drogenanalytik
11/1999 04/1998 – 11/1998	**Merchandising** Cruwys-Lemmings OEG geringfügig beschäftigt

05/1997 und 05/1998	**Kamera, Videoproduktion und Verkauf** Videoteam des Pensionistenverbandes
07/1995 - 08/1995 02/1995	**Urlaubsvertretung Proteinanalytik** Bender & Co GmbH
07/1994 – 09/1994	**Praktikantin Proteinanalytik** Bender & Co GmbH
07/1993 – 09/1993	**Praktikantin** Ciba Geigy , Basel Entwicklung von Papierfarbstoffen
08/1992 – 09/1992	**Praktikantin** Chemie Linz GmbH Synthese von Monomeren

Studium und Ausbildung

2/2013 – 9/2014	**Masterarbei**t am Institut für Anorganische Chemie der Universität Wien, Gruppe Umweltchemie, Thema: Eisen-Huminstoffkomplexe
21.11.2001	**Pharmareferentenprüfung**
10/1999 – 06/2001	**Universität Wien** Universitätslehrgang für Öffentlichkeitsarbeit
11/1991 – 06/1996	**Universität Wien** Diplomstudium Chemie, 2. Abschnitt, Schwerpunkte: Analytische Chemie, Biochemie
03/1993 – 07/1994	**Universität Wien** Studium Volkswirtschaft (3 Semester)
10/1988 – 11/1991	**Universität Wien** Diplomstudium Chemie, 1. Abschnitt abgeschlossen 27.11.1991, am 5.10.2011 anerkannt als Abschluss Bachelor of Science
09/1980 – 07/1988	**Naturwissenschaftliches Realgymnasium, 1120 Wien** Matura

Kenntnisse und Qualifikationen

Software	MS Office, Photoshop, Premiere, Chromelion, Siebel
Sprachen	**Deutsch**: Muttersprache **Englisch**: verhandlungssicher in Wort und Schrift **Portugiesisch**: Grundkenntnisse
Führerschein	Klassen A, B

LIST OF FIGURES

LIST OF TABLES

REFERENCES

Aitkenhead, J. A., Hope, D., and Billet, M. F. "The relationship between dissolved organic carbon in stream water and soil organic carbon pools at different spatial scales", *Hydrol. Processes*, 123 (8), 1289–1302, 1999

Boyd, Philip W., et al. "Mesoscale iron enrichment experiments 1993-2005: Synthesis and future directions." *Science* 315.5812 (2007): 612-617.

Byrne, Robert H., and Dana R. Kester. "Solubility of hydrous ferric oxide and iron speciation in seawater." *Marine Chemistry* 4.3 (1976): 255-274.

Bliefert C., „Umweltchemie", Wiley-VCH, (2002)

Cassar, Nicolas, et al. "The Southern Ocean biological response to aeolian iron deposition." *Science* 317.5841 (2007): 1067-1070.

Clarke, E. T., Loeppert, R. H. & Ehrman, J. M. "Crystallization of iron oxides on calcite surfaces in static systems." *Clays and Clay Minerals* 33.2 (1985): 152-158

Colditz, G. *Auen, Moore, Feuchtwiesen Gefährdung und Schutz von Feuchtgebieten*, Birkhäuser Verlag. (1994).

Elder, J. F., Rybicki, N. B., Carter, V., and Weintraub, V. "Sources and yields of dissolved carbon in northern Wisconsin stream catchments with different amounts of peatland", *Wetlands*, 20(1), 113–125, 2000.

Falkowski, P. G., R. T. Barber, et al. "Biogeochemical Controls and Feedbacks on Ocean Primary Production." *Science* 281.5374 (1998): 200-206.

GE Healthcare (2006) Instructions 56-1190-97 AD Sephadex LH-20

Gledhill, M.; Van den Berg, C. M. G. "Determination of complexation of iron(III) with naturalorganic complexing ligands in seawater using cathodic stripping voltammetry." *Marine Chemistry* 47(1) (1994): 41-54

Gledhill, M. and Buck, KN "The organic complexation of iron in the marine environment: a review." *Front.Microbio*. **3**:69 (2012): 1-17

Hamidatou Lylia, H. Slamene, T. Akhal and B. Zouranen Concepts, "Instrumentation and Techniques of Neutron Activation" *InTech*, http://dx.doi.org/10.5772/53686

Hiemstra, Tjisse, and Willem H. van Riemsdijk. "Biogeochemical speciation of Fe in ocean water." *Marine chemistry* 102.3 (2006): 181-197.

Hernes, Peter J., and Ronald Benner. "Terrigenous organic matter sources and reactivity in the North Atlantic Ocean and a comparison to the Arctic and Pacific oceans." *Marine chemistry* 100.1 (2006): 66-79.

Hollemann A.F., Nils Wiberg. *Lehrbuch der Anorganischen Chemie*. Walter de Gruyter, Berlin, (1985)

Hopkinson, Brian M., and François MM Morel. "The role of siderophores in iron acquisition by photosynthetic marine microorganisms." *Biometals* 22.4 (2009): 659-669.

IHSS. "Source Materials for IHSS Samples." Retrieved from http://www.humicsubstances.org/sources.html

IHSS. (2007). "What are Humic Substances." Retrieved from http://www.humicsubstances.org/whatarehs.html.

Kendall, Brian, Anbar, A. D., Kappler, A. and Konhauser, K. O. "The Global Iron Cycle", *Fundamentals of Geobiology* (eds A. H. Knoll, D. E. Canfield and K. O. Konhauser), Wiley, Chichester, (2012): 65-92

Kester, Dana R., et al. "Preparation of artificial seawater." *Limnology and Oceanography* 12.1 (1967).

Kittinger, R. „Terrestrische Huminstoffe in Oberflächengewässern als Eisenkomplexbildner unter salinen Bedingungen." (2010)

Krachler, R., F. Jirsa, and S. Ayromlou. "Factors influencing the dissolved iron input by river water to the open ocean." *Biogeosciences* 2.4 (2005): 311-315.

Krachler, Regina, Rudolf F. Krachler, Frank von der Kammer, Altan Süphandag, Franz Jirsa, Shahram Ayromlou, Thilo Hofmann, Bernhard K. Keppler. "Relevance of peat-draining rivers for the riverine input of dissolved iron into the ocean." *Science of the Total Environment* 408.11 (2010): 2402-2408.

Kuhn, K. M., Maurice, P. A., Neubauer, E., Hofmann, T. & von der Kammer, F. "Accessibility of humic-associated Fe to a microbial siderophore: Implications for bioavailability." *Environmental Science and Technology* 48**.**2, (2014): 1015-1022.

Kuma, Kenshi, Jun Nishioka, and Katsuhiko Matsunaga. "Controls on iron(III) hydroxide solubility in seawater: the influence of pH and natural organic chelators." *Limnology and Oceanography* 41.3 (1996): 396-407.

Laglera, Luis M., and Constant MG van den Berg. "Evidence for geochemical control of iron by humic substances in seawater." *Limnology and Oceanography* 54.2 (2009): 610.

Liu, Xuewu & Millero, Frank J. „The solubility of iron hydroxide in sodium chloride solutions." *Geochimica et Cosmochimica Acta* 63.19/20 (1999): 3487-3497

Liu, Xuewu, and Frank J. Millero. "The solubility of iron in seawater." *Marine Chemistry* 77.1 (2002): 43-54.

Martin, John H., and Steve E. Fitzwater. "Iron deficiency limits phytoplankton growth in the north-east Pacific subarctic." *Nature* (1988): 341-343.

Martinez JS, Carter-Franklin JN, Mann EL, Martin JD, Haygood MG, Bulter "A Structure and membrane affinity of a suite of amphiphilic siderophores produced by a marine bacterium." *Proc Natl Acad Sci USA* 100(2003): 3754– 3759

Mawji, Edward, M. Gledhill, J. A. Milton, G. A. Tarran, S. Ussher, A. Thompson, G. A. Wolff, P. J. Worsfold, and E. P. Achterberg "Hydroxamate Siderophores: Occurrence and Importance in the Atlantic Ocean" *Environmental Science & Technology* 42.23, (2008): 8675-8680

Plessl, Christof Andreas Reinold. "Charakterisierung von gelöstem organischem Material in Moorwässern." (2012)

Raven, J. A., and P. G. Falkowski. "Oceanic sinks for atmospheric CO2." *Plant, cell & environment* 22.6 (1999): 741-755.

Riedel, E. *Anorganische Chemie*, de Gruyter (2004)

Rose, Andrew L., and T. David Waite. "Kinetics of iron complexation by dissolved natural organic matter in coastal waters." *Marine chemistry* 84.1 (2003): 85-103.

Rue, Eden L., and Kenneth W. Bruland. "Complexation of iron(III) by natural organic ligands in the Central North Pacific as determined by a new competitive ligand equilibration/adsorptive cathodic stripping voltammetric method." *Marine Chemistry* 50.1 (1995): 117-138.

Skoog, Douglas,James Holler, Stanley Couch, *Instrumentelle Analytik*, 6. Auflage, Springer Berlin, Heidelberg (2013)

Smetacek, Victor, et al. "Deep carbon export from a Southern Ocean iron-fertilized diatom bloom." *Nature* 487.7407 (2012): 313-319.

Stevenson, Frank J. *Humus chemistry: genesis, composition, reactions*. John Wiley & Sons, (1994)

Turner, David R. and Keith A. Hunter, eds. *The Biogeochemistry of Iron in Seawater.* Wiley, Chichester, (2001)

Ziechmann, W. *Huminstoffe und ihre Wirkungen,* Spektrum, Akademischer Verlag (1996).

APPENDIX

Chromatograms:

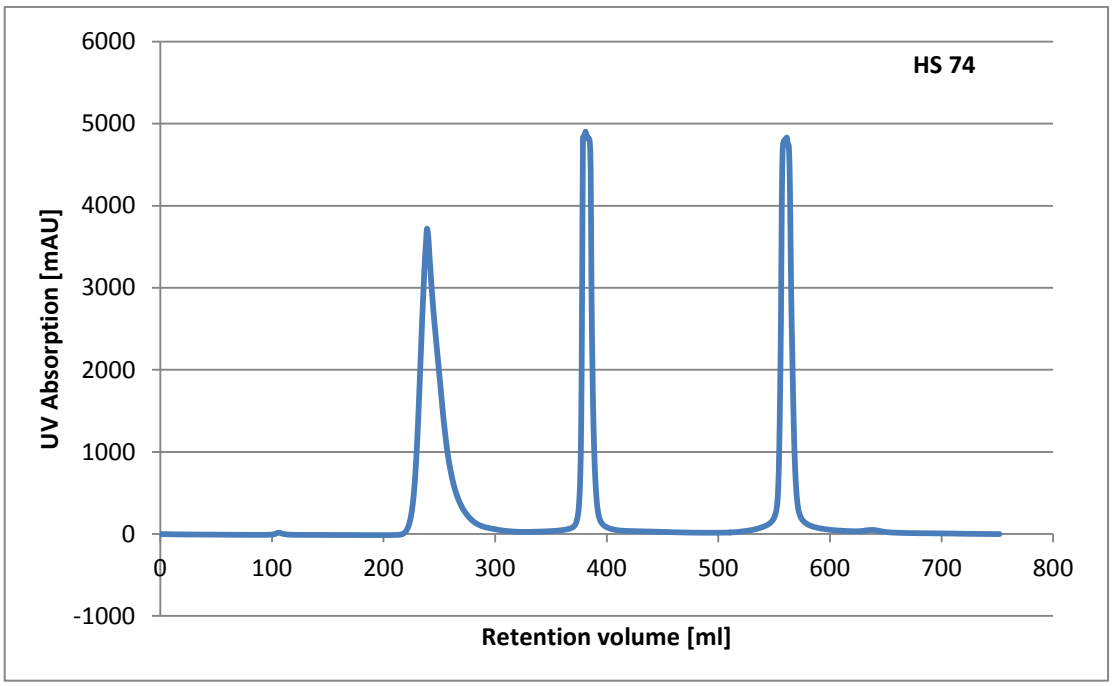

Figure 26: HS 74 Craggie burn

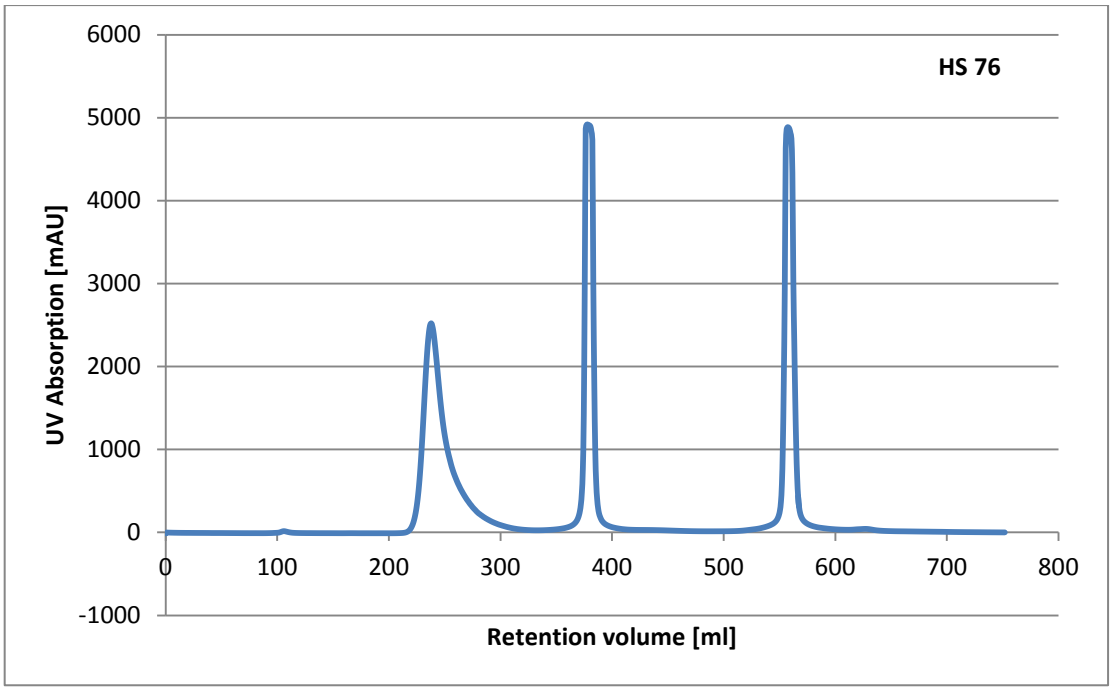

Figure 27: HS 76 Craggie burn

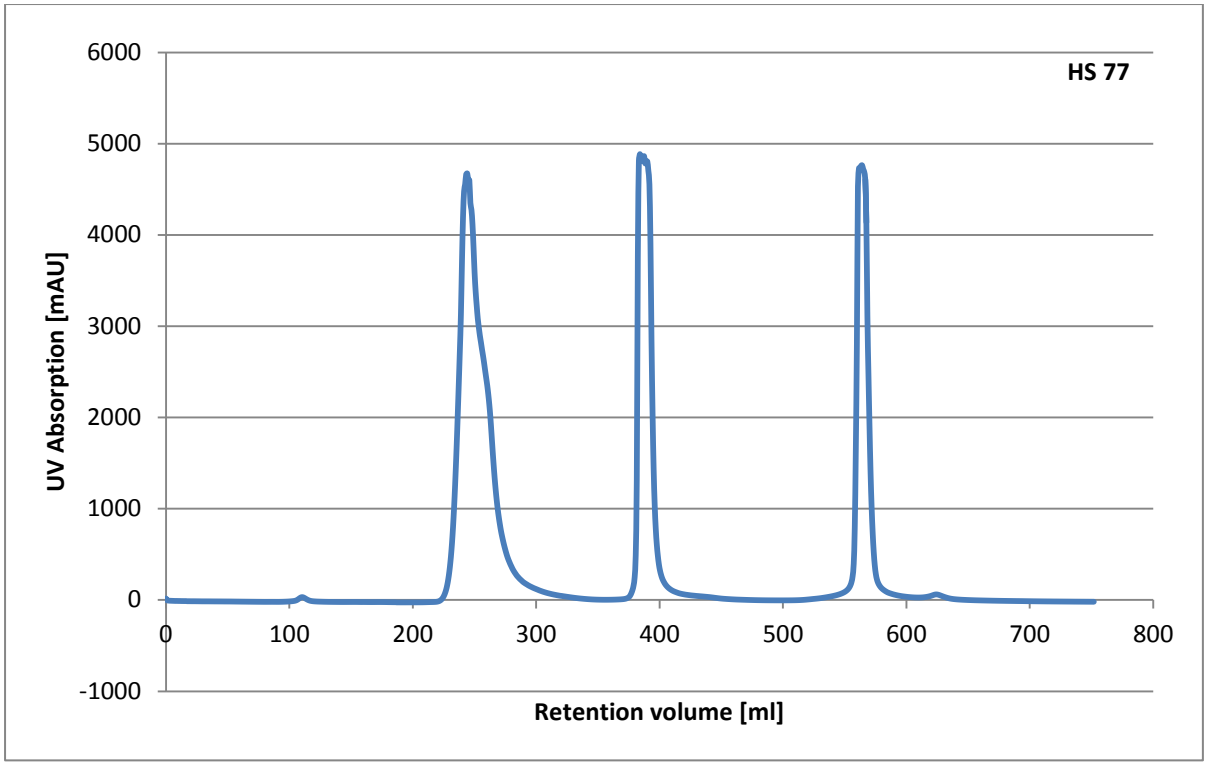

Figure 28: HS 77 Craggie burn

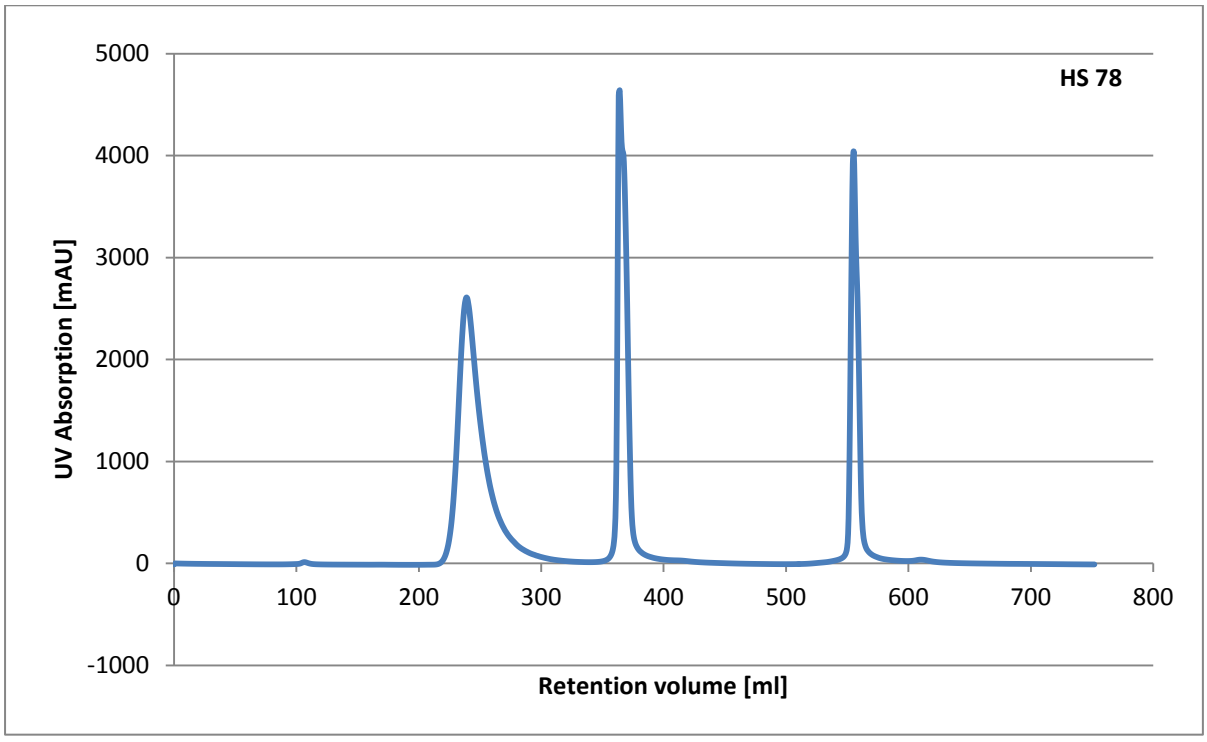

Figure 29: HS 78 Craggie burn

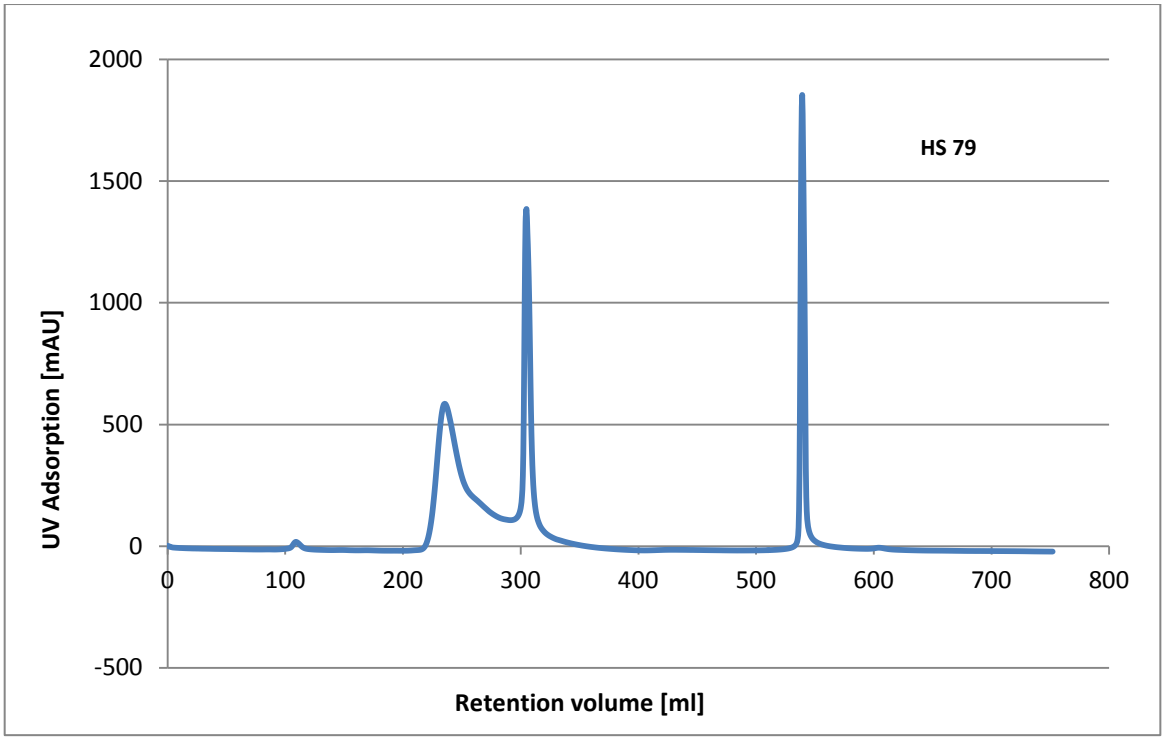

Figure 30: HS 79 Craggie burn

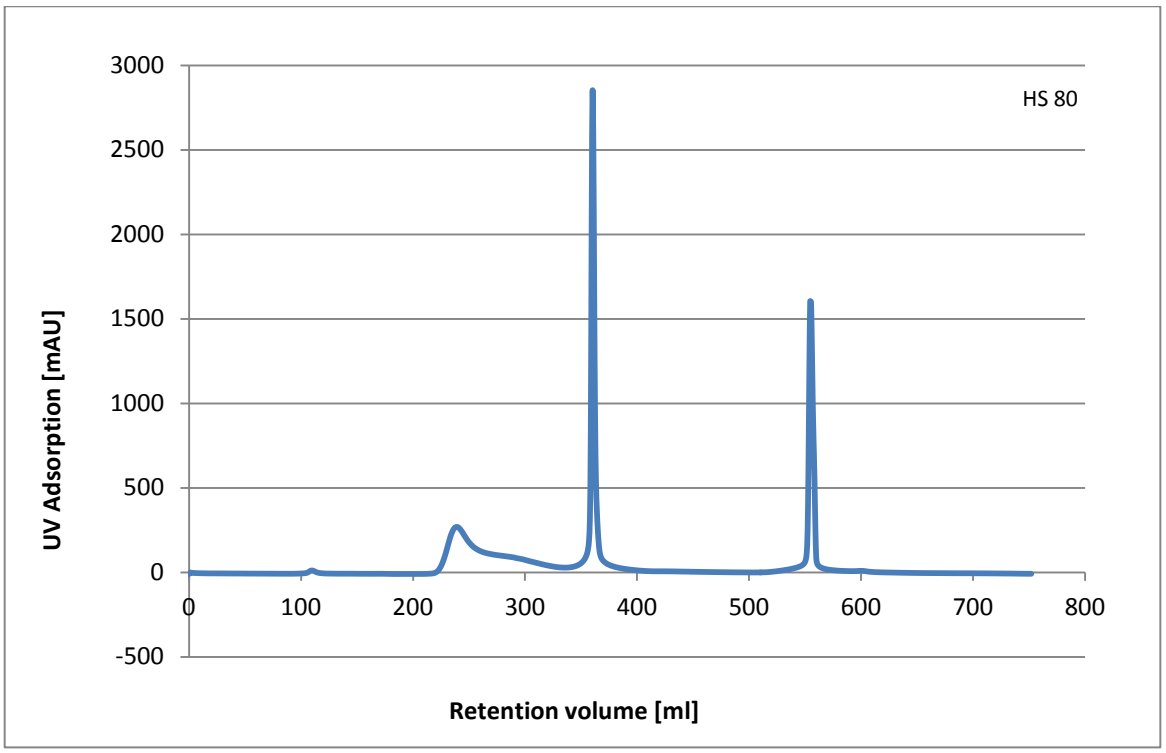

Figure 31: HS 80 Suwannee river

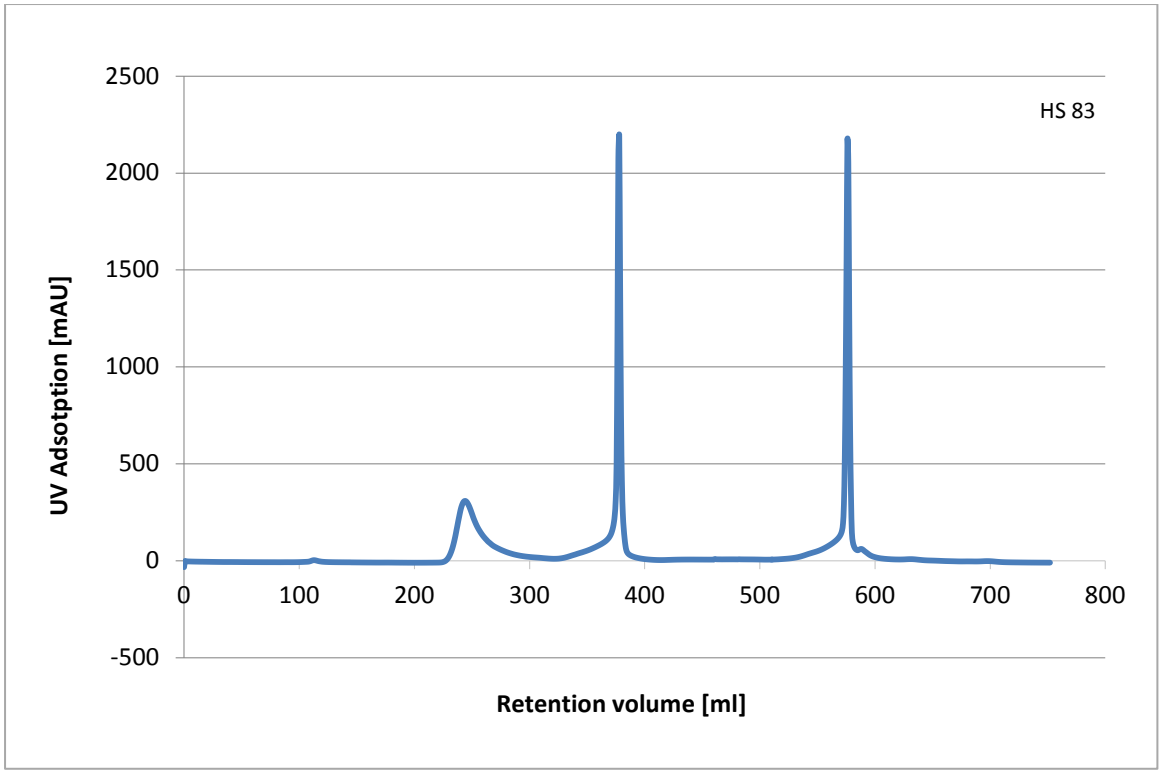

Figure 33: HS 83 Nordic Reservoir

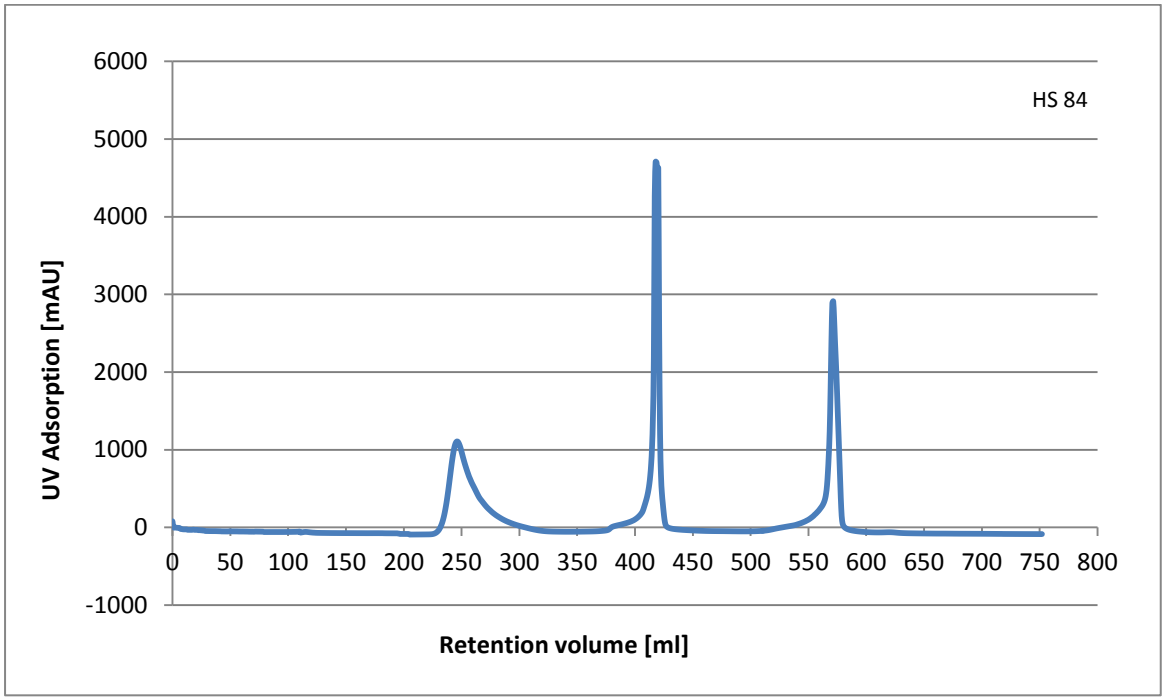

Figure 34 HS 84 Craggie Burn

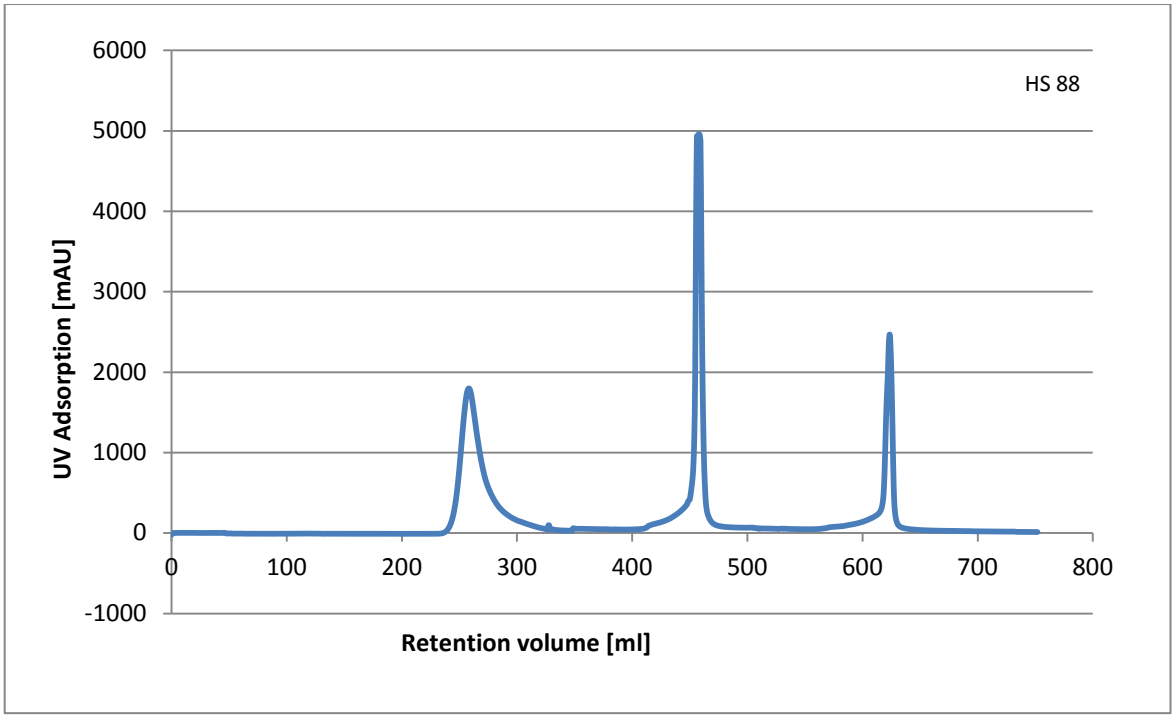

Figure 35: HS 88 Tannermoor

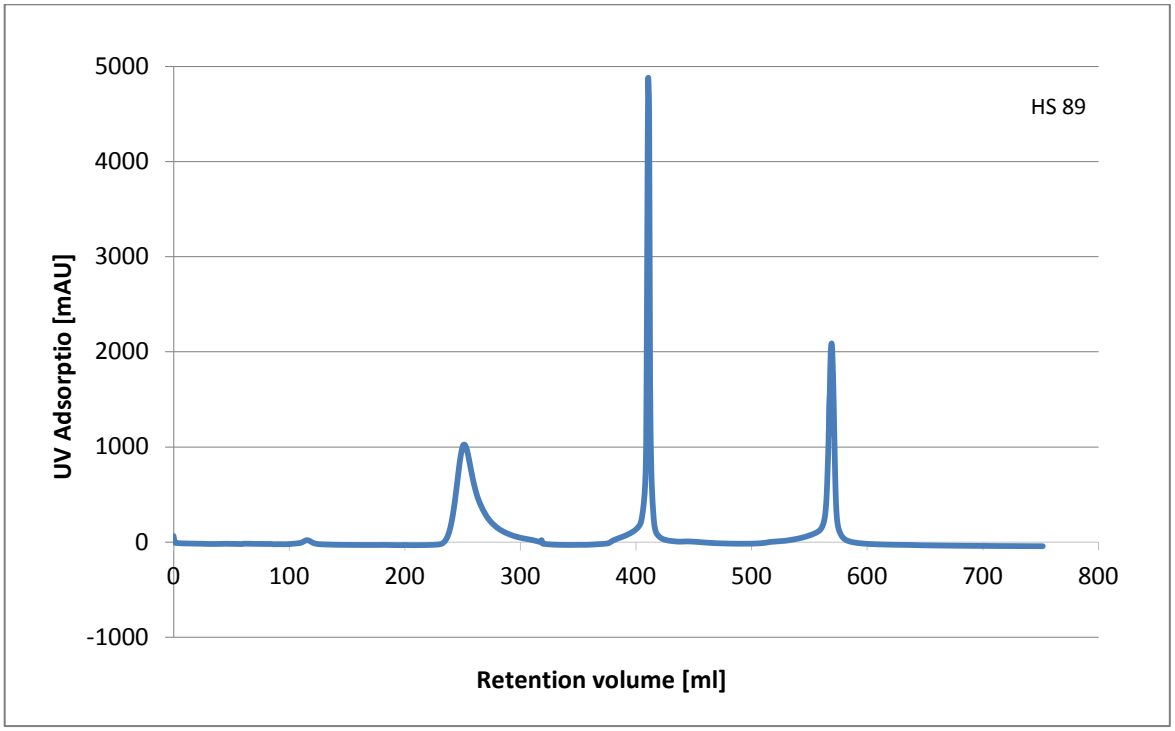

Figure 36: HS 89 Tannermoor

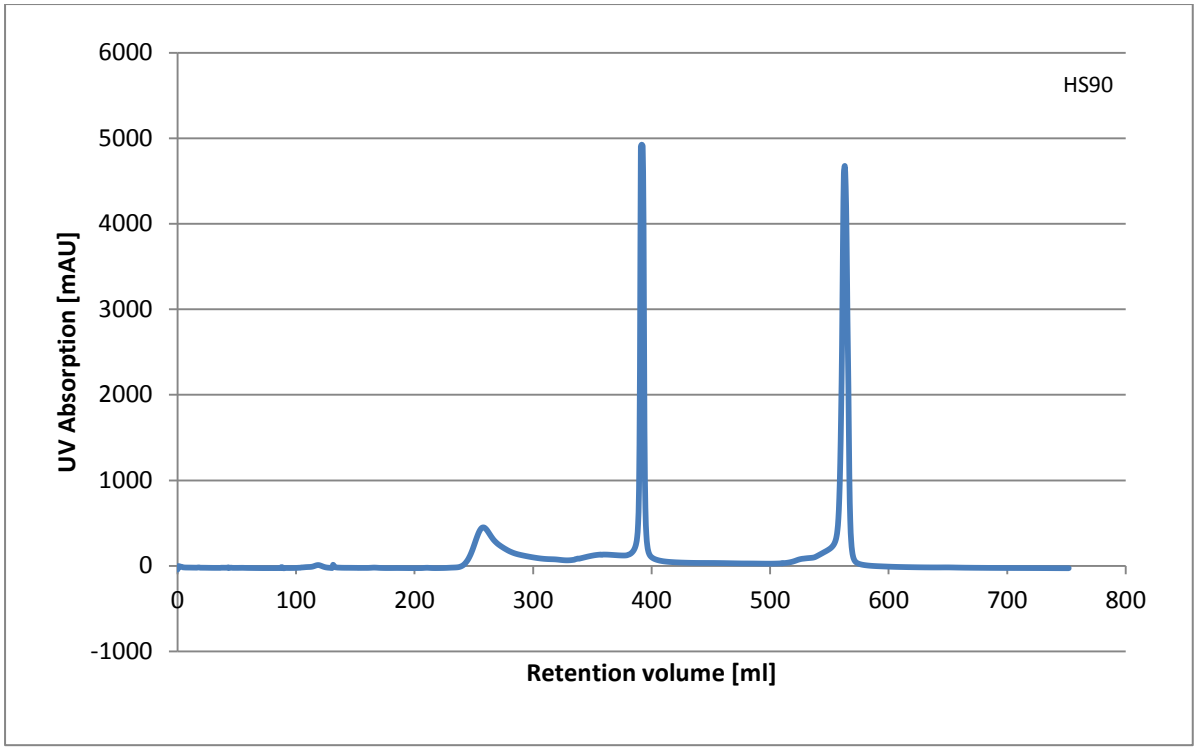

Figure 37: HS 90 Suwannee River

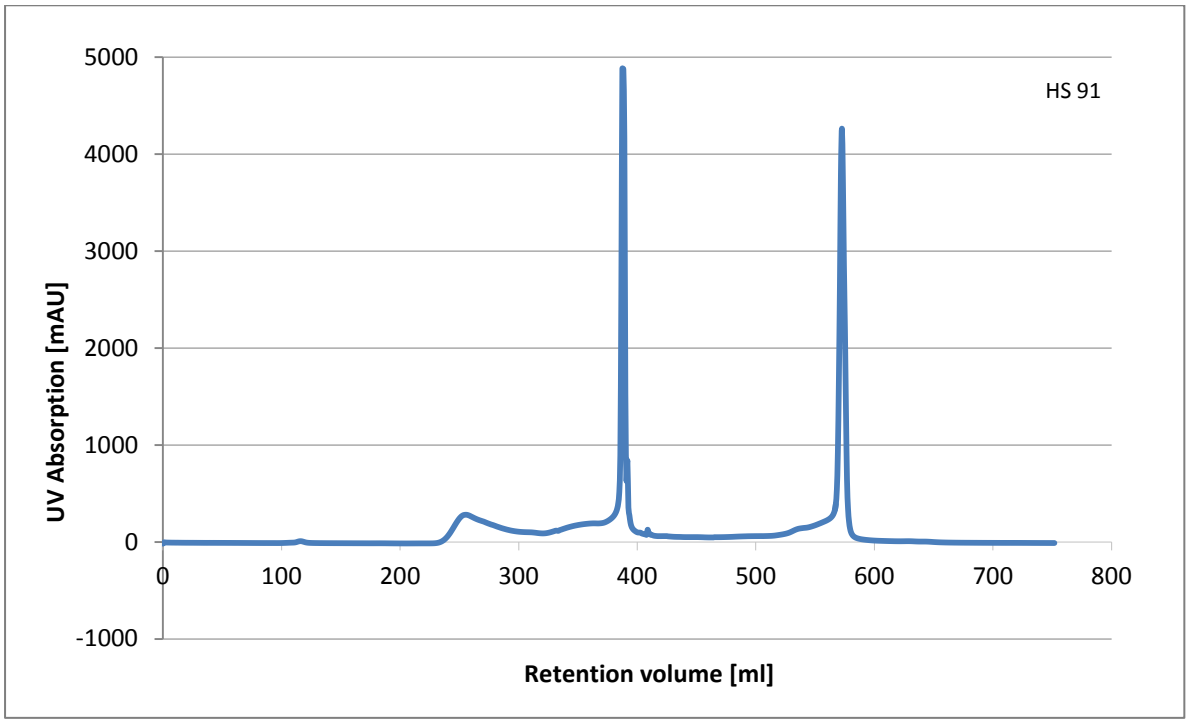

Figure 38: HS 91 Suwannee River

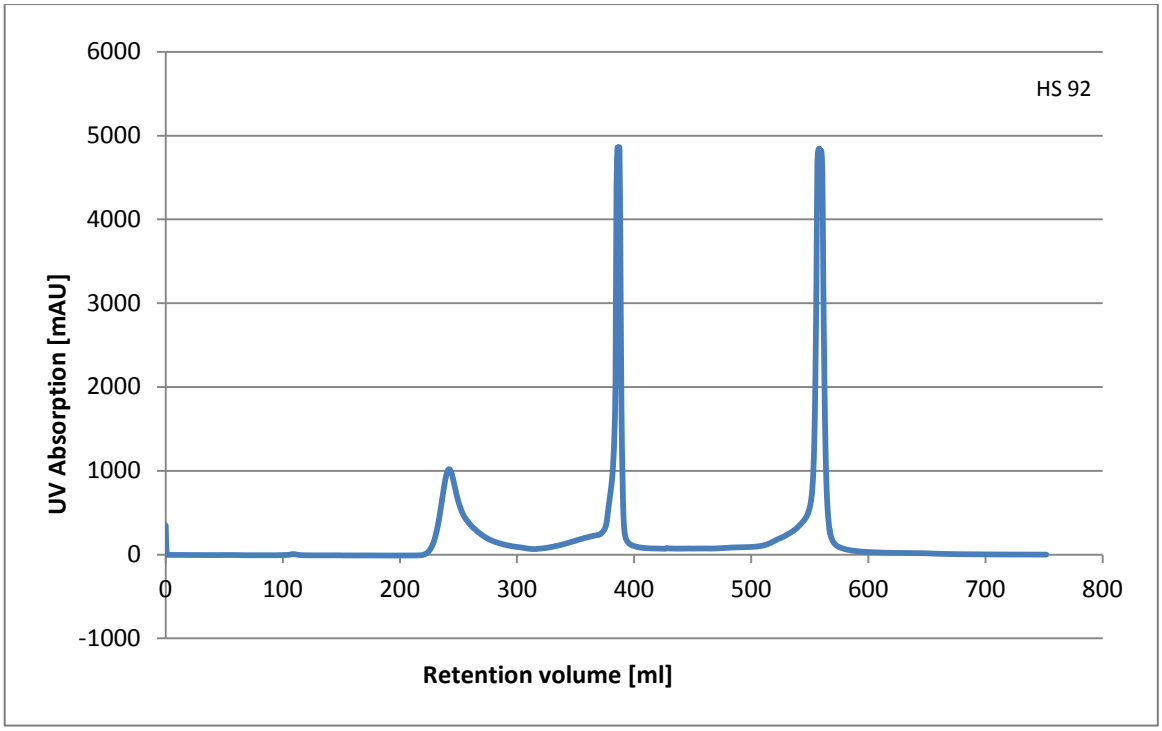

Figure 39: HS 92 Nordic Reservoir

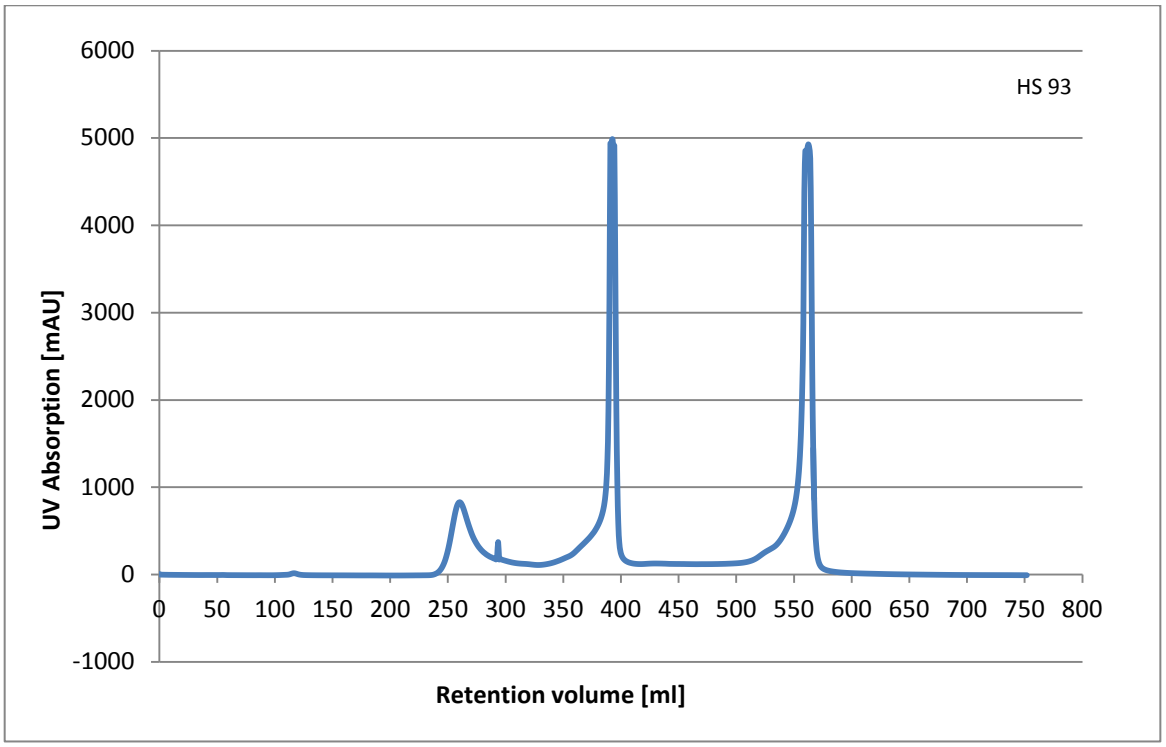

Figure 40: HS 93 Suwannee River

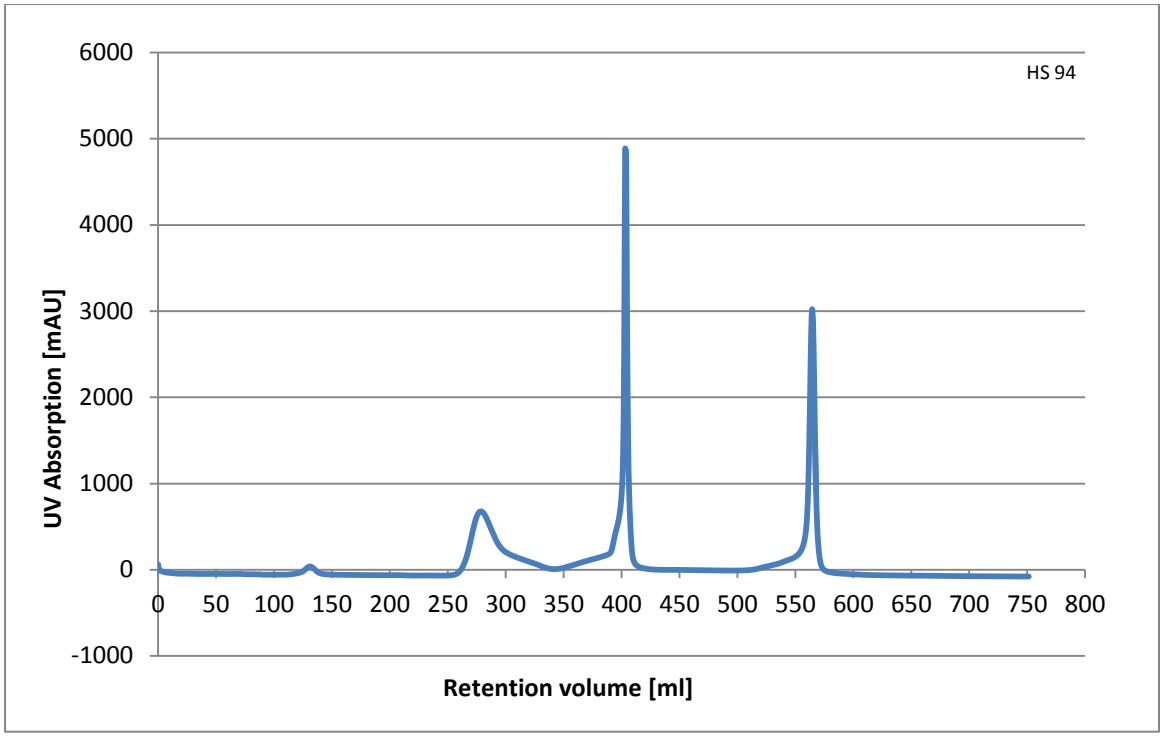

Figure 41: HS 94 Tannermoor

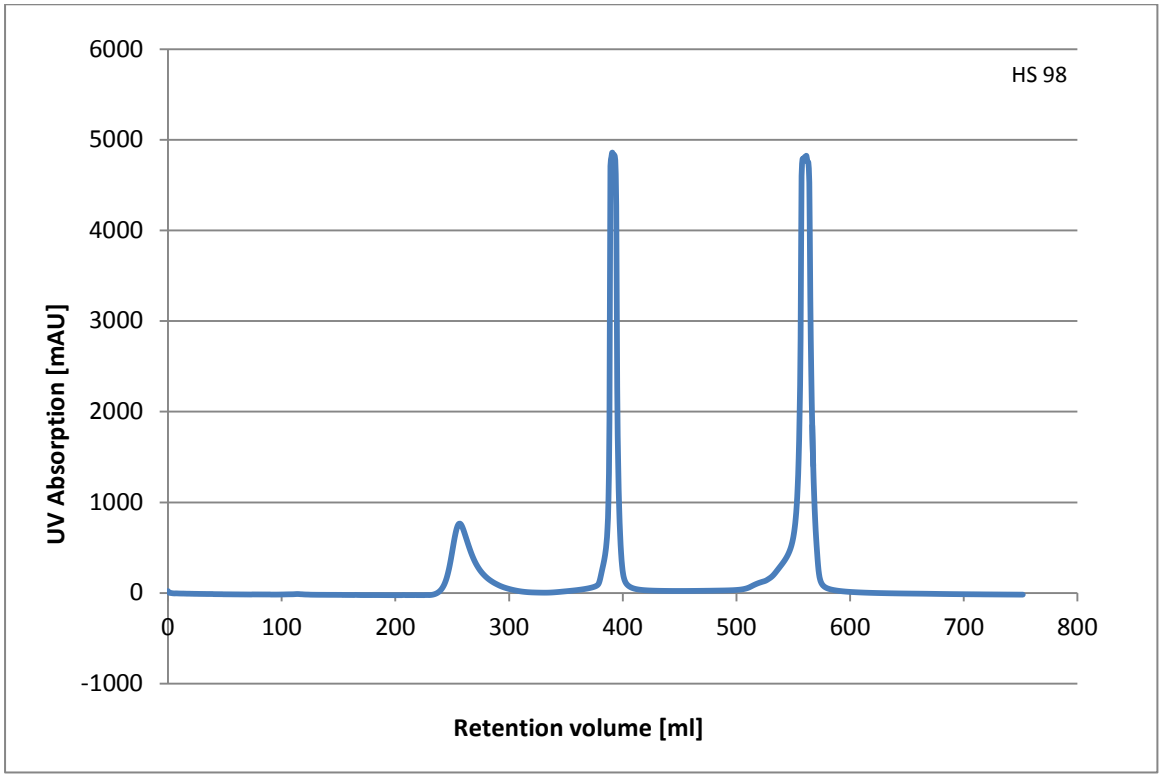

Figure 42: HS 98 Suwannee River

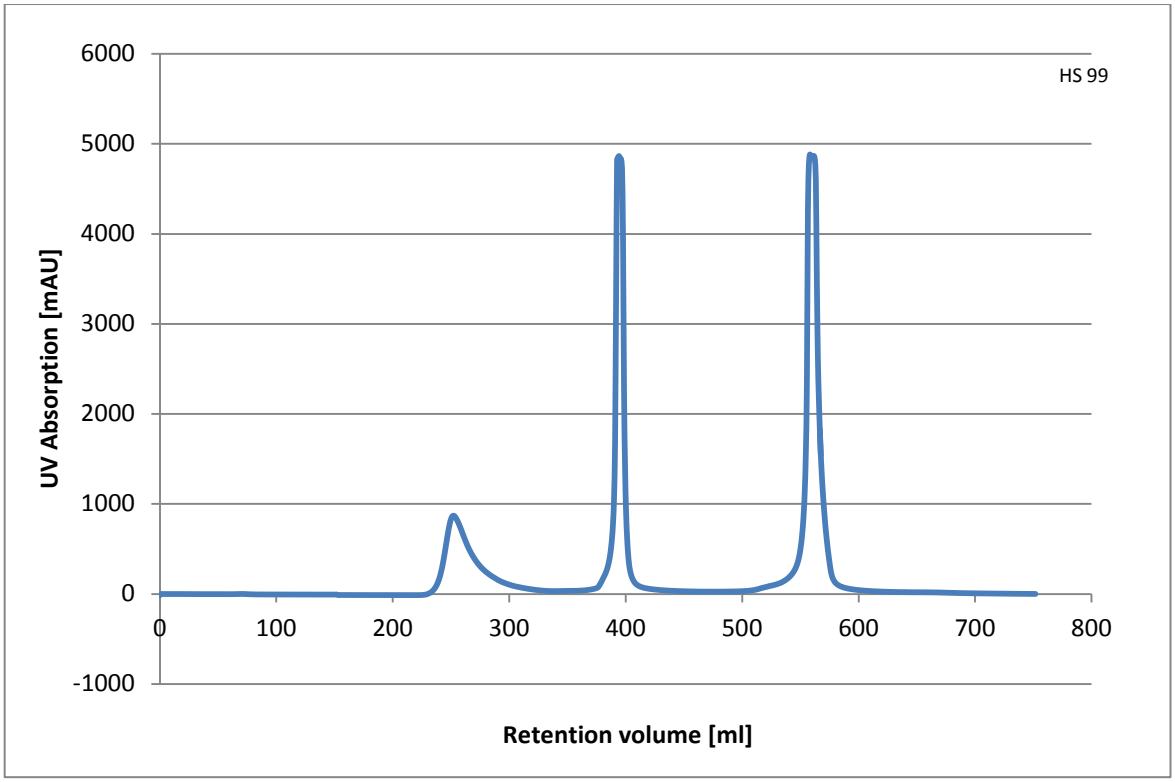

Figure 43: HS 99 Nordic Reservoir

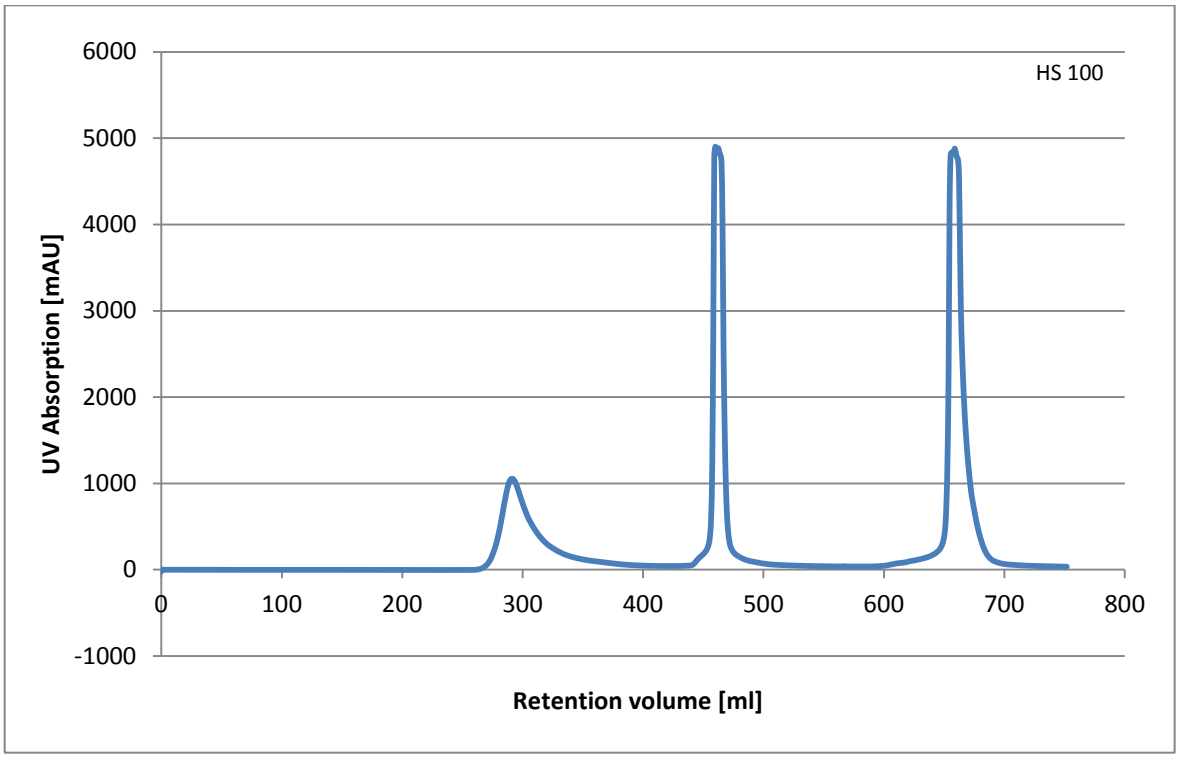

Figure 44: HS 100 Nordic Reservoir

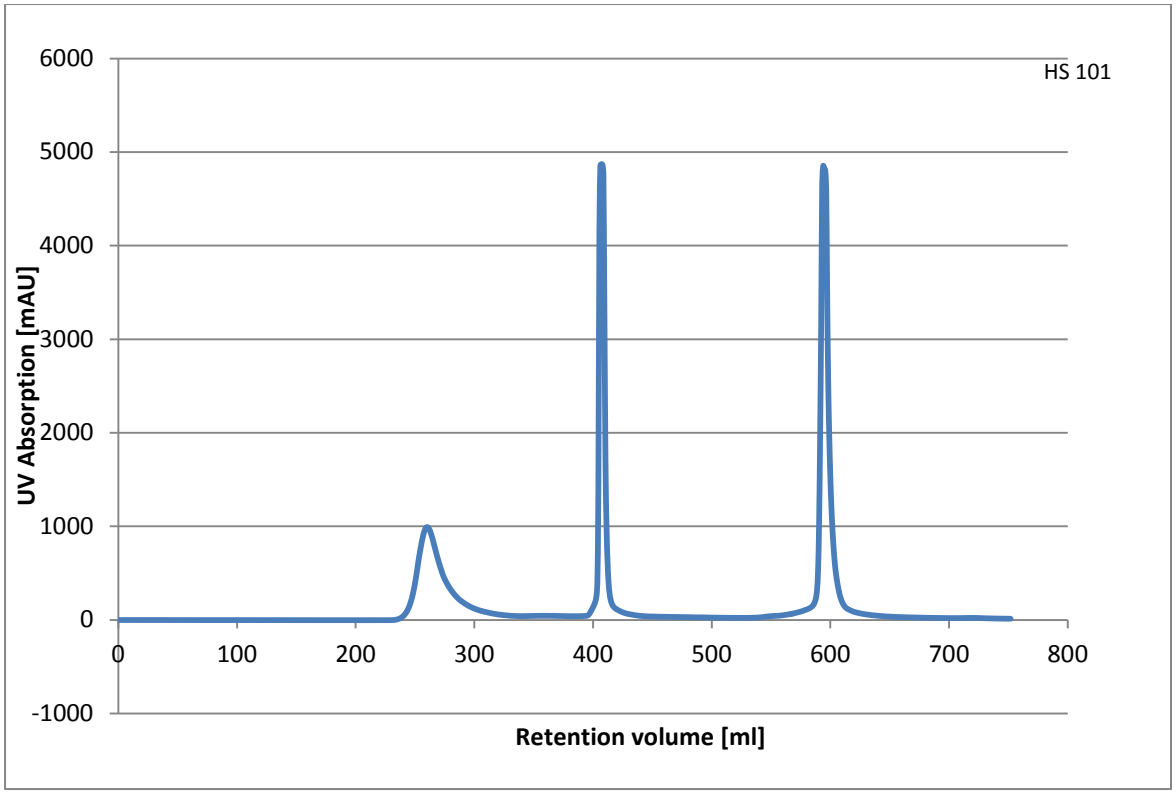

Figure 45: HS 101 Craggie Burn

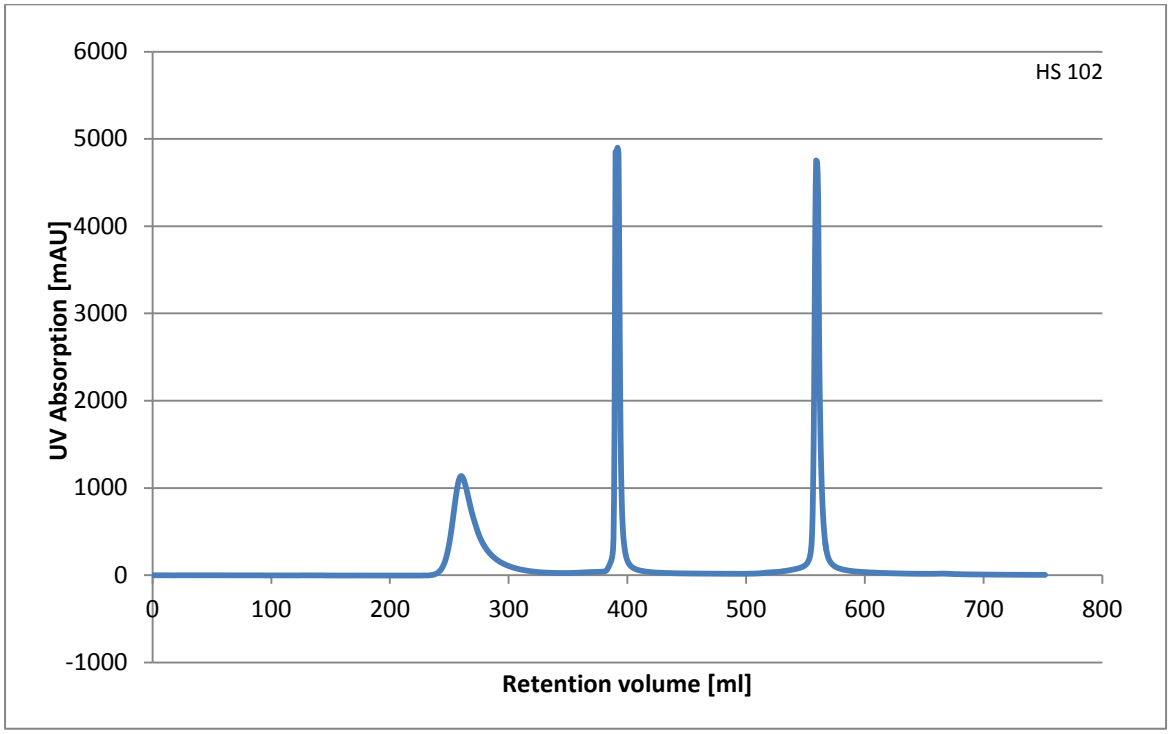

Figure 46: HS 102 Craggie Burn

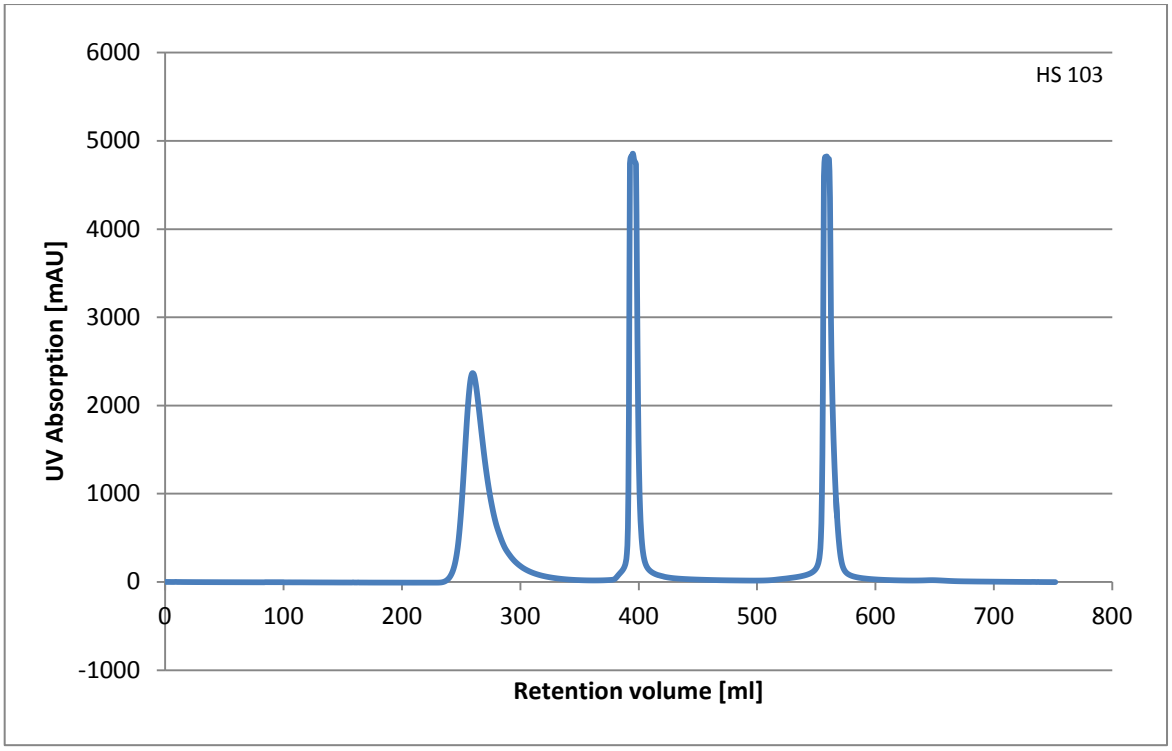

Figure 47: HS 103 Nordic Reservoir

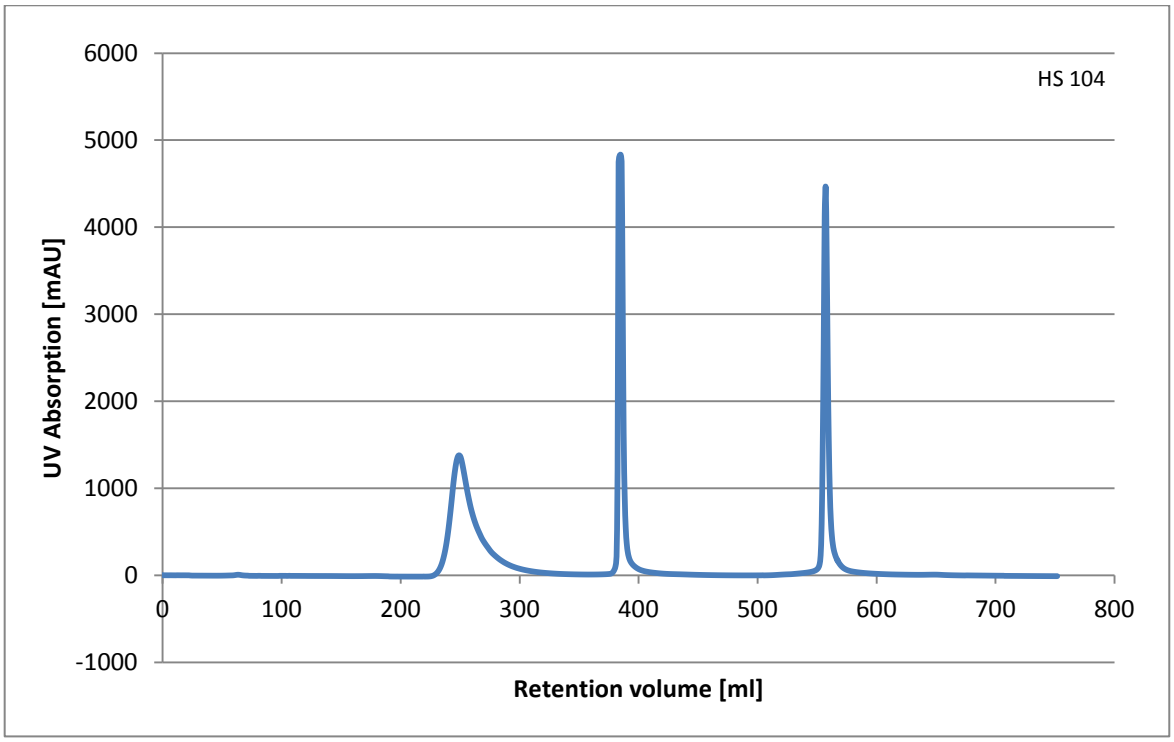

Figure 48: HS 104 Craggie Burn

Tables

Table 5: Results of Run Ito IV (Ferrioxamine)

Run Nr,	Sample	DOC (ng/L)	pH	$FeCl_3$ added (ng)	Fe in Sample (ng)	Sum of Fe from $FeCl_3$ + Sample Fe_S (ng)	cpm (HCl)	cpm (Sample)	Fe solubility Fe_T (ng/L)	log Fe_T (mol/L)
I 1	Seawater	0,00	7.26	558400	0.0	558400	1220	56.3	644219	-4.937
I 2	0.5M HCl	0.0	0.81	558400	0.0	558400	1220	1220	13960000	-
I 3	DMA	4.25	7.19	558400	-	558400	1220	63.3	724317	-4.887
I 4	DMA	4.25	7.21	558400	-	558400	1220	47.6	544668	-5.011
II 1	Seawater	0.00	7.94	10.2	0.0	10.2	1140	51.2	9.07	-9.789
II 2	DMA	4.25	7.93	10.2	-	10.2	1140	75.0	16.8	-9.522
II 3	DMA	4.25	7.95	10.2	-	10.2	1140	72.6	16.2	-9.536
II 4	DMA	4.25	7.93	10.2	-	10.2	1140	74.2	16.6	-9.527
III 1	Seawater	0.00	7.3	102	0.0	102	749	12.4	42.2	-9.119
III 2	CB0	38.75	7.5	102	0.05	102.05	749	12.1	41.4	-9.130
III 3	CB0	38.75	7.4	102	0.05	102.05	749	13.7	46.7	-9.077
III 4	CB0	38.75	7.5	102	0.05	102.05	749	11.2	38.1	-9.165
IV 1	Seawater	0.0	7.3	102	0.0	102	749	5.3	18.0	-9.490
IV 2	CB0	3875	7.6	102	5.3	107.3	749	26.6	95.3	-8.768
IV 3	CB0	387.5	7.6	102	0.53	102.53	749	7.3	25.0	-9.349
IV 4	CB0	38.75	7.6	102	0.05	102.05	749	5.9	20.1	-9.444

Table 6: Results of Run V to VIII (Ferrioxamine)

Run Nr.	Sample	DOC (ng/L)	pH	$FeCl_3$ added (ng)	Fe in Sample (ng)	Sum of Fe from $FeCl_3$ + Sample Fe_S (ng)	cpm (HCl)	cpm (Sample)	Fe Solubility Fe_T (ng/L)	log Fe_T (mol/L)
V 1	Seawater	0.0	6.5	1020	0.0	1020	749	0.5	17.0	-9.516
V 2	CB0	38.75	6.4	1020	0.05	1020.05	749	2.7	91.9	-8.783
V 3	CB0	38.75	6.4	1020	0.05	1020.05	749	6.3	214	-8.415
V 4	CB0	38.75	6.4	1020	0.05	1020.05	749	3.6	123	-8.658
VI 1	Seawater	0.00	7.9	9.5	0.0	9.5	693	8.9	3.05	-10.262
VI 2	CB0	19.38	7.9	9.5	0.03	9.53	693	6.3	2.17	-10.411
VI 3	CB0	19.38	7.8	9.5	0.03	9.53	693	7.6	2.61	-10.330
VI 4	CB0	19.38	7.9	9.5	0.03	9.53	693	5.2	1.79	-10.494
VII 1	Seawater	0.00	7.8	4.75	0.03	4.75	693	4.2	0.72	-10.889
VII 2	CB0	19.38	7.9	4.75	0.03	4.78	693	3.1	0.53	-11.019
VII 3	CB0	19.38	7.8	4.75	0.03	4.78	693	7.5	1.29	-10.635
VII 4	CB0	19.38	7.9	4.75	0.03	4.78	693	3.7	0.64	-10.942
VIII 1	Seawater	0.00	8.0	10.2	0.0	10.2	603	6.5	2.75	-10.307
VIII 2	DMA	4.25	8.0	10.2	-	10.2	603	5.8	2.45	-10.357
VIII 3	DMA	21.25	8.0	10.2	-	10.2	603	5.2	2.20	-10.404
VIII 4	DMA	42.5	7.9	10.2	-	10.2	603	6.2	2.62	-10.328

Table 7: Results of Run IX to XII (Ferrioxamine)

Run Nr.	Sample	DOC (ng/L)	pH	$FeCl_3$ added (ng)	Fe in Sample (ng)	Sum of Fe from $FeCl_3$ + Sample Fe_S (ng)	cpm (HCl)	cpm (Sample)	Fe Solubility Fe_T (ng/L)	log Fe_T (mol/L)
IX 1	Seawater	0.00	7.9	10.2	0.0	10.2	583	8.5	3.72	-10.176
IX 2	CB0	387.5	8.0	10.2	0.53	10.73	583	8.6	3.96	-10.149
IX 3	CB0	387.5	7.9	10.2	0.53	10.73	583	7.8	3.59	-10.192
IX 4	CB0	387.5	7.9	10.2	0.53	10.73	583	7.8	3.59	-10.192
X 1	Seawater	0.0	8.2	0.51	0.0	0.51	505	14.0	0.35	-11.198
X 2	CB2	53.75	8.2	0.51	0.01	0.52	505	16.5	0.42	-11.118
X 3	CB2	53.75	8.2	0.51	0.01	0.52	505	13.7	0.35	-11.199
X 4	CB2	53.75	8.2	0.51	0.01	0.52	505	14.0	0.36	-11.190
XI 1	Seawater	0.00	7.1	0.51	0.0	0.51	505	5.1	0.13	-11.637
XI 2	Seawater	0.00	7.3	0.51	0.0	0.51	505	3.7	0.09	-11.776
XI 3	Seawater	0.00	7.6	0.51	0.0	0.51	505	4.0	0.10	-11.742
XI 4	Seawater	0.00	8.1	0.51	0.0	0.51	505	5.3	0.13	-11.620
XII 1	Seawater	0.00	8.2	0.51	0.0	0.51	208	3.5	0.21	-11.415
XII 2	SR0	115	8.2	0.51	0.054	0.564	208	3.7	0.25	-11.347
XII 3	SR0	115	8.2	0.51	0.054	0.564	208	3.5	0.24	-11.371
XII 4	SR0	115	8.2	0.51	0.054	0.564	208	3.6	0.24	-11.359

Table 8: Results of Run XIII to XIV (Ferrioxamine)

Run Nr.	Sample	DOC (ng/L)	pH	$FeCl_3$ added (ng)	Fe in Sample (ng)	Sum of Fe from $FeCl_3$ + Sample Fe_S (ng)	cpm (HCl)	cpm (Sample)	Fe Solubility Fe_T (ng/L)	log Fe_T (mol/L)
XIII 1	Seawater	0.00	7.9	0.51	0.0	0.51	208	3.9	0.24	-11.368
XIII 2	CB1	130	7.9	0.51	0.05	0.56	208	3.9	0.26	-11.328
XIII 3	CB1	130	8.2	0.51	0.05	0.56	208	3.6	0.24	-11.362
XIII 4	CB1	130	7.9	0.51	0.05	0.56	208	3.4	0.23	-11.387
XIV 1	Seawater	0.00	7.9	0.51	0.0	0.51	208	4.1	0.25	-11.346
XIV 2	CB0	132	7.9	0.51	0.09	0.60	208	4.6	0.33	-11.226
XIV 3	CB0	132	7.9	0.51	0.09	0.60	208	4.3	0.31	-11.255
XIV 4	CB0	132	7.9	0.51	0.09	0.60	208	4	0.29	-11.287

Table 9: Results of Run XV to XVIII (Ferrioxamine)

Run Nr.	Sample	DOC (ng/L)	pH	$FeCl_3$ added (ng)	Fe in Sample (ng)	Sum of Fe from $FeCl_3$ + Sample Fe_S (ng)	cpm (HCl)	cpm (Sample)	Fe Solubility Fe_T (ng/L)	log Fe_T (mol/L)
XV 1	Seawater	0.00	8.0	0.5	0	0.50	2913	0.46	0.001975	-13.45
XV 2	Ferrioxamine	610.24	7.2	0.5	4.5	4.70	2913	0.51	0.020368	-12.44
XV 3	Ferrioxamine	610.24	7.8	0.5	4.5	4.70	2913	0.49	0.019916	-12.45
XV 4	Ferrioxamine	610.24	7.5	0.5	4.5	4.70	2913	0.57	0.023084	-12.38
XVI 1	Seawater	0.00	7.8	0.5	0	0.50	3252	0.51	0.001942	-13.46
XVI 2	Ferrioxamine	1220.49	7.8	0.5	8.4	8.90	3252	0.64	0.043762	-12.11
XVI 3	Ferrioxamine	1220.49	7.7	0.5	8.4	8.90	3252	0.83	0.056813	-11.99
XVI 4	Ferrioxamine	1220.49	7.7	0.5	8.4	8.90	3252	0.85	0.058349	-11.98
XVII 1	Seawater	0.00	7.3	0.5	0	0.50	2633	0.22	0.001066	-13.72
XVII 2	Ferrioxamine	1830.73	7.5	0.5	12.6	13.10	2633	0.63	0.078160	-11.85
XVII 3	Ferrioxamine	1830.73	7.4	0.5	12.6	13.10	2633	0.64	0.079556	-11.85
XVII 4	Ferrioxamine	1830.73	7.5	0.5	12.6	13.10	2633	0.75	0.093513	-11.78
XVIII 1	Seawater	0.00	7.3	0.5	0	0.50	2633	0.27	0.001279	-13.64
XVIII 2	Ferrioxamine	2440.98	7.6	0.5	16.79	17.29	2633	0.68	0.112434	-11.70
XVIII 3	Ferrioxamine	2440.98	7.6	0.5	16.76	17.29	2633	0.65	0.106905	-11.72
XVIII 4	Ferrioxamine	2440.98	7.6	0.5	16.79	17.29	2633	0.65	0.106905	-11.72

Table 10: Results of Run XIX to XXII (Ferrioxamine)

Run Nr.	Sample	Coment	DOC (ng/L)	pH	$FeCl_3$ added (ng)	Fe in Sample (ng)	Sum of Fe from $FeCl_3$ + Sample Fe_S (ng)	cpm (HCl)	cpm (Sample)	Fe Solubility Fe_T (ng/L)	log Fe_T (mol/L)
XIX 1	Seawater		0	7.6	0.5	0	0.50	2331	0.41	0.002199	-13.40
XIX 2	Ferrioxamine		3423.63	7.4	0.5	23.55	24.05	2331	0.76	0.196069	-11.45
XIX 3	Ferrioxamine		3423.63	7.4	0.5	23.55	24.05	2331	0.75	0.193489	-11.46
XIX 4	Ferrioxamine		3423.63	7.7	0.5	23.55	24.05	2331	1.1	0.283784	-11.29
XX 1	Seawater		0	7.6	0.5	0	0.50	2331	0.54	0.002896	-13.28
XX 2	Ferrioxamine		4108.63	7.0	0.5	28.27	28.77	2331	2.1	0.647914	-10.94
XX 3	Ferrioxamine		4108.63	7.1	0.5	28.27	28.77	2331	0.89	0.274592	-11.31
XX 4	Ferrioxamine		4108.63	7.1	0.5	28.27	28.77	2331	1.07	0.330128	-11.23
XXI 1	Seawater		0	7.6	0.5	0	0.50	2260	0.38	0.002102	-13.42
XXI 2	Ferrioxamine		5267.65	7.1	0.5	36.24	36.74	2260	1.43	0.581197	-10.98
XXI 3	Ferrioxamine		5267.65	7.7	0.5	36.24	36.74	2260	0.88	0.357660	-11.19
XXI 4	Ferrioxamine		5267.65	7.1	0.5	36.24	36.74	2260	1.037	0.421470	-11.12
XXII 1	Seawater		0	7.2	0.5	0	0.50	2124	0.3	0.001766	-13.50
XXII 2	Ferrioxamine		6848.63	7.1	0.5	47.12	47.62	2124	2.55	1.429230	-10.59
XXII 3	Ferrioxamine		6848.63	7.2	0.5	47.12	47.62	2124	1.31	0.734232	-10.88
XXII 4	Ferrioxamine	Sample destroyed	6848.63	-	0.5	47.12	47.62	2124			

Table 11: Results of Run XXIII to XXV (Ferrioxamine)

Run Nr.	Sample	Coment	DOC (ng/L)	pH	$FeCl_3$ added (ng)	Fe in Sample (ng)	Sum of Fe from $FeCl_3$ + Sample Fe_S (ng)	cpm (HCl)	cpm (Sample)	Fe Solubility Fe_T (ng/L)	log Fe_T (mol/L)
XXIII 1	Seawater		0	7.3	0.5	0	0.50	2124	0.62	0.003649	-13.18
XXIII 2	Ferrioxamine	Sample destroyed	8217.26	-	0.5	56.53	57.03	2124			
XXIII 3	Ferrioxamine		8217.26	7.5	0.5	56.53	57.03	2124	1.8	1.208363	-10.66
XXIII 4	Ferrioxamine		8217.26	7.3	0.5	56.53	57.03	2124	1.56	1.047248	-10.73
XXIV 1	Seawater		0	7.3	0.5	0	0.50	2124	0.72	0.004237	-13.12
XXIV 2	Tannermoor Peak 1		20	7.5	0.5	0.037	0.537	2124	0.82	0.005182	-13.03
XXIV 3	TM1		20	7.4	0.5	0.037	0.537	2124	1.29	0.008152	-12.84
XXIV 4	TM1		20	7.3	0.5	0.037	0.537	2124	1.5	0.009479	-12.77
XXV 1	Seawater		0	7.2	0.5	0	0.500	1885	0.43	0.002851	-13.29
XXV 2	TM1		40	7.5	0.5	0.074	0.574	1885	0.42	0.003196	-13.24
XXV 3	TM1		40	7.5	0.5	0.074	0.574	1885	0.4	0.003044	-13.26
XXV 4	TM1		40	7.3	0.5	0.074	0.574	1885	0.6	0.004566	-13.09

Table 12: Results Run XXVI to XXVIII (Ferrioxamine)

Run Nr.	Sample	DOC (ng/L)	pH	$FeCl_3$ added (ng)	Fe in Sample (ng)	Sum of Fe from $FeCl_3$ + Sample Fe_S (ng)	cpm (HCl)	cpm (Sample)	Fe Solubility Fe_T (ng/L)	log Fe_T (mol/L)
XXVI 1	Seawater	0	7.5	0.5	0	0.500	1885	0.63	0.004178	-13.13
XXVI 2	TM1	60	7.5	0.5	0.111	0.611	1885	0.65	0.005267	-13.03
XXVI 3	TM1	60	7.5	0.5	0.111	0.611	1885	0.46	0.003728	-13.18
XXVI 4	TM1	60	7.4	0.5	0.111	0.611	1885	1.0	0.008103	-12.84
XXVII 1	Seawater	0	8.1	0.5	0	0.500	1885	5.2	0.034483	-12.21
XXVII 2	TM1	5992.5	7.9	0.5	11.054	11.554	1885	3.2	0.490353	-11.06
XXVII 3	TM1	5992.5	8.0	0.5	11.054	11.554	1885	2.8	0.429059	-11.11
XXVII 4	TM1	5992.5	7.9	0.5	11.054	11.554	1885	2.2	0.337117	-11.22
XXVIII 1	Seawater	0	8.2	0.5	0	0.500	1885	1.8	0.011936	-12.67
XXVIII 2	TM1	4982	8.0	0.5	9.19	9.690	1885	2.1	0.269879	-11.32
XXVIII 3	TM1	4982	7.9	0.5	9.19	9.690	1885	2.0	0.257028	-11.34
XXVIII 4	TM1	4982	7.9	0.5	9.19	9.690	1885	2.0	0.257028	-11.34

Table 13: Results of Tannermoor Fraction Peak 0

Run Nr.	Sample	DOC (µg/L)	pH	$FeCl_3$ added (ng)	Fe in Sample (ng)	Sum of Fe from $FeCl_3$ + Sample Fe_S (ng)	cpm (HCl)	cpm (Sample)	Fe Solubility Fe_T (ng/L)	log Fe_T (mol/L)
TM0 0.1	Seawater	0.00	7.6	0.5	0.0	0.5	3243	62.6	0.241289	-11.36
TM0 0.2	Seawater	0.00	7.4	0.5	0.0	0.5	2889	83.6	0.361717	-11.19
TM0 2.1	Tannermoor Peak 0	2.00	7.2	1.68	2.9	4.58	3243	61.5	2.171369	-10.41
TM0 2.2	TM0	2.00	7.5	1.68	2.9	4.58	3148	60.0	2.182338	-10.41
TM0 4.1	TM0	3.99	7.6	3.36	5.3	8.66	2889	77.4	5.800312	-9.98
TM0 4.2	TM0	3.99	7.4	3.36	5.3	8.66	2889	66.5	4.983472	-10.05
TM0 6.1	TM0	5.99	7.4	5.04	7.7	12.74	2889	51.6	5.688681	-9.99
TM0 6.2	TM0	5.99	7.3	5.04	7.7	12.74	2889	79.8	8.797612	-9.80
TM0 8.1	TM0	7.98	7.5	6.72	10.1	16.82	2889	68.8	10.013984	-9.75
TM0 8.2	TM0	7.98	7.5	6.72	10.1	16.82	2889	74.4	10.829076	-9.71
TM0 10.1	TM0	9.98	6.2	8.40	12.5	20.90	3243	404	65.090965	-8.93
TM0 10.2	TM0	9.98	7.3	8.40	12.5	20.90	2889	60.7	10.978107	-9.71
TM0 12	TM0	11.97	7.4	10.08	14.9	24.98	3148	65.0	12.894695	-9.64
TM0 14	TM0	13.97	7.5	11.76	17.3	29.06	3148	63.0	14.539231	-9.58
TM0 16	TM0	15.96	7.6	13.44	19.7	33.14	3148	62.0	16.317344	-9.53
TM0 18	TM0	17.96	7.7	15.12	22.1	37.21	3243	48.9	14.026896	-9.60

Table 14: Results of Tannermoor Fraction Peak 0

Run Nr.	Sample	DOC (µg/L)	pH	$FeCl_3$ added (ng)	Fe in Sample (ng)	Sum of Fe from $FeCl_3$ + Sample Fe_S (ng)	cpm (HCl)	cpm (Sample)	Fe Solubility Fe_T (ng/L)	log Fe_T (mol/L)
TM0 20	TM0	19.95	7.3	16.80	24.5	41.29	3243	62.8	19.989300	-9.45
TM0 22	TM0	21.95	7.7	18.48	26.9	45.37	3243	51	17.837419	-9.50
TM0 24	TM0	23.94	6.9	20.16	29.3	49.45	3243	124	47.269504	-9.07
TM0 26	TM0	25.94	7.0	21.84	31.7	53.53	3243	149	61.486047	-8.96
TM0 28	TM0	28.07	7.0	23.64	34.1	57.73	3243	233	103.693262	-8.73
TM0 30	TM0	30.07	7.0	25.32	36.5	61.81	3243	235	111.974638	-8.70
TM0 32	TM0	32.06	7.0	27.00	38.9	65.89	3243	207	105.143617	-8.72
TM0 34	TM0	34.07	7.0	16.68	41.3	57.97	3243	265	142.939023	-8.59
TM0 36	TM0	36.05	6.9	30.36	43.7	74.05	3243	228	130.152636	-8.63
TM0 38	TM0	38.05	7.0	32.04	46.1	78.13	3243	233	140.335261	-8.60
TM0 40	TM0	40.04	7.0	33.72	48.5	82.21	3148	235	153.425588	-8.56
TM0 42	TM0	42.04	7.0	35.40	50.9	86.29	3148	283	193.933212	-8.46
TM0 44	TM0	44.03	7.2	37.08	53.3	90.37	3148	207	148.559323	-8.57
TM0 46	TM0	46.03	7.0	38.76	56.2	94.95	3148	334	251.852764	-8.35
TM0 48	TM0	48.02	7.0	40.44	58.1	98.53	3148	310	242.569091	-8.36
TM0 50	TM0	50.02	7.0	42.12	60.5	102.61	3148	332	270.540978	-8.31

Table 15: Results Run XXIX to XXXI (Ferrioxamine)

Run Nr.	Sample	DOC (µg/L)	pH	$FeCl_3$ added (ng)	Fe in Sample (ng)	Sum of Fe from $FeCl_3$ + Sample Fe_S (ng)	cpm (HCl)	cpm (Sample)	Fe Solubility Fe_T (ng/L)	log Fe_T (mol/L)
XXIX 1	Meerwasser	0	7.0	0.5	0	0.5	2595	126	0.606936	-10.96
XXIX 2	Ferrioxamin	2.5	7.0	0.5	17.048	17.548	2595	315	53.252601	-9.02
XXIX 3	Ferrioxamin	2.5	6.9	0.5	17.048	17.548	2595	240	40.573410	-9.14
XXIX 4	Ferrioxamin	2.5	6.4	0.5	17.048	17.548	2595	243	41.080578	-9.13
XXX 1	Meerwasser	0	6.8	0.5	0	0.5	2485	130	0.653924	-10.93
XXX 2	Ferrioxamin	1.5	6.8	0.5	10.229	10.729	2485	218	23.530402	-9.38
XXX 3	Ferrioxamin	1.5	7.1	0.5	10.229	10.729	2485	175	18.889085	-9.47
XXX 4	Ferrioxamin	1.5	7.0	0.5	10.229	10.729	2485	137	14.787455	-9.58
XXXI 1	Meerwasser	0	7.2	0.5	0	0.5	2485	82	0.412475	-11.13
XXXI 2	Ferrioxamin	1.0	6.6	0.5	6.819	7.319	2485	128	9.424869	-9.77
XXXI 3	Ferrioxamin	1.0	7.0	0.5	6.819	7.319	2485	147	10.823873	-9.71
XXXI 4	Ferrioxamin	1.0	6.8	0.5	6.819	7.319	2485	178	13.106459	-9.63

Table 16: Results of Ferrioxamine with different equilibration times

Run Nr.	Sample	DOC (µg/L)	pH	$FeCl_3$ added (ng)	Fe in Sample (ng)	Sum of Fe from $FeCl_3$ + Sample Fe_S (ng) (ng)	cpm (HCl)	cpm (Sample)	Fe Solubility Fe_T (ng/L)	log Fe_T (mol/L)
MW 2D	Seawater	0	7.7	0.5	0	0.5	2889	724	3.132572	-10.25
FOD 2D	Ferrioxamine	2.0	8.0	0.5	13.638	14.138	2889	357	43.676584	-9.11
FOD 3D.1	FO	2.0	7.8	0.5	13.638	14.138	2889	124	15.170578	-9.57
FOD 3D.2	FO	2.0	7.8	0.5	13.638	14.138	2889	884	108.151540	-8.71
FOD 7D.1	FO	2.0	7.9	0.5	13.638	14.138	2595	123	16.753121	-9.52
FOD 7D.2	FO	2.0	7.8	0.5	13.638	14.138	2595	113	15.391079	-9.56
FO MW 8D	Seawater	0	7.7	0.5	0	0.5	2595	115	0.553950	-11.00
FOD 8D	FO	2.0	7.7	0.5	13.638	14.138	2595	156	21.247861	-9.42
FOD 1a 14d	FO	2.0	7.5	0.5	13.638	14.138	2312	651	99.522470	-8.75
FOD 2a 14d	FO	2.0	7.6	0.5	13.638	14.138	2312	107	16.357764	-9.53

Table 17: Results of Ferrioxamine with concentration 0 [Fe']

Run Nr.	Sample	DOC (µg/L)	pH	$FeCl_3$ added (ng)	Fe in Sample (ng)	Sum of Fe from $FeCl_3$ + Sample Fe_S (ng)	cpm (HCl)	cpm (Sample)	Fe Solubility Fe_T (ng/L)	log Fe_T (mol/L)
FO MW 1	Seawater	0	8.3	0.5	0	0.5	2312	259	1.400303	-10.60
FO MW 2	Seawater	0	8.3	0.5	0	0.5	2312	560	3.027682	-10.27
FO MW 3	Seawater	0	8.2	0.5	0	0.5	2312	757	4.092777	-10.13
FO MW 4	Seawater	0	8.2	0.5	0	0.5	2312	784	4.238754	-10.12

Table 18: Results of Ferrioxamine with different concentrations

Run	Sample	DOC (µg/L)	pH	$FeCl_3$ added (ng)	Fe in Sample (ng)	Sum of Fe from $FeCl_3$ + Sample Fe_S (ng)	cpm (HCl)	cpm (Sample)	Fe Solubility Fe_T (ng/L)	log Fe_T (mol/L)
FOX 1	Ferrioxamine	0.4	8.3	0.5	2.728	3.228	2312	487	16.998659	-9.52
FOX 2	Ferrioxamine	0.4	8.3	0.5	2.728	3.228	2312	367	12.810078	-9.64
FOB 1	Ferrioxamine	1.0	8.2	0.5	6.819	7.319	2312	483	38.225314	-9.16
FOB 2	Ferrioxamine	1.0	8.3	0.5	6.819	7.319	2312	274	21.684753	-9.41
FOD 1	Ferrioxamine	2.0	8.2	0.5	13.638	14.138	2312	653	99.828222	-8.75
FOD 2	Ferrioxamine	2.0	8.2	0.5	13.638	14.138	2312	461	70.475973	-8.90
FOF 1	Ferrioxamine	3.0	8.3	0.5	20.458	20.958	2312	489	110.818144	-8.70
FOF 2	Ferrioxamine	3.0	8.3	0.5	20.458	20.958	2312	619	140.279001	-8.60
FOG 1	Ferrioxamine	4.0	8.2	0.5	27.277	27.777	2312	730	219.260489	-8.41
FOG 2	Ferrioxamine	4.0	8.1	0.5	27.277	27.777	2312	426	127.952011	-8.64
FOI 1	Ferrioxamine	6.0	8.2	0.5	34.096	34.596	2312	236	88.285640	-8.80
FOI 2	Ferrioxamine	6.0	8.3	0.5	34.096	34.596	2312	674	252.137803	-8.34
FOJ 1	Ferrioxamine	8.0	8.2	0.5	40.915	41.415	2312	747	334.526438	-8.22
FOJ 2	Ferrioxamine	8.0	8.2	0.5	40.915	41.415	2312	1153	516.344020	-8.03
FOK 1	Ferrioxamine	10.0	8.2	0.5	54.554	55.054	2312	875	520.893707	-8.03
FOK 2	Ferrioxamine	10.0	8.2	0.5	54.554	55.054	2312	981	583.996259	-7.98

Table 19: Results Run XXII to XXXIII (Ferrioxamine)

Run Nr.	Sample	Coment	DOC (µg/L)	pH	$FeCl_3$ added (ng)	Fe in Sample (ng)	Sum of Fe from $FeCl_3$ + Sample Fe_S (ng)	cpm (HCl)	cpm (Sample)	Fe Solubility Fe_T (ng/L)	log Fe_T (mol/L)
XXXII 1	Seawater	Not centrifuged	0	8.3	10	0	10	1363	349	64.013206	-8.94
XXXII 2	Ferrioxamine	Not centrifuged	1.0	8.3	10	6.882	16.882	1363	338	104.660968	-8.73
XXXII 3	Ferrioxamine	Not centrifuged	2.0	8.3	10	13.764	23.764	1363	269	117.250844	-8.68
XXXII 4	Ferrioxamine	Not centrifuged.	4.0	8.3	10	17.205	27.205	1363	265	132.232667	-8.63
XXXII 5	Ferrioxamine	Not centrifuged	6.0	8.3	10	20.646	30.646	1363	355	199.547506	-8.45
XXXII 6	Ferrioxamine	Not centrifuged	8.0	8.3	10	27.528	37.528	1363	269	185.161996	-8.48
XXXIII 1	Seawater		0	8.4	10	0.000	10.000	1363	229	42.002935	-9.12
XXXIII 2	Ferrioxamine		1.0	8.3	10	6.882	16.882	1363	115	35.609501	-9.20
XXXIII 3	Ferrioxamine		2.0	8.3	10	13.764	23.764	1363	169	73.663169	-8.88
XXXIII 4	Ferrioxamine		4.0	8.3	10	17.205	27.205	1363	231	115.266966	-8.68
XXXIII 5	Ferrioxamine		6.0	8.3	10	20.646	30.646	1363	230	129.284299	-8.64
XXXIII 6	Ferrioxamine		8.0	8.3	10	27.528	37.528	1363	331	227.838738	-8.39

Table 20: Results of Tannermoor fraction Peak 0

Run	Sample	DOC (µg/L)	pH	$FeCl_3$ added (ng)	Fe in Sample (ng)	Sum of Fe from $FeCl_3$ + Sample Fe_S (ng)	cpm (HCl)	cpm (Sample)	Fe Solubility Fe_T (ng/L)	log Fe_T (mol/L)
TM0 MW	Seawater	0	8.3	0.5	0	0.5	2165	923	5.329099	-10.02
TM0 1	Tannermoor Peak 0	1.0		1.35	1.35	2.70	2165	605	18.862587	-9.47
TM0 2	TM0	2.0	8.2	2.7	2.69	5.39	2165	533	33.174018	-9.23
TM0 5	TM0	5.0	8.1	6.75	6.73	13.48	2165	373	58.060508	-8.98
TM0 10	TM0	10.0	7.9	13.5	13.48	26.98	2165	227	70.721247	-8.90
TM0 15	TM0	14.96	8.3	20	20.18	40.18	2165	420	194.868360	-8.46
TM0 20	TM0	20.02		27	26.97	53.97	2165	401	249.907275	-8.35
TM0 30	TM0	30.07	8.2	40.5	40.01	80.51	2165	344	319.808776	-8.24
TM0 40	TM0	40.04	8.2	54	53.93	107.93	2165	294	366.413626	-8.18
TM0 50	TM0	50.02	8.1	67.5	66.98	134.48	2165	228	354.058199	-8.20

Table 21: Results of Tannermoor fraction Peak 1

Run	Sample	DOC (µg/L)	pH	$FeCl_3$ added (ng)	Fe in Sample (ng)	Sum of Fe from $FeCl_3$ + Sample Fe_S (ng)	cpm (HCl)	cpm (Sample)	Fe Solubility Fe_T (ng/L)	log Fe_T (mol/L)
TM1 MW	Seawater	0	8.4	0.5	0	0.5	1532	140	1.142298	0.020471
TM1 1	Tannermoor Peak 1	1.00	8.4	1.85	1.84	3.69	1532	213	12.825881	0.229855
TM1 2	TM1	2.02	8.3	3.70	3.72	7.42	1532	126	15.256527	0.273414
TM1 5	TM1	4.99	8.1	9.25	9.21	18.46	1532	73	21.990535	0.394096
TM1 10	TM1	9.98	8.4	18.50	18.42	36.92	1532	190	114.471279	2.051457
TM1 15	TM1	15.04	8.3	27.50	27.74	55.24	1532	267	240.683420	4.313323
TM1 20	TM1	20.16	8.3	37.00	37.19	74.19	1532	170	205.814295	3.688428
TM1 30	TM1	30.08	8.2	55.50	55.48	110.98	1532	276	499.844648	8.957789
TM1 40	TM1	40.00	8.2	74.00	73.78	147.78	1532	207	499.191580	8.946086
TM1 50	TM1	49.92	8.1	92.5	92.08	184.58	1532	208	626.511749	11.227809

Table 22: Results of Tannermoor fraction Peak 2

Run	Sample	DOC (µg/L)	pH	$FeCl_3$ added (ng)	Fe in Sample (ng)	Sum of Fe from $FeCl_3$ + Sample Fe_S (ng)	cpm (HCl)	cpm (Sample)	Fe Solubility Fe_T (ng/L)	log Fe_T (mol/L)
TM2 MW	Seawater	0	8.2	0.5	0	0.5	1971	711	4.509132	-10.09
TM2 1	Tannermoor Peak 2	1.00	8.2	1.6	1.58	3.18	1971	574	23.152207	-9.38
TM2 2	TM2	2.00	8.3	3.15	3.16	6.31	1971	61	4.882166	-10.06
TM2 5	TM2	4.99	8.1	7.95	7.91	15.86	1971	81	16.294521	-9.53
TM2 10	TM2	9.98	7.8	15.9	15.82	31.72	1971	66	26.554033	-9.32
TM2 15	TM2	14.96	8.3	24	23.73	47.73	1754	82	55.784778	-9.00
TM2 20	TM2	19.95	8.2	31.5	31.64	63.14	1754	443	398.674743	-8.15
TM2 30	TM2	29.93	8.2	47.5	47.46	94.96	1754	347	469.656784	-8.07
TM2 40	TM2	39.90	8.2	63.5	63.28	126.78	1754	88	159.017104	-8.55
TM2 50	TM2	49.88	8.2	79.5	79.10	158.60	1754	72	162.759407	-8.54

Table 23: Results of Suwannee River fraction Peak 0

Run	Sample	DOC (µg/L)	pH	$FeCl_3$ added (ng)	Fe in Sample (ng)	Sum of Fe from $FeCl_3$ + Sample Fe_S (ng)	cpm (HCl)	cpm (Sample)	Fe Solubility Fe_T (ng/L)	log Fe_T (mol/L)
SR0 MW	Seawater	0	8.3	0.5	0	0.5	2165	769	4.439954	-10.10
SR0 1	Suwannee River Peak 0	1.0	8.2	1.35	1.35	2.70	2165	616	19.205543	-9.46
SR0 2	SR0	2.0		2.7	2.69	5.39	2165	644	40.082679	-9.14
SR0 5	SR0	5.0	8.1	6.75	6.73	13.48	2165	368	57.282217	-8.99
SR0 10	SR0	10.02	7.9	13.5	13.48	26.98	2165	231	71.967436	-8.89
SR0 15	SR0	14.99	8.3	20	20.18	40.18	2165	460	213.427252	-8.42
SR0 20	SR0	20.03		27	26.97	53.97	2165	418	260.501848	-8.33
SR0 30	SR0	29.73	8.2	40.5	40.01	80.51	2165	501	465.768014	-8.08
SR0 40	SR0	40.07	8.2	54	53.93	107.93	2165	260	324.039261	-8.24
SR0 50	SR0	49.76	8.1	67.5	66.98	134.48	2165	239	371.139954	-8.18

Table 24: Results of Suwannee River fraction Peak 1

Run	Sample	DOC (µg/L)	pH	$FeCl_3$ added (ng)	Fe in Sample (ng)	Sum of Fe from $FeCl_3$ + Sample Fe_S (ng)	cpm (HCl)	cpm (Sample)	Fe Solubility Fe_T (ng/L)	log Fe_T (mol/L)
SR1 MW	Seawater	0	8.4	0.5	0	0.5	1532	176	1.436031	0.025735
SR1 1	Suwannee River Peak 1	1.00	8.4	1.85	1.85	3.70	1532	266	16.060705	0.287826
SR1 2	SR1	2.01	8.3	3.70	3.70	7.40	1532	160	19.321149	0.346257
SR1 5	SR1	4.99	8.1	9.25	9.20	18.45	1532	140	42.150783	0.755390
SR1 10	SR1	9.97	8.4	18.50	18.39	36.89	1532	162	97.522520	1.747715
SR1 15	SR1	14.89	8.4	27.50	27.47	54.97	1532	111	99.570333	1.784415
SR1 20	SR1	20.07	8.3	37.00	37.02	74.02	1532	142	171.521540	3.073863
SR1 30	SR1	30.11	8.2	55.50	55.54	111.04	1532	107	193.885117	3.474644
SR1 40	SR1	40.15	8.2	74.00	74.05	148.05	1532	136	328.570496	5.888360
SR1 50	SR1	49.86	8.0	92.5	91.96	184.46	1532	117	352.183747	6.311537

Table 25: Results of Suwannee River fraction Peak 2

Run	Sample	DOC (µg/L)	pH	$FeCl_3$ added (ng)	Fe in Sample (ng)	Sum of Fe from $FeCl_3$ + Sample Fe_S (ng)	cpm (HCl)	cpm (Sample)	Fe Solubility Fe_T (ng/L)	log Fe_T (mol/L)
SR2 MW	Seawater	0	8.2	0.5	0	0.5	1971	547	3.469051	0.062169
SR2 1	Suwannee River Peak 2	0.99	8.3	1.6	1.58	3.18	1971	538	21.700152	0.388892
SR2 2	SR2	2.01	8.3	3.15	3.16	6.31	1971	67	5.362380	0.096100
SR2 5	SR2	4.99	8.1	7.95	7.91	15.86	1971	71	14.282851	0.255965
SR2 10	SR2	9.95	7.8	15.9	15.82	31.72	1971	34	13.679351	0.245150
SR2 15	SR2	15.02	8.3	24	23.73	47.73	1971	64	38.745814	0.694369
SR2 20	SR2	20.09	8.2	31.5	31.64	63.14	1971	34	27.229325	0.487981
SR2 30	SR2	30.03	8.2	47.5	47.46	94.96	1971	329	396.268899	7.101593
SR2 40	SR2	39.98	8.2	63.5	63.28	126.78	1971	43	69.146880	1.239191
SR2 50	SR2	49.92	8.1	79.5	79.10	158.60	1971	49	98.571791	1.766520

Table 26: Results of Craggie Burn fraction Peak 0

Run	Sample	Coment	DOC (ng/L)	pH	$FeCl_3$ added (ng)	Fe in Sample (ng)	Sum of Fe from $FeCl_3$ + Sample Fe_S (ng)	cpm (HCl)	cpm (Sample)	Fe Solubility Fe_T (ng/L)	log Fe_T (mol/L)
CB0 MW	Seawater		0	8.2	20	0	20	1122	181	80.659537	-8.84
CB0 1	Craggie Burn Peak 0	precipitate	1.00	8.2	20	1.35	21.35	1122	140	66.599822	-8.92
CB0 2	CB0		2.00	8.3	20	2.69	22.69	1122	246	124.370321	-8.65
CB0 5	CB0		4.95	8.3	20	6.66	26.66	1122	207	122.963904	-8.66
CB0 10.1	CB0		10.01	8.3	20	13.47	33.47	1122	234	174.509358	-8.50
CB0 10.2	CB0		10.01	8.4	20	13.47	33.47	1122	209	155.865196	-8.55
CB0 15.1	CB0		14.96	8.2	20	20.13	40.13	1122	164	146.642602	-8.58
CB0 15.2	CB0		14.96	8.3	20	20.13	40.13	1122	200	178.832442	-8.49
CB0 20.1	CB0		20.02	8.2	20	26.94	46.94	1122	172	179.894831	-8.49
CB0 20.2	CB0		20.02	8.4	20	26.94	46.94	1122	321	335.733957	-8.22

Table 27: Results of Craggie Burn fraction Peak 1

Run	Sample	DOC (µg/L)	pH	$FeCl_3$ added (ng)	Fe in Sample (ng)	Sum of Fe from $FeCl_3$ + Sample Fe_S (ng)	cpm (HCl)	cpm (Sample)	Fe Solubility Fe_T (ng/L)	log Fe_T (mol/L)
CB1 MW	Seawater		8.3	20	0	20	1122	167	74.420677	-8.87
CB1 1	Craggie Burn Peak 1	1.00	8.3	20	1.84	21.84	1122	131	63.748663	-8.94
CB1 2	CB1	2.00	8.3	20	3.69	23.69	1122	201	106.098262	-8.72
CB1 5	CB1	5.00	8.3	20	9.21	29.21	1122	191	124.311720	-8.65
CB1 10.1	CB1	9.99	8.2	20	18.43	38.43	1122	207	177.250668	-8.50
CB1 10.2	CB1	9.99	8.3	20	18.43	38.43	1122	209	178.963235	-8.49
CB1 15.1	CB1	14.99	8.2	20	27.64	47.64	1122	186	197.438503	-8.45
CB1 15.2	CB1	14.99	8.2	20	27.64	47.64	1122	221	234.590909	-8.38
CB1 20.1	CB1	19.98	8.1	20	36.86	56.86	1122	149	188.773173	-8.47
CB1 20.2	CB1	19.98	8.3	20	36.86	56.86	1122	201	254.653743	-8.34

Table 28: Results of Craggie Burn fraction Peak 2

Run	Sample	DOC (µg/L)	pH	$FeCl_3$ added (ng)	Fe in Sample (ng)	Sum of Fe from $FeCl_3$ + Sample Fe_S (ng)	cpm (HCl)	cpm (Sample)	Fe Solubility Fe_T (ng/L)	log Fe_T (mol/L)
CB2 MW	Seawater	0.00	8.2	20	0	20.00	330	5	7.575758	-9.87
CB2 1	Craggie Burn Peak 2	1.00	8.2	20	1.58	21.58	330	5.9	9.647279	-9.76
CB2 2	CB2	2.02	8.2	20	3.21	23.21	330	6.9	12.131289	-9.66
CB2 5	CB2	5.00	8.2	20	7.92	27.92	330	6.1	12.901832	-9.64
CB2 10.1	CB2	9.90	8.2	20	15.68	35.68	330	5.7	15.405826	-9.56
CB2 10.2	CB2	9.90	8.3	20	15.68	35.68	330	6.6	17.838325	-9.50
CB2 15.1	CB2	14.97	8.2	20	23.72	43.72	330	7.7	25.500975	-9.34
CB2 15.2	CB2	14.97	8.2	20	23.72	43.72	330	6	19.870890	-9.45
CB2 20.1	CB2	20.05	8.2	20	31.76	51.76	330	7.1	27.838059	-9.30
CB2 20.2	CB2	20.05	8.2	20	31.76	51.76	330	5.9	23.133035	-9.38

Table 29: Results of Nordic Reservoir fraction Peak 0

Run	Sample	Coment	DOC (ng/L)	pH	$FeCl_3$ added (ng)	Fe in Sample (ng)	Sum of Fe from $FeCl_3$ + Sample Fe_S (ng)	cpm (HCl)	cpm (Sample)	Fe Solubility Fe_T (ng/L)	log Fe_T (mol/L)
NR0 MW	Seawater		0	8.2	20	0	20	1122	127	56.595365	-8.99
NR0 1	Nordic reservoir Peak 0	Precipitate!	1.00	8.2	20	1.35	21.35	1122	167	79.444073	-8.85
NR0 2	NR0		2.01	8.3	20	2.70	22.70	1122	251	126.954100	-8.64
NR0 5	NR0		5.01	8.3	20	6.74	26.74	1122	89	53.027184	-9.02
NR0 10.1	NR0		10.02	8.3	20	13.48	33.48	1122	184	137.262032	-8.61
NR0 10.2	NR0		10.02	8.3	20	13.48	33.48	1122	177	132.040107	-8.63
NR0 15.1	NR0		15.15	8.3	20	20.38	40.38	1122	288	259.122995	-8.33
NR0 15.2	NR0		15.15	8.2	20	20.38	40.38	1122	234	210.537433	-8.42
NR0 20.1	NR0		20.10	8.3	20	27.05	47.05	1122	208	218.057041	-8.41
NR0 20.2	NR0		20.10	8.3	20	27.05	47.05	1122	146	153.059269	-8.56

Table 30: Results of Nordic Reservoir fraction Peak 1

Run	Sample	DOC (µg/L)	pH	$FeCl_3$ added (ng)	Fe in Sample (ng)	Sum of Fe from $FeCl_3$ + Sample Fe_S (ng)	cpm (HCl)	cpm (Sample)	Fe Solubility Fe_T (ng/L)	log Fe_T (mol/L)
NR1 MW	Seawater	0	8.4	20	0	20	1122	90	40.106952	-9.14
NR1 1	Nordic reservoir Peak 1	1.00	8.2	20	1.85	21.85	1122	131	63.777852	-8.94
NR1 2	NR1	2.01	8.2	20	3.70	23.70	1122	98	51.751337	-9.03
NR1 5	NR1	5.02	8.2	20	9.25	29.25	1122	94	61.263369	-8.96
NR1 10.1	NR1	10.03	8.3	20	18.51	38.51	1122	94	80.658200	-8.84
NR1 10.2	NR1	10.03	8.2	20	18.51	38.51	1122	185	158.742201	-8.55
NR1 15.1	NR1	14.97	8.2	20	27.62	47.62	1122	92	97.616756	-8.76
NR1 15.2	NR1	14.97	8.3	20	27.62	47.62	1122	121	128.387255	-8.64
NR1 20.1	NR1	20.06	8.3	20	37.01	57.01	1122	106	134.649287	-8.62
NR1 20.2	NR1	20.06	8.2	20	37.01	57.01	1122	163	207.055036	-8.43

Table 31: Results of Nordic Reservoir fraction Peak 2

Run	Sample	DOC (µg/L)	pH	$FeCl_3$ added (ng)	Fe in Sample (ng)	Sum of Fe from $FeCl_3$ + Sample Fe_S (ng)	cpm (HCl)	cpm (Sample)	Fe Solubility Fe_T (ng/L)	log Fe_T (mol/L)
NR2 MW	Seawater	0	8.3	20	0	20.00	330	5	7.575758	-9.87
NR2 1	Nordic reservoir Peak 2	1.00	8.3	20	1.59	21.59	330	22	35.976998	-9.19
NR2 2	NR2	2.00	8.2	20	3.17	23.17	330	29.5	51.786798	-9.03
NR2 5	NR2	5.01	8.2	20	7.93	27.93	330	26.1	55.227194	-9.00
NR2 10.1	NR2	10.01	8.2	20	15.86	35.86	330	5.2	14.127450	-9.60
NR2 10.2	NR2	10.01	8.2	20	15.86	35.86	330	6.6	17.930995	-9.49
NR2 15.1	NR2	14.96	8.2	20	23.69	43.69	330	5.1	16.881229	-9.52
NR2 15.2	NR2	14.96	8.2	20	23.69	43.69	330	1.5	4.965067	-10.05
NR2 20.1	NR2	20.03	8.2	20	31.72	51.72	330	17.4	68.181608	-8.91
NR2 20.2	NR2	20.03	8.2	20	31.72	51.72	330	4.4	17.241326	-9.51